INSTITUTO POLITÉCNICO NACIONAL

*Centro de Investigación en Ciencia Aplicada y Tecnología Avanzada*

*Unidad Querétaro*


# *EXPERT SYSTEM TO SUPPORT THE DETECTION OF HUMAN FOOTPRINT ALTERATIONS*

**THESIS**

SUBMITTED AS A PARTIAL REQUIREMENT TO OBTAIN THE DEGREE OF DOCTOR IN ADVANCED TECHNOLOGY


**By:**

M. in A.T. JULIAN ANDRES RAMIREZ BAUTISTA

**Under the supervision of:**

Dr. ANTONIO HERNÁNDEZ ZAVALA

Dr. JORGE ADALBERTO HUERTA RUELAS



September 2020, Santiago de Querétaro, Qro.

SIP-13
REP 2017

# INSTITUTO POLITÉCNICO NACIONAL
## SECRETARIA DE INVESTIGACIÓN Y POSGRADO

*ACTA DE REGISTRO DE TEMA DE TESIS*
*Y DESIGNACIÓN DE DIRECTOR DE TESIS*

Ciudad de México, a 3 de septiembre del 2020

El Colegio de Profesores de Posgrado de **CICATA** Unidad Querétaro en su Sesión **ordinaria** No. **200902** celebrada el día **2** del mes **septiembre** de **2020**, conoció la solicitud presentada por el alumno:

| Apellido Paterno: | Ramirez | Apellido Materno: | Bautista | Nombre (s): | Julian Andres |
|---|---|---|---|---|---|

Número de registro: B 1 6 1 2 2 8

del Programa Académico de Posgrado: Doctorado en Tecnologia Avanzada

Referente al registro de su tema de tesis; acordando lo siguiente:

1.- Se designa al aspirante el tema de tesis titulado:

Expert system to support the detection of human footprint alterations

Objetivo general del trabajo de tesis:

Implementar un sistema experto para apoyar la detección de alteraciones ortopédicas en la huella humana mediante el uso de datos cinéticos de sensores de presión.

2.- Se designa como Directores de Tesis a los profesores:

Director: Dr. Antonio Hernández Zavala

2° Director: Dr. Jorge Adalberto Huerta Ruelas

No aplica: ☐

3.- El Trabajo de investigación base para el desarrollo de la tesis será elaborado por el alumno en:

CICATA-Unidad Queretaro

que cuenta con los recursos e infraestructura necesarios.

4.- El interesado deberá asistir a los seminarios desarrollados en el área de adscripción del trabajo desde la fecha en que se suscribe la presente, hasta la aprobación de la versión completa de la tesis por parte de la Comisión Revisora correspondiente.

Director de Tesis

Dr. Antonio Hernández Zavala

Aspirante

Julian Andres Ramirez Bautista

2° Director de Tesis

Dr. Jorge Adalberto Huerta Ruelas

Presidente del Colegio

Dr. Juan Bautista Hurtado Ramos

SECRETARIA DE EDUCACIÓN PÚBLICA
INSTITUTO POLITÉCNICO NACIONAL
CENTRO DE INVESTIGACIÓN EN CIENCIA APLICADA Y TECNOLOGÍA AVANZADA
UNIDAD QUERÉTARO
DIRECCIÓN

SIP-14
REP 2017

# INSTITUTO POLITÉCNICO NACIONAL
## SECRETARÍA DE INVESTIGACIÓN Y POSGRADO

*ACTA DE REVISIÓN DE TESIS*

En la Ciudad de Querétaro siendo las 18:00 horas del día 24 del mes de Agosto del 2020 se reunieron los miembros de la Comisión Revisora de la Tesis, designada por el Colegio de Profesores de Posgrado de: CICATA-IPN unidad Qro. para examinar la tesis titulada:

EXPERT SYSTEM TO SUPPORT THE DETECTION OF HUMAN FOOTPRINT ALTERATIONS del (la) alumno (a):

| Apellido Paterno: | RAMIREZ | Apellido Materno: | BAUTISTA | Nombre (s): | JULIAN ANDRES |
|---|---|---|---|---|---|

Número de registro: B 1 6 1 2 2 8

Aspirante del Programa Académico de Posgrado: Doctorado en Tecnología Avanzada

Una vez que se realizó un análisis de similitud de texto, utilizando el software antiplagio, se encontró que el trabajo de tesis tiene 54 % de similitud. **Se adjunta reporte de software utilizado**.

Después que esta Comisión revisó exhaustivamente el contenido, estructura, intención y ubicación de los textos de la tesis identificados como coincidentes con otros documentos, concluyó que en el presente trabajo **SI** ☐ **NO** ☒ **SE CONSTITUYE UN POSIBLE PLAGIO.**

**JUSTIFICACIÓN DE LA CONCLUSIÓN:** *(Por ejemplo, el % de similitud se localiza en metodologías adecuadamente referidas a fuente original)*
En el presente trabajo de tesis, al contar con gran parte de su contenido previamente publicado por el mismo autor como resultados parciales de su investigación, se tiene un reporte derivado de una investigación exhaustiva que merece la pena sea difundida a través de ésta tesis y no constituye un caso de plagio dado que se otorga el crédito correspondiente a los comentarios acerca de otros trabajos.

****Es responsabilidad del alumno como autor de la tesis la verificación antiplagio, y del Director o Directores de tesis el análisis del % de similitud para establecer el riesgo o la existencia de un posible plagio.**

Finalmente y posterior a la lectura, revisión individual, así como el análisis e intercambio de opiniones, los miembros de la Comisión manifestaron **APROBAR** ☒ **SUSPENDER** ☐ **NO APROBAR** ☐ la tesis por **UNANIMIDAD** ☒ o **MAYORÍA** ☐ en virtud de los motivos siguientes:

Cumple con todos los requisitos solicitados para poder continuar con el trámite de graduación

**COMISIÓN REVISORA DE TESIS**

| | | |
|---|---|---|
| Dr. Antonio Hernández Zavala<br>Director de Tesis | Dr. Joaquín Salas Rodríguez | Dr. Ruth Magdalena Gallegos Torres |
| Dr. Jorge Adalberto Huerta Ruelas<br>2° Director de Tesis (en su caso) | Dr. Juan Bautista Hurtado Ramos | Dr. Alejandro Lozano Guzmán<br>**PRESIDENTE DEL COLEGIO DE PROFESORES** |

INSTITUTO POLITÉCNICO NACIONAL
CENTRO DE INVESTIGACIÓN EN CIENCIA APLICADA
DIRECCIÓN

**INSTITUTO POLITÉCNICO NACIONAL**
**SECRETARÍA DE INVESTIGACIÓN Y POSGRADO**

*CARTA CESIÓN DE DERECHOS*

En la Ciudad de México, D.F. el día 07 del mes de septiembre del año 2020, el que suscribe Julian Andres Ramirez Bautista alumno del Programa de Doctorado en Tecnología Avanzada, con número de registro B161228, adscrito al CICATA-IPN unidad Querétaro, manifiesto que es el autor intelectual del presente trabajo de Tesis bajo la dirección del Dr. Antonio Hernández Zavala y del Dr. Jorge Adalberto Huerta Ruelas y cede los derechos del trabajo titulado EXPERT SYSTEM TO SUPPORT THE DETECTION OF HUMAN FOOTPRINT ALTERATION, al Instituto Politécnico Nacional para su difusión, con fines académicos y de investigación.

Los usuarios de la información no deben reproducir el contenido textual, gráficas o datos del trabajo sin el permiso expreso del autor y/o directores del trabajo. Este puede ser obtenido escribiendo a las siguientes direcciones julianramirez@ieee.org, anhernandezz@ipn.mx, jhuertar@ipn.mx. Si el permiso se otorga, el usuario deberá dar el agradecimiento correspondiente y citar la fuente del mismo.

JulianRamirezB.

Julian Andres Ramirez Bautista
Nombre y firma del alumno

## Abstract

Mobility is an essential part of our daily life, and this is where the health of our lower limbs is essential. Gait analysis using kinetic data, together with a medical decision support system or computer-assisted diagnosis, provides the physician with assistance in detecting gait disorder and the risk of foot ulcers, especially in diabetic patients, leg discrepancy, and footprints pathologies and many other applications in biomedical diagnosis.

The purpose of this study was to establish a procedure to correlate plantar pressure data to foot disorders. With that aim, we review the state of the art of hardware and software, plantar pressure acquisition devices and the algorithms that researchers and medical practitioners have used in this matter. Based on this background, we decided to use electronic baropodometry equipment and Fuzzy Cognitive Map (FCM) to analyze plantar pressure data. In this sense, two FCM architectures with different configurations were used to achieve the established goals.

In the first experiment, an FCM type I trained by a genetic algorithm was implemented, with one hundred and fifty-one local volunteers subject (aged 7 to 77), which were classified previously with a flat foot (n=70) and cavus foot (n=81) by specialized physicians of the Piédica diagnostic center. The trial walking was conducted using plantar pressure platforms FreeMed ®. The foot surface was divided into 14 areas that included toe 1st to 5th, metatarsal joint 1st to 5th, lateral midfoot, medial midfoot, lateral heel, and medial heel.

In the second experiment, an FCM Type II trained by Bacterial Foraging Optimization Algorithm was used, in which one hundred twenty-five local volunteers subject (20 to 68 years) participate. Foot classification into normal (n=31), flat (n=32), cavus type III (n=31), and cavus type IV (n=31) to train the system was carried out by specialized physicians. A FreeMed® platform was used to obtain the database.

A graphical user interface (GUI) was developed to implement intended methodologies. In our GUI, the user enters plantar pressure data, and as a result, the system gives probability percentages of an alteration.

Our results indicate that our methods resulted in a high-performance classification of the plantar foot alteration according to the plantar pressure. Results can be improved using the knowledge of physicians in the training process to avoid possible bias and including more population with similar morphological characteristics of other countries, to obtain results that may be applicable and scalable in other places.

## Resumen

La movilidad es una parte esencial de nuestro día a día, y es aquí donde la salud de nuestras extremidades inferiores es fundamental. El análisis de la marcha utilizando datos cinéticos, junto con un sistema de apoyo a la toma de decisiones médicas o diagnóstico asistido por computadora, proporciona al médico asistencia en la detección de trastornos de la marcha, riesgo de úlceras en el pie, especialmente en pacientes diabéticos, además de discrepancia en las piernas, patologías de huellas y muchas otras aplicaciones en diagnóstico biomédico.

El propósito de este estudio fue establecer un procedimiento para correlacionar los datos de la presión plantar con los trastornos del pie. Con ese objetivo, revisamos el estado del arte del hardware y software, los dispositivos de adquisición de presión plantar y los algoritmos que investigadores y médicos han utilizado en esta materia. Basándonos en estos antecedentes, decidimos utilizar equipos de baropodometría electrónica y Fuzzy Cognitive Map (FCM) para analizar los datos de presión plantar. En este sentido, se utilizaron dos arquitecturas FCM con diferentes configuraciones para lograr los objetivos establecidos.

En el primer experimento se implementó un FCM tipo I entrenado por un algoritmo genético, con ciento cincuenta y un sujetos voluntarios locales (de 7 a 77 años), que fueron clasificados previamente con pie plano (n = 70) y pie cavo (n = 81) por médicos especialistas del centro de diagnóstico Piédica. La marcha de prueba se realizó utilizando plataformas de presión plantar FreeMed®. La superficie del pie se dividió en 14 áreas que incluían dedo del pie 1º al 5º, articulación metatarsiana 1º al 5º, mediopié lateral, mediopié medial, talón lateral y talón medial.

En el segundo experimento, se utilizó un FCM Tipo II entrenado por un Algoritmo de Optimización de Forrajeo Bacteriano. En el experimento participaron ciento veinticinco sujetos voluntarios locales (de 20 a 68 años). La clasificación del pie en normal (n = 31), plano (n = 32), cavo tipo III (n = 31) y cavo tipo IV (n = 31) para entrenar el sistema fue realizada por médicos especializados. Se utilizó una plataforma FreeMed® para obtener la base de datos.

Se desarrolló una interfaz gráfica de usuario (GUI) para implementar las metodologías previstas. En nuestra GUI, el usuario ingresa datos de presión plantar y, como resultado, el sistema proporciona porcentajes de probabilidad de una alteración.

Nuestros resultados indican que los métodos tienen un alto grado de rendimiento para la clasificación de alteración del pie de acuerdo con la presión plantar. Los resultados se pueden mejorar utilizando el conocimiento de más médicos en el proceso de entrenamiento de los algoritmos para evitar posibles sesgos e incluir más población con características morfológicas similares de otros países, para obtener resultados que puedan ser aplicables y escalables en otros lugares.

# CONTENTS

## ACKNOWLEDGMENTS

Studying a doctorate is a long but very rewarding journey; during the journey, you not only learn technical and theoretical concepts but also to live, to endure how difficult life is sometimes. Nobody says that reaching a goal is easy; you have to be persistent and constant.

I would like to thank my wife, who has been my greatest company during this adventure that I call life and with whom I have my greatest treasure, my son. I also want to thank my parents and brother for supporting me during these four years. The support of all of them was essential to achieve my goal. A thank you to my entire advisory and evaluation team for their valuable suggestions, advice, and guidance. And also to the Centro de Investigación en Ciencia Aplicada y Tecnología Avanzada, Qro unit from Instituto Politécnico Nacional, for its valuable contribution and especially to CONACyT for the scholarship, fundamental to achieve my goal.

# Chapter 1. Introduction

In this chapter, a brief introduction will be made related to plantar pressure measurements, applications, and the parts required for a system to help in the detection of alterations in the human footprint. It includes its history and evolution in the academic and commercial environments. Afterwards, we describe the purpose and scope of our research, highlighting the requirements of the system to process and analyze the signals and correlate them with footprint alterations. In last section, it is described thesis content organization.

## 1.1 Background and scope

Plantar pressure measurements provide detailed information for the evaluation of diseases or abnormalities, involving the function of the ankle, knee, hip, the back, and other pathologies reflected in the footprint. It also allows for understanding the human foot's mechanical behavior in static and dynamic load conditions.

Biomedical signal classification systems give rise to the development of medical diagnostic support systems, which have been working for a couple of decades using flexible computing methods. These systems benefit medical centers; since they contribute to positive aspects as low rates of false-positive results, low-cost, and relatively simple tests, among others [1]. An accurate and efficient application can increase the possibility of early diagnosis of many diseases and prevent deterioration of health [1].

There are three types of plantar pressure systems: Pressure platforms, imaging technologies, and instrumented footwear systems, in which the latest are the most efficient, flexible, portable, and lowest cost systems [2]. The measurement of pressures between the foot and the shoe during walking has been studied area since 1963 when Bauman et al. [3] reported a device and method to evaluate footwear for leprosy patients through plantar measurements simple tools. At this time, the pressure measurement systems were wired, until 1997, when Lawrence et al. [4] [5] reported a device and method to evaluate footwear for patients with leprosy through plantar measurements with simple tools such as gyros, accelerometers, humidity and temperature sensors.

Biomedical signal classification systems led to the development of medical diagnostic support systems, providing benefits for medical centers; as they contribute to aspects such as low false-positive results, low cost, and relatively simple tests, among others [1]. These diagnostic systems are leaving aside the physicians' unanimous decision, which can sometimes be wrong, to support them, with systems that have medical records of patients who have been used in recent years [6]. In this study, the analysis software is an expert system capable of automatically classifying plantar pressure data in normal, flat, cavus type 3 and cavus type 4 foot.

A healthy walk requires coordination of both the neural and musculoskeletal systems to provide balance and stabilization of the body. It is possible to determine many diseases that are reflected through the abnormal distribution of weight using the footprint. For obtaining gait or footprint data, it is necessary to use specific devices. There are three types of plantar pressure systems: Pressure platforms, imaging technologies, and instrumented footwear [2], These systems use different sensor technologies and produce quantities of signals that can be normalized, classified, and interpreted to develop systems that help in the monitoring and early diagnosis of diseases.

Computer-Aided Diagnosis (CAD) or Clinical Decision Support Systems (DSS) are an active research area since the beginning of artificial intelligence. There is an application area for any innovative computing approach, which handles the massive amounts of imprecise or ambiguous data in this field. The hybrid approach seeks to exploit each component's individual advantage, obtaining improved performance for their combination[6]. With the footprint analysis study, it is possible to diagnose and treat many diseases that affect the lower extremities. On the downside, one has to analyze complex and dependent data, with non-linear correlations since each person walks differently. It is at that point where the physician gives importance to the use and robustness of efficient systems, able to process and interpret significant amounts of data to diagnose, monitor, and suggest treatment options to different gait disorders [7]. Therefore, the need for robust development systems that are versatile and easy to use in supporting medical diagnosis is evident. These systems must leverage emerging technologies based on sensors, along with computational intelligence techniques that allow performing successful real-time applications. Other benefits of DSS are the reduction of long recording times, and to dispense the gait laboratories mounting, getting portable, continuously monitoring, and cost-effective solutions [6].

The main goal of this work was to implement an expert system for supporting the detection of orthopedic alteration in the human footprint by using kinetic data from pressure sensors. The milestones required to obtain main goal were:

- Determine the characteristic patterns in the human footprint that indicate orthopedic alterations, through kinetic pressure data.
- Analyze databases with existing baropodometric equipment on normal and altered footprints.
- Define the techniques for using the pressure data classification system.
- Experimentally validate the developed technique obtained with an acquisition system, in patients with and without alterations.

## 1.2 Hypothesis formulated at the beginning of project

By having a system for the analysis of plantar pressures that can be adapted to different foot sizes and weight of people, to associate them with normal or pathological footprints, will provide a useful tool to help doctors in the detection and monitoring of pathologies in patients. The system must interpret and analyze complex data from the electronic insole and give output as a percentage of the possible alteration.

### 1.3 Methodology employed in project

For the development of the project, the methodology proposed by Buchanan was used, which is described below:

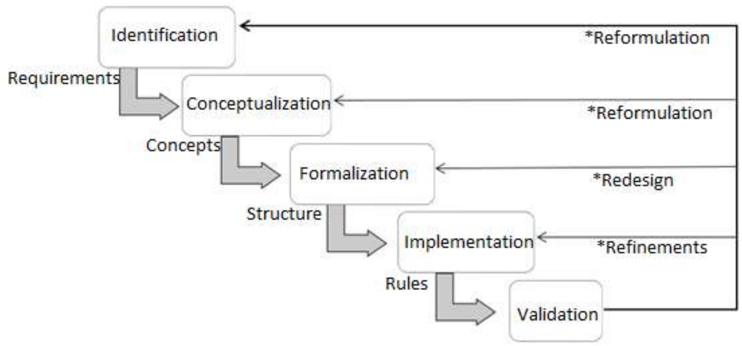


Figure 1. Diagram that shows steps defined in Buchanan methodology

Each stage performed during the project is described as follows:

a) Identification

The problem was identified. Interviews with experts in the field of plantar pressure analysis were carried out, as well as searches in the literature to contemplate the solutions proposed above. This phase was essential to obtain the problem, which was addressed together with the possible solution, the target population, the objectives and goals to be achieved with the system. With the identification stage, the computational functions are established, enter symptoms, provide a diagnosis expressed in percentage, low computational cost, and provide an easy-to-use GUI.

b) Conceptualization

The concepts obtained from the field experts were analyzed, as well as all the information reported in the literature. Variables that indicate a specific pathology were defined, as well as obtaining a healthy reference standard, normalized in weight and size. At this stage, two searches were considered, on the one hand, everything related to plantar pressure acquisition systems and, on the other, the algorithms used by previous authors to analyze biomedical data.

c) Formalization

Based on the information obtained in the previous stage, the relevant concepts that were considered to classify plantar pressures were identified. The programming paradigm and the representation of the knowledge base were determined.

d) Implementation

Visual Studio IDE was chosen as an environment to develop the entire project, with the *C#* and *R* languages. For the graphical part, Windows Forms was used, which was the name given to the graphical application programming interface, which provides access to the elements of the native Microsoft Windows interface, this in *C#* language. For the analysis and classification of plantar pressure data, the *R* language was used, which can be integrated with the graphical interfaces programmed in *C#*, and it was one of the most important languages used by data scientists and programmers.

e) Validation

The system's performance was verified using a plantar pressure acquisition system in patients with and without alterations.

## 1.4 Content Summary

This thesis is structured with four additional chapters. The second Chapter presents the state of art of adquisition systems, reviewing the technologies used in the sensors and the developments that have been made commercially and academically, highlighting the need to create systems that correlate these signals with footprint alterations, regardless of foot size and patient weight. Besides the algorithms used for recognizing patterns in the plantar pressure data, their current state, and the improvement aspects reported by the authors. The third Chapter presents the phases of obtaining human plantar pressure data through a plantar pressure platform; in addition, we describe the procedure for acquiring and preprocessing plantar pressure data. The fourth Chapter presents the algorithms and the experiments used for the classification of alterations in the human plantar foot. The last chapter, describe the conclusion of the work and the future work recommended to follow on the classification of the alteration of the human plantar foot using Fuzzy approaches. Fig. 2 shows the content summary.

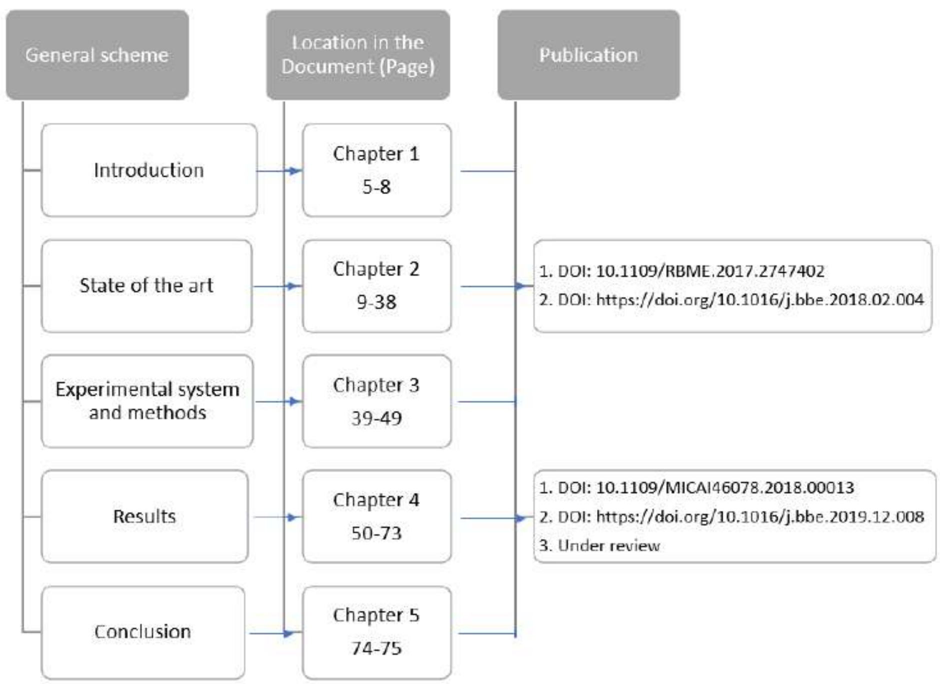


Figure 2. Content Diagram

# Chapter 2. Acquisition System and Algorithms for Plantar Pressure Analysis

This chapter presents the antecedents related to plantar measurement systems, focusing on instrumented footwear or instrumented insole, disclosing in detail the development of this type of system, their scope, and future work reported by the authors academically or commercially. The last part deals with the alterations that can be detected and the algorithms used for plantar pressure data pattern recognition considering the scope and the aspects to improve reported by the authors. Appendices 1.1 and 1.2 show the original documents.

## 2.1 Acquisition System for Plantar Pressure Kinetic Data

Plantar pressure measurement provides important information about the pleople´s health, the human body structure, and foot functionality [8]. Advancements have been made in the development of measurement technologies for plantar pressure to get systems for understanding general behavior and/or pathologies by analyzing the pressure generated by the feet during human motion [9], [10]. Plantar foot measurement systems can be classified into three types: pressure platforms, imaging technologies, and instrumented footwear systems [2], [11].

Foot pressure measurement by instrumented shoes has been an exciting area since 1963, when Bauman, J.H et al. [3] described this equipment and method to evaluate footwear for leprosy patients through plantar measurements with simple devices. The measuring pressure systems were wired until 1997 when Tracie L. Lawrence et al. [4] presented a wireless in-shoe force system for analyzing normal and paraplegic patients. In recent times, both commercial and academic groups have been developing instrumented shoes with different types of sensor technologies, allowing wireless communication and low power consumption in simple systems for improving data acquisition. These advances have been made to achieve significant social acceptation [5]. The inclusion of other types of sensors, such as gyroscopes, accelerometers, humidity, and temperature sensors, makes these instrumented insoles a helpful tool for detecting many diseases.

These devices have been widely used in the clinical and research field to evaluate patients with structural disorders, foot illness, or early diagnosis pathologies [8]. Plantar pressure analysis lets us estimate many parameters, such as mean pressure, peak pressure, center pressure, and displacement speed of the center of pressure [12]. Allowing to determine balance analysis [13], [14]; measuring of spatiotemporal gait [15], [16]; and ground reaction forces (GRFs) [17] in sports and medicine. For detecting abnormalities, such as the type of foot, cavus, or flat [18], flat-valgus, and clubfoot [19]. But also for monitoring and diagnosing many diseases as insensible feet [20], Parkinson, peripheral neuropathy, frailty, dementia [21], and pressure peak in diabetic foot [22]. Detectable when the inappropriate forces are present in the measuring [23].

By utilizing pressure-sensitive elements and inertial sensors such as accelerometers in conjunction with gyroscopes, both commercial and academic groups are developing ergonomic and wearable systems intended to be used in real life for long periods.

The main requirements for measuring plantar pressure and gait parameters are:

*Flexible electronics:* Allows the best place of the measurement electronics for obtaining accurate information. Also, the device can be more flexible and adaptable to the natural human movements [2], [24].

*Sensor placement:* The foot surface can be divided into areas to obtain more relevant data. Reports show that the sole can be divided into 15 differentiable areas [2]. The minimum number of recommended sensors is 15, but it is limited to the changes in foot size, resulting in the displacement of interest pressure points [25], [21].

*Sensor size:* The sensor size recommended by the previous works is 5mm x 5mm [26], [27]. A larger sensor can underestimate the peak pressure. And with a smaller sensor, it is difficult to control the displacement of the points of interest during gait.

*Embedded electronics:* The completely integrated micro-electro-mechanical systems MEMs technology (sensors, communication, battery, storage, etc.), becomes an excellent option since there are not strange elements perceived by the users [24], [28]. Studies report that a device attached to the shoe weighing less than 300 g does not affect gait [2].

*Low power consumption:* The system must operate through a complete day to obtain sufficient data for research and/or continuous monitoring of the patients [8].

*Low cost:* The cost of the system is an essential factor because current systems are efficient and comfortable but not affordable.

The development is being carried out in the commercial and academic groups, obtaining the following results.

### 2.1.1 Commercial systems

There are entirely integrated commercial devices such as the German company Moticon [29], which develops, manufactures, and distributes sensor products for motion analysis in medicine and sports applications. Moticon products are characterized by fully integrated design and easy handling with 13 capacitive sensors per insole, 3D accelerometer sensor, wireless communication, flash memory, and power supply, all integrated into the insole, as shown in Fig. 3a. The Chinese InsoleX, developed by Sennotech [30], is a wearable monitoring product with high accuracy and reliability. This insole is easy-to-use and integrates approximately 48 smart textile pressure sensors (depending on the insole size) in the 30-1200 kPa range, 3D accelerometer, 3D gyroscope, 3D compass, and wireless communication, among other features (Fig. 3b).


a)
b)


Figure 3. Insoles completely integrated, unobtrusive to the user. a) Moticon system [29]. b) InsoleX system [30].

These systems reduce space constraints in the rehabilitation or research centers and offer freedom of movement for the patient. The summary of these systems is shown in Table 1.

Table I. Commercially Available Instrumented Insole

| **Insole** | **Sensor Technology** | **Sensors per insole** | **Other sensors** | **Battery** | **Communication** | **Sampling (Hz)** | **Image** |
|---|---|---|---|---|---|---|---|
| F-Scan [31] | Resistive | 960 | ------ | 2 hours | USB | 100 |  |
| Moticon [29] | Capacitive | 13 | 3D accelerometer | ------ | Wireless | 100 |  |
| Pedar-X Insoles [32] | Piezo electric | 99 | ------ | 4.5 hours | Bluetooth/ USB/ Optic Fiber | 100 |  |
| Footwork Insole [33] | Capacitive | 80 | ------ | 3 hours | Bluetooth / USB | 400 |  |
| Biofoot/IB V [34] | Piezo electric | 64 | ------ | ------ | Wi-Fi/ USB | 750 |  |
| ParoTec [35] | Hydro-cell, piezo resistive | 24 ó 36 | ------ | ------ | Memory card | 300 |  |
| Dynafoot2 [36] | Resistive | 58 | Accelerometer | 3.5 hours | Bluetooth | 100 |   |
| Wiisel [37] | Resistive | 14 | Accelerometer Gyroscope | ------ | Bluetooth | ------ | |

| | | | | | | | |
|---|---|---|---|---|---|---|---|
| Sennopro Insole X [30] | Textile sensor | 48 | Accelerometer<br>Gyroscope<br>Compass | 48 hours | Bluetooth | 100 |  |
| Medilogic insole [38] | ------ | 240 | ------ | 16 hours | Wireless | 300 |  |
| Orpyx LogR [39] | ------ | 8 | ------ | 12-8 hours | Bluetooth | 100 |  |
| Sensor Medica Flexinfit [40] | Resistive | 214 | ------ | 4 hours | Bluetooth | 25 to 50 |  |

### 2.1.2 Academical systems

Due to the high cost of the commercial systems, academicals have been developing different devices with novel sensor technology [41] while determining their best positions to obtain a significant amount of features from both, gait parameters and plantar pressure [2]. In these systems, they are integrating up to 64 sensing elements. For example, Donati M. et al. [42] developed a system composed of flexible matrices of 64 optoelectric sensors covered by soft silicone, called Pressure Sensor Pads (PSP), as in Fig. 4a. The system has an excellent performance in terms of accuracy, sensitivity, dynamic behavior, and compliance with the mechanical requirements.

Leemets K et al. [43], presents a lightweight, and robust sensor array system for the instrumented insole. The setup enables the use of both resistive sensing and capacitive sensing, but the authors used a capacitive setup because it turned out to be the most reliable and consistent. The system is composed of layers (Fig. 4b).

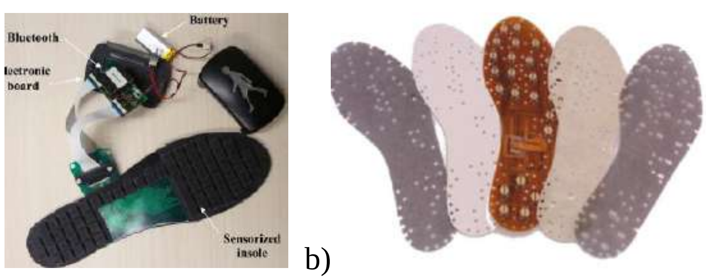

a) b)

Figure 4. Development of the sensor arrays for pressure measurement. a) Opto-electric system by Donati M. et al. [42]. b) The multi-layer system by Leemets K. et al. [43].

There are many academic efforts to obtain better systems covering different interesting issues like low-cost, size reduction, sensitivity, measurement range, accuracy, and spatial resolution.

A summary of these developments is shown in Table 2. This review intends to present the advances in plantar measurement systems that have been developed since 1963.

Table II. Academic instrumented insoles

| Technology | Sensors per insole | Other sensors | Sampling (Hz) | Reference |
|---|---|---|---|---|
| **Resistive** | 1 to 5 | Accelerometer<br>Gyroscope<br>Humidity<br>Temperature | 24 to 100 | [15], [21], [51]–[55], [25], [44]–[50], [56] |
| | >5 to 10 | ---- | 25 to 25000 | [4], [57]–[62], [63] |
| | >10 to 20 | Humidity<br>Temperature | 25 to 30 | [18], [58], [64], [65], [66] |
| **Capacitive** | 1 to 5 | ---- | 100 | [67], [68] |
| | >20 to 30 | ---- | ---- | [43] |
| **Piezo-resistive and piezo-electric** | <1 to 10 | Accelerometer | 60 to 155 | [46], [69]–[73] |
| | > 30 | Accelerometer<br>Temperature | 5 to 13 | [13], [74] |
| | other array | ---- | 10 to 1000 | [41], [75] |
| **Opto-electronic** | 4 | None | 1000 | [17] |
| | 64 | None | 100 | [42] |
| **Conductive compound** | 7 | Electrotactile stimulator | 20 | [76] |
| | 8 | Accelerometer<br>Humidity<br>Temperature | ---- | [22] |
| **EMFI-Film** | 16 | None | 10 | [77] |
| **Elastometer** | 5 | None | 240 | [65] |
| **Conductive rubber** | 7 | None | 20 | [78] |
| **Air pressure** | 4 | None | ---- | [79] |
| **Tri-axial force transducers** | 5 | None | 100 to 300 | [80], [81] |
| **Six-axial force sensors** | 3 | Gyroscope<br>Accelerometer<br>Magnetometer | ---- | [82] |
| **Optical fiber** | 6 | None | 960 | [83] |
| **Textile sensor** | 1 to 6 | ---- | 100 | [12], [84] |
| | 48 | Accelerometer<br>Gyroscope<br>Compass | 100 | [85] |

| | | | | |
|---|---|---|---|---|
| | 1040 | None | 30 | [86] |

### 2.1.3 Pressure sensor technologies

The literature has reported different sensing elements for measuring plantar pressure, which can be divided in:

*Capacitive sensors*

It is composed of two electrical conducting plates separated by a dielectric elastic layer in which the distance changes according to the force applied, producing a voltage variation [8]. Some studies have reported this technology [29], [33], [43], [67].

*Resistive sensors*

They are made of a conductive polymer that varies its resistance according to the applied force, i.e., the higher the pressure, the lower the resistance. Is the most common type and has been used in several studies [18], [20], [31], [57], [64], [87]–[90].

*Opto-electronic sensors*

These sensors are composed of a light transmitter and a photodiode receiver separated by an external silicone bulk structure. When a load is applied, the cover deforms itself, the light is screened, and the sensor changes its output voltage proportionally [42], [17].

*Piezo-resistive and piezo-electric Sensors*

These devices can be constructed using a miniature pressure sensor based on MEMS technology. Studies with this type of technology are reported in [32], [13], [91], [41] and [92].

*Other Technologies*

There are systems developed with different technologies such as textile sensors, as used by Wenyao et al. [85] and Sennotech [30]; this technology is based on conductive inks to create a stretchable, thin, and pressure-sensitive textile, in which it is possible to include a higher number of sensing elements [48]. Kyoungchul et al. [23] developed a system based on air pressure sensors composed of air bladders made of winding soft silicone tubes and an air pressure sensor.

### 2.1.4 Detected and monitored disorders

Plantar pressure measurement systems are widely used in sports, research, and medical applications, these systems allow to estimate several biomechanical and foot disorders [93]. These devices aim to provide support for researchers and medics by generating reports for studying the patient progress or by aiding in identifying pathologies. Many of the reported developments were made for application in fields like monitoring, pattern extraction, rehabilitation, disorder detection, among others.

### *Monitoring and disorder detection applications*

The first study in 1963 was the design of orthopedic shoes for patients with leprosy [3]. In 1990 began the development of systems for monitoring diseases as diabetes [60], which is the most widely studied disease. The diabetic patients lose pain and temperature sensations in their feet. For this, the monitoring of the foot is transcendental to prevent complications as ulcerations, pathological neuropathy, infections, and even amputation due to the lack of sense. The absence of adequate sensation produces changes in the walking pattern as abnormal pressure distributions indicating a risk area when the plantar pressure increases [94], [95].

In 1995 Hausdorff et al. [47] presented a simple footswitch system that provides accurate estimations of the start and end of the stance phase for distinguishing normal and pathologic gait. The systems developed by Shu Lin et al. [22], Torres et al. [20], Patil et al. [59], Benbakhti et al. [61], Wenyao et al.[85], Talavera et al. [96], [37], and Orpyx [39] are focused on monitoring reduced or inexistent sensation in the foot, avoiding the excessive friction with the skin. They also allow proper orthopedic prescriptions preventing ulcers or amputation due to sensory failure. Besides, they have used other sensors for measuring temperature and humidity to give feedback in both friction and humidity rates. In many cases to determinate the higher-pressure areas, they refer to previous works to obtain the six main areas where foot ulcerations are more common [97] (Toe, Medial Forefoot, Lateral Forefoot, Medial Med-foot, Lateral Mid-foot, and Heel) allowing a smaller number of sensors used.

The combination of plantar pressure analysis and inertial sensors allows for monitoring patient balance to assess neurological disorders, early disease detection, monitoring new medication or training, and elderly fall risk [70], [98]. The lack of balance is a secondary effect of a large number of diseases. Ghaida et al [99] used only 3 sensors to study the human equilibrium determining the displacement and velocity of the center of pressure in real-time. By doing this, they obtained a portable monitoring system with low-power consumption focused on fall risk detection, encouraging new studies in comparing healthy and unhealthy people.

Finally, developments such as those made by Ahmad et al.[87], Kawsar et al. [100], Crea et al. [42] and, Meng et al. [52], are focused on monitoring and detecting abnormalities in human gait, giving a low-cost tool for future studies. Many devices have been tested in healthy and unhealthy people of different ages and weights to obtain more reliable results, providing medical specialists a tool to analyze and evaluate patients' progress, as reported by Pineda et al. [18]. They developed a device for capturing the distribution of loads in the feet during quiet, standing, and gait cycles. It provides valuable information for medics using a graphical interface (Fig. 5b) to determine possible dysfunctions of the foot, postural abnormalities, and the symmetry ratio between feet. This system is shown in Fig 5a.

a)  b) 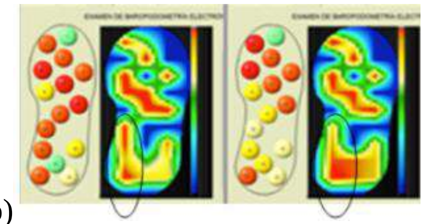

Figure 5. System for children's postural and gait analysis proposed by Pineda et al. [18]. a) System for acquire signals. b) Example of information maps to assist in medical diagnostic.

### *Rehabilitation applications*

In this topic Qin et al. [57] developed a device that provides real-time feedback for monitoring the evolution in post-stroke rehabilitation (Fig. 6). The authors used a tailored insole to be adapted to the deformity of the paralyzed foot, and they obtained that the peak contact area was significantly more significant in the 3D insoles than in the flat insoles.

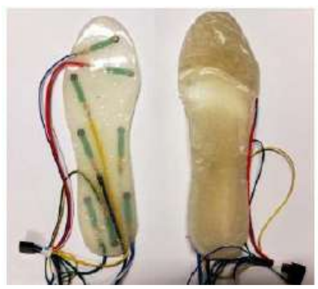

Figure 6. Instrumented insole for analysis of post-stroke rehabilitation, flat insole (left) and 3D insole (right) [57].

Many efforts in the development of devices seek to offer an efficient tool that the researchers and medics can use to assess rehabilitation treatments [101]. Authors present innovative wearable monitoring systems for studying walking patterns in ill and healthy people, providing more and better treatment methods [49], [91].

### *Monitoring athletes*

Analyzing the load differences in the foot is determinant in assessing success factors and risks of injury in an athlete, as well as the comfort of his footwear [102]. Besides, it is useful to develop motion protocols for athletes when they are injured, providing a source of information to analyze and understand the injury mechanisms [103]. In this field, researchers have carried out an analysis to improve sports achievements as in the soccer players as it is reported in [104]. Their purpose was to evaluate the balance ability in the players both before and after soccer training session. In [84], a textile pressure sensor is used for snowboarding applications; in [68], the instrumented insole is used for javelin; and [69] mentions other applications in which researchers have worked, such as tennis, skiing, running and soccer, among others. Additional references are focused on providing a tool that benefits the sports community because these systems can help to increase the performance of the athletes [105], [75], and improve the comfort of sports shoes [106].

The instrumented insoles are fundamental for plantar pressure analysis required for many applications. One of their major limitations is the price for massive use, as it is reported in many works. In many cases, these systems do not have the necessary comfort and efficiency features. With the technology evolution and the facility to miniaturize measurement systems, systems nowadays tend to be more efficient, smaller, and capable of measuring more extensive ranges.

The number of pressure sensing elements in the insoles is an essential consideration since the ideal instrumented insole requires a large number of sensors to provide smaller detection areas to achieve better analysis results. Unfortunately, the increase in the sensor number is reflected in the energy consumption, and in the computational cost to analyze and process the signals to converge to a solution.

By experience, to obtain the most representative signals of the whole foot, the minimum necessary sensors are fifteen as the foot can be divided into this number of representative regions. Still, this quantity is not enough for measuring different foot sizes since the position of pressure points changes. Besides, the system's weight is another factor to consider; it is reported that 300 g or less do not affect gait while the system is attached to the shoe (including sensors, electronics, and batteries) [2].

## 2.2 Algorithms for Plantar Pressure Analysis

Medical diagnosis depends strongly on the medical's experience, which cannot be inherited incoming generation, repeating the training processes with new doctors. For this reason, it is needed to develop diagnosis systems that help to store and manage the information acquired with the experience to provide a tool for improving the diagnostic processes [107]. Traditionally, hospitals continuously collect vast amounts of information by monitoring the physiological parameters of patients. This becomes a great opportunity and a challenge because the manual analysis of large amounts of medical data is complicated [108], [109]. Clinical decision support systems (CDSS) are currently useful for analyzing medical data, and much work has been done in medical diagnosis problems [110]–[118], but in the case of diagnosis of diseases related to plantar pathologies, only a few works have been reported.

### 2.2.1 Plantar pressure analysis

There are many systems developed with different technologies for measuring the footprint pressure distribution [119], [2], [5], [9]. The development of algorithms to analyze load distributions between healthy and unhealthy people allows us to obtain useful information for medicals and researchers [120]. The foot is divided into different areas that support all bodyweight and balance adjusting to get more efficient and precise plantar pressure measurements and to facilitate its analysis.

For example, in [121]–[123], the authors sectioned the foot into four areas; in the case of [124]–[128], it is divided from eight to fifteen areas. In many cases, those areas satisfy the requirements of a particular study, but when not all the regions are considered, there is a risk of losing important information. After analyzing the previous studies, we propose that a foot divided into fourteen areas is suitable for making studies without losing information. These relevant areas are medial heel, lateral heel, medial midfoot, lateral midfoot, 1st to 5th metatarsal joint, and 1st to 5th toe, as presented in Fig. 7. For perceiving every move and impulse of the human footprint, it is required a sampling rate of around 300 Hz, reported by [38]. For the analysis of fast-moving actions in sports, this sampling rate is adequate to capture short time force peaks, such as those produced by a fast motion of 7 km/h.

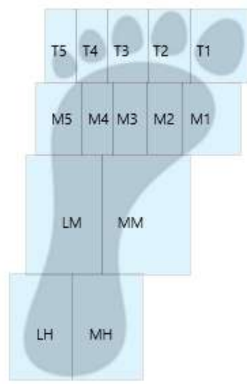


Figure 7. Interest regions on the foot surface. Lateral heel (LH), medial heel (MH), lateral midfoot (LM), medial midfoot (MM), metatarsal joint 1st to 5th (M1-M5), toe 1st to 5th (T1-T5).

### *Pressure analysis for diabetes*

Biomechanical observations on the footprint could reflect clinical pathologies such as the diabetic foot. It is a disease caused by diabetes disease that affects the patient's quality of life, and the authors reported that it would exceed 365 million in 2030 [129]. Table III summarizes the reported outcomes obtained in this area, taking into account the most relevant features of each study.

Table III. Syntesis of diabetic foot analysis reports

| Author | Sampled population | Age (years) | Mass | Acquisition System | Technical Details | Regions of Interest | Sampling Rate |
|---|---|---|---|---|---|---|---|
| Z. Pataky et al. [121] | 33 diabetic patients, 10 with callus, 10 without callus and 13 treatment group | ----- | ----- | Own system made of Force Sensing Resistors (International Electronics & Engineering, Luxembourg) | Thick: Unspecified<br>Sensor: 174 attached on the foot<br>Resolution: Unspecified | 1st, 3rd, and 5th metatarsal head | 250 Hz |
| Bacarin T. et al. [122] | 20 control patients, 17 without foot ulcers, 10 history of ulcers | Control patients: 48.7(9.4),<br>Without foot ulcers:54.7(7.8),<br>History of ulcers: 58.8(6.7) | BMI<br>Control patients:24.3+-2.6 kg/m2,<br>Without foot ulcers:26.1+-4.6 kg/m2,<br>History of ulcers: 27+-5.5 kg/m2 | Pedar-X system insoles | Thick: 2.5 mm<br>Sensor: 99 capacitive pressure sensors<br>Resolution: 1.6 to 2.2 cm2 | Rearfoot, midfoot, lateral forefoot, medial forefoot, and hallux | 50 Hz |
| Z. Pataky et al. [130] | 15 diabetic and 15 non-diabetic patients | Diabetic patient: 43.5+- 9.1<br>Non-diabetic patient: 43.4+-10.8 | Diabetic patient: 85.3+- 11.50kg<br>Non-diabetic patient: 82.0+-10.3kg | Own system made of Force Sensing Resistors (International Electronics & Engineering, Luxembourg) | Thick: Unspecified<br>Sensor: 174 attached on the foot<br>Resolution: Unspecified | 1st, 3rd, and 5th metatarsal head | 96Hz |

| | | | | | | | |
|---|---|---|---|---|---|---|---|
| Linah Wafai et al. [131] | 16 diabetic and 16 control patients | Control female: 33.7+-11.6<br>Control male: 37.4+-13.0<br>Diabetic female: 32.8+-14.1<br>Diabetic male: 40.8+-13.8 | Control female: 64.6+-13.8kg<br>Control male:<br>85.9+-7.6kg<br>Diabetic female:<br>63.0+-6.4kg<br>Diabetic male:<br>82.0+-18.8kg | F-scan in-shoe (Tekscan, MA, USA) | Thick: 0.178 mm<br>Sensor: 960 resistive pressure sensors<br>Resolution: 3.9 sensels / cm2 | Interphalangeal joint and 1st to 5th metatarsophalangeal joints | ----- |
| Chi-Wen Lung et al. [123] | 19 diabetic and 8 control patients | Diabetic: 42.2+- 12.6<br>Control patients: 23.1+-3.2 | Diabetic: 94.0+-21.7kg<br>Control patients: 66.8+-21.3kg | F-scan in-shoe (Tekscan, South Boston, MA, USA) | Thick: 0.178 mm<br>Sensor: 960 resistive pressure sensors<br>Resolution: 3.9 sensels / cm2 | 1st toe, 1st metatarsal head, 2nd metatarsal head, and heel | 200Hz |
| A. Veves et al. [132] | 58 neuropathic and 28 non-neuropathic | Neuropathic: 28-77,<br>Non-neuropathic: 17-66 | Neuropathic: 74.8+-17.2kg<br>Non-neuropathic: 74.4+-15.0kg | Optical pedobaro-graph | Thick: Unspecified<br>Sensor: Unspecified<br>Resolution: Unspecified | 1st to 5th metatarsal head, heel, and toes | ----- |
| T. Duckworth [126] | 41 patients with diabetic neuropathy and 41 healthy patients | ------ | ------ | Optical pedobaro-graph | Thick: Unspecified<br>Sensor: monochrome television camera<br>Resolution: Unspecified | 1st to 5th metatarsal head, heel, toes, and forefoot | ----- |

| | | | | | | | |
|---|---|---|---|---|---|---|---|
| Zequera et al. [133] | 40 diabetic and 40 non-diabetic patients | ------- | ------ | Parotec system insole | Thick: 3.5 mm<br>Sensor: 24 with Hydrocell technology<br>Resolution: Unspecified | ------ | 300 Hz |
| Madavi et al. [128] | ------- | ------- | ------ | Own system made of piezo-resistive sensors | Thick: Unspecified<br>Sensor: 6<br>Resolution: Unspecified | Toe area, metatarsal area, heel and mid-foot | ------ |

### *Orthopedic alterations*

According to its arch, another condition that can be detected and analyzed through plantar pressure is the foot type [134]. The most studied foot types in previous work are: flat foot, cavus foot, and hallux valgus foot, as shown in Table IV. The flat foot condition occurs in childhood when the arch of the foot is not totally developed, causing pain in feet, ankles, and knees, besides the mechanical instability during the gait, abduction, and valgus of the hindfoot. It is caused by the insufficiency of the posterior tibial tendon in adults [135]. This condition is observed in the work from Vorlickova et al. [136] showed in Fig. 8.

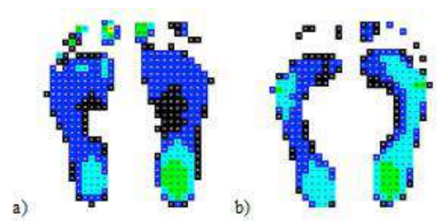


Figure 8. Plantar pressure distribution is taken from Vorlickova et al. [136]. a) Flat foot. B) Flat foot after therapy.

The opposite condition is called cavus foot, characterized by a medial longitudinal arch higher than the normal. In most cases, it is associated with claw toe or hammer toe, with the contracture of the plantar fascia, or with metatarsalgia, and callosities. An example of this condition is shown in Fig. 9.

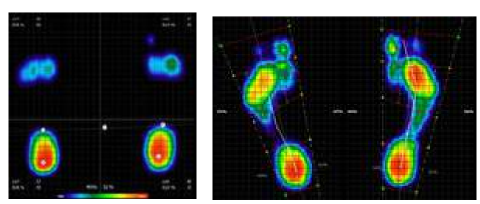

Figure 9. Cavus foot map [137].

The hallux valgus foot is associated with a prominent protuberance on the inside of the forefoot produced by the medial deviation of the first metatarsal [127] as shown in Fig. 10.

Figure 2. Hallux valgus foot. Left, radiological image. Right, plantar pressure mapping [138].

Table IV. Syntesis of foot type analysis reports

| Author | Sampled population | Age | Mass | Acquisition System | Regions of Interest | Sampling Rate |
|---|---|---|---|---|---|---|
| **Flat foot** | | | | | | |
| Ledoux et al. [139] | 16 flat foot and 22 normal foot | Flat foot: 25.6<br>Normal: 26.6 | Flat foot: 78.88kg<br>Normal: 79.64kg | Pressure plate Musgrave Medical | Sub-hallucal, five sub-metatarsals, and sub-calcaneal area | 28 Hz |
| Queen et al. [140] | 12 normal feet and 10 flat feet | Flat foot: 25+-3.6<br>Normal:25+-3.6 | Flat foot: 78.8+-18.5kg<br>Normal: 80.5+-17.9kg | Insole by Pedar-X system | Side-cut, shuttle run, cross-cut, and landing | 50 Hz |
| Vorlickova et al. [136] | 3 patients | 6.3+-1.7 | 21.0+-3.6kg | Emed platform | Midfoot, forefoot, thumbs, and 2nd to 5th toe | ----- |
| **Cavus foot** | | | | | | |
| Fernández Seguín et al. [141] | 34 patients with pes cavus and 34 patients with normal feet | Cavus foot: 24.21+-5.18<br>Normal: 27.88+-10.49 | Cavus foot: 22.10+-2.64kg/m2<br>Normal: 22.28+-3.02kg/m2 | Footscan platform | 1st to 5th metatarsal heads, forefoot, midfoot, and heel | 500 Hz |
| Burns et al. [142] | 30 with cavus foot, 10 with Charcot-Marie-Tooth and 30 normal patients | Cavus foot:30.6+-13.5<br>Charcot-Marie-Tooth:56+-18.6<br>Normal: 31.7+-11.1 | Cavus foot: 25.4+-5.3 kg/m2<br>Charcot-Marie-Tooth: 25.9+-1.9 kg/m2<br>Normal: 24.3+-3.6 kg/m2 | EMED-SF platform | Rearfoot and forefoot | 50 Hz |
| **Hallux valgus foot** | | | | | | |
| Wen et al. [127] | 248 with pain, 210 without pain and 70 normal patients | Pain:51.2+-12.14<br>Without:49.4+-Normal:16.14<br>46.7+-9.76 | Pain:61.9+-7.71kg<br>Without:60.4+-8.16kg<br>Normal:66.5+-13.17kg | Pressure plate | Hallux, the 2nd to 5th toe as a region, metatarsal joints 1st to 5th, middle foot, medial heel and lateral heel | 250 Hz |

| | | | | | | |
|---|---|---|---|---|---|---|
| Wafai et al. [131] | 16 unhealthy patients, and 16 control patients | Unhealthy female: 32.8+-14.1<br>Control female: 33.7+-11.6<br>Unhealthy male: 40.8+-13.8<br>Control male: 37.4+-13.0 | Unhealthy female: 63.0+-6.4kg<br>Control female: 64.6+-13.8kg<br>Unhealthy male: 82.0+-18.8kg<br>Control male: 85.9+-7.6kg | F-scan in-shoe | Interphalangeal joint and the metatarsophalangeal joints 1st to 5th | ----- |
| Koller et al. [138] | 61 feet of 55 patients | 57.7+-11.3 | ------ | Emed-at platform | Hallux valgus angle | 60 Hz |
| **Club-foot** | | | | | | |
| Giacomozzi et al. [143] | 20 patients with club-foot and 20 control patients | Control: 11.5+-2.8<br>Club-foot: 11.0+-3.3 | Control: 18.1+-3.1kg/m2<br>Club-foot: 19.5+-4.0kg/m2 | Emed-m platform | Medial hind foot, lateral hind foot, midfoot, medial forefoot and lateral forefoot | 50 Hz |
| **Normal foot, flat foot, cavus foot, hallux-valgus foot and Hallux varus foot** | | | | | | |
| Costea et al. [144] | 67 patients | 52-84 | 45-70kg | RSscan pressure plate | Foot length, heel width, toe width, hallux-valgus angle, middle foot width | ----- |

### *Other pathologies*

There are other relevant pathologies that researchers have been studied as summarized in Table V. Rouhani et al. [145], analyzed the initial contact time, terminal contact time, maximum force time, peak pressure time, maximum force and peak pressure, to demonstrate that it is possible to use plantar pressure parameters as a tool for assessing patients with total ankle replacement (TAR) and ankle arthrodesis (AA).

Zammit et al. [146] found changes in the load function of the foot, which may produce other effects, such as plantar callus formation and hyperextension of the hallux interphalangeal joint, as is shown in Fig. 11.

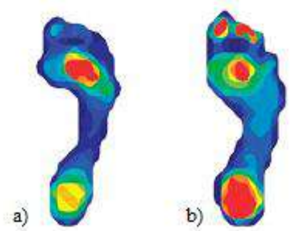


Figure 11. Comparison of a normal foot (a) and foot with osteoarthritis in the first metatarsophalangeal joint (b) [146].

These analyses indicate the importance of realizing studies using plantar pressure measurements for early detecting changes in plantar loading characteristics and their relationship to foot pain in patients as the case of rheumatoid arthritis [147]. Another possible issue to analyze through plantar pressure is the pathological gait because during standing, the foot assists in controlling the delicate muscular activity required to keep balance [148]. Hayafune et al. [149] analyzed normal force distribution pattern of the forefoot during the push-off phase to obtain more information when the forefoot carries the whole weight.

Another related application is to detect leg length discrepancy. This condition affects gait and posture, for which it is important to understand the biomechanics of these patients, Abu-Faraj et al. [150]. Choi et al. [151], [152], studied the possibility of detecting a slip-off event early through identifying plantar pressure distribution differences during heel contact between normal and slipped step. Patients with Parkinson or Hemiparesis can be analyzed through plantar pressure. Okuno et al. [153] concluded that it is possible to separate patients with Parkinson´s disease from normal patients taking as a feature the time of step cycle and the step length. Meyring et al. [154] reported that gait pressure distribution analysis improves the assessment and therapy of hemiparetic patients.

### *Plantar pressure for people characterization*

The purpose of others authors is to compare the plantar pressure distribution between young, adults, and elderly [155], children and adults [156], obese and non-obese [157], [158], or visually impaired and normal people [159], as shown in Table VI.

Table V. Some other reported analysis

| **Disease** | **Sampled population** | **Age** | **Mass** | **Acquisition System** | **Regions of interest** | **Sampling Rate** | **Reference** |
|---|---|---|---|---|---|---|---|
| Ankle Osteoarthritis (AO) | 47 patients | Control: 59+-27<br>AO:60.5+-17<br>TAR:66.5+-19<br>AA: 65+-13.3 | Control: 66.6+-12.6kg<br>AO: 80.6+-18.3kg<br>TAR: 80.5+-8.8kg<br>AA: 87.7+-9.2kg | Insole Pedar-X | Medial and lateral hind foot; medial and lateral midfoot; medial, central, and lateral forefoot; and 1st to 5th toe | 200 Hz | [145] |
| Osteoarthritis (OA) on the first metatarso-phalangeal joint | 197 patients | Control: 74.8+-7.8<br>OA:76.6+-8.1 | Control: 73.2+-17.9kg<br>OA: 78.7+-14.7kg | Mat-Scan system | Heel, midfoot, 1st to 5th metatarsophalangeal joint, hallux, and lesser toes | 40 Hz | [146] |
| Rheumatoid arthritis (RA) | 112 patients RA and 20 control | RA: 55.0+-11.0<br>Control: 53.2+-12.3 | RA1: 25.1+-4.1kg/m2<br>RA2: 26.0+-6.9kg/m2<br>RA3: 28.2+-5.4kg/m2<br>Control: 25.2+-4.7kg/m2 | Plat-form Emed ST4 | Medial and lateral heel; medial and lateral midfoot; 1st to 2nd metatarsal, lateral metatarsals, hallux, 2nd toe and lateral | 50 Hz | [147] |
| Normal force distribution pattern | 42 healthy patients | 34.8+-10.2 | 66.4+-10.8kg | EMED-SF4 system | 1st to 5th metatarsal head, big toe, 2nd to 5th toe. | ---- | [149] |
| Leg discrepancy (LD) | 2 patients | Normal: 22<br>LD:44 | Normal: 68kg<br>LD:65kg | Insole system Pedar-x | Lateral and medial heel; midfoot; lateral and forefoot; lesser toes, and hallux | ---- | [150] |
| Slip event early detection | 11 patients | 25 to 39 | 55 to 88 kg | Insole system Pedar-C | Toes, metatarsal head, arch and heel | 50 Hz | [151] |

| | | | | | | | |
|---|---|---|---|---|---|---|---|
| Reduction of plantar sensation | 40 patients | 25.3+-3.3 | 70.8+-10.6kg | EMED ST4 platform (Novel GmbH, Munich) | Medial and lateral heel, medial and lateral midfoot, medial, central and lateral forefoot, hallux, 2nd toe and lateral toes | 50 Hz | [152] |
| Parkinson disease (PD) | 6 PD patients and 14 control | PD: 45 to 81<br>Control: 55 to 85 | ------- | Pressure sensors (Nitta Co.) | Spatial-temporal plantar pressure patterns | 60 Hz | [153] |
| Hemiparetic patients (HP) | 18 HP and 111 control | HP: 50.2+-16.4<br>Control:27.2+-8.4 | HP: 175.9+-8.4kg<br>Control:175.5+-8.2kg | Platform EMED-FOI system | Medial, lateral heel, midfoot, hallux, and 1st, 3rd and 5th metatarsal heads | 20 Hz | [154] |

Table VI. Studies and comparisons of plantar pressure distribution

| Study | Sampled population | Age | Mass | Acquisition System | Regions of interest | Sampling Rate | Reference |
|---|---|---|---|---|---|---|---|
| Foot sensitivity between young adults and elderly | 19 young adults and 19 elderly | Young adults: 24.7+-5.8<br>Elderly: 78.6+-4.2 | Young adults: 63.2+-10kg<br>Elderly: 68.8+-9.5kg | Pressure plate Matscan | Forefoot, midfoot, and rear foot | 100 Hz | [155] |
| Compares young school children and adults | 125 children and 111 adults | Boys: 102+-14.3 months<br>Girls: 100+-12.1 months<br>Adults: 27.4+-8.4years | Boys: 30.3+-6.7kg<br>Girls:28.1+-5.3kg<br>Adults: 70.0+-11.8kg | Pressure platform<br>System EMED | Medial and lateral heel; midfoot; 1st, 3rd and 5th metatarsal heads; and hallux | 20 Hz | [156] |
| Compares obese and non-obese adults | 25 obese (O) and non-obese (NO) adults | NO: 48.0+-12.2<br>O: 53.0+-9.5 | Non-obese: 24.0+-3.4kg/m2<br>Obese: 32.2+-2.0kg/m2 | Pressure platform<br>System Mini-EMED | Peak pressure of forefoot, and rear foot. Total plantar force | ----- | [157] |
| Compares obese and non-obese adults | 35 obese (O) and non-obese (NO) adults | Women(N): 35.1+-9.6<br>Women(O): 44.6+-13.5<br>Men(N): 42.3+-11.7<br>Men(O): 42.6+-10.0 | Women (N): 65.7+-10.9kg/m2<br>Women(O): 101.7+-21.2kg/m2<br>Men(N): 83.6+-10.7kg/m2<br>Men(O): 127.2+-22.5kg/m2 | Pressure platform<br>System EMED F01 | Heel, mid-foot, 1st to 5th metatarsal heads, and hallux | 20 Hz | [158] |
| Plantar pressures in visually-impaired individuals | 2 control patients and 3 visually-impaired patients (VIP) | Control: 22 and 21<br>VIP: 17-37 | Control: 62 and 58kg<br>VIP: 60-80kg | In-shoe system pedar-x | Lateral and medial heel; midfoot; lateral and medial forefoot; hallux; lesser toes | 100 Hz | [159] |
| Pressures during walking in older people | 172 older people | 80.0+-6.4 | 26.7+-4.2kg/m2 | Pressure platform<br>System Mat-Scan | 1st to 5th metatarsophalangeal joint, midfoot and heel | 40 Hz | [160] |

### 2.2.2 Automatic plantar pathologies diagnosis

The most commonly used techniques are clustering, artificial neural networks, and fuzzy logic.

*Clustering* is an unsupervised pattern classifications method that uses the existing relationships in the data for creating groups, based on a measure of similarity [161]. In this field, the most common algorithms are Fuzzy C-means and K-means.

Fuzzy c-means is the most common fuzzy clustering technique in data mining. It is based on each object's membership value to determine which cluster belongs to [162]. This technique was used by Wang et al. [163] in the Anterior Cruciate Ligament Deficiency (ACLD) analysis, related to plantar pressure.

K-means is another unsupervised clustering method used to partition a data set into k groups in which each observation belongs to the group whose mean value is the nearest [164]. This technique has been used by many authors as Bennetts et al. [129] to obtain typical local peak plantar pressure distributions. De Cock et al. [165], analyzed the loading patterns during jogging and developed a foot-type classification, Giacomozzi et al. [166], detected gait alterations in rheumatoid arthritis patients. Niemann et al. [167] classified the regional plantar pressure distributions in diabetic patients, as shown in Fig. 12. Deschamps et al. [168], [169] identified patterns of forefoot loading in patients with and without diabetes. In this case, Niemann et al. observed that using four clusters allows for the observation of differences between patients with and without diabetic foot, potentially using its prevention and/or treatment.

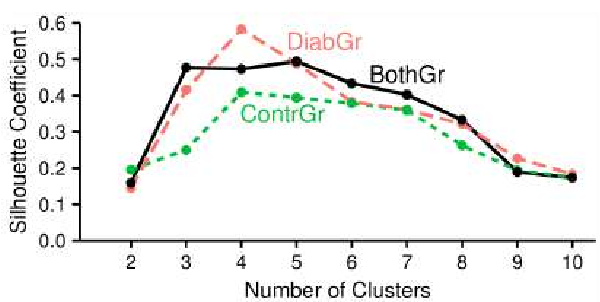


Figure 12. The image is taken from Niemann et al. [167]. The quality of separation between classes based on a number of clusters k set.

*Artificial Neural Networks (ANN)* are another popular technique, which consists of a mathematical representation of the behavior of the human brain, formed by a series of one or more layers of neurons joined by links. The ANNs are widely used in many applications fields [170], specifically in medicine has been applied in medical diagnosis, since through the models generated by the ANNs, it is possible to solve difficult problems when you have a lot of data to analyze.

The technique has been used by Keijsers [171] to classify between patients with and without forefoot pain, based on plantar pressure measurements. Sazonov et al. [172], identified abnormal gait patterns and reduced risk factors. Piecha et al. [173], developed a walk-abnormalities diagnosis system. Oh et al. [174] used an ANN to study the Ground Reaction Force (GRF), helping the farmers that present musculoskeletal disorders caused by harvesting posture. Joo et al. [175], realized a method to predict 6-axis ground reaction forces. Finally, Acharya et al. [176], compared the Gaussian mixture model (GMM) and a four-layer feed-forward neural network to classify between normal, diabetic and neuropathy patients; as a result, they reported that both the ANN and GMM have an accuracy of 86% and 83%, respectively.

*Fuzzy logic* is characterized by the robustness of its interpolative reasoning mechanism. It tries to imitate human reasoning, in the sense of considering all available information to infer using partial truths. The principles of fuzzy logic are simple, and its implementation in software is relatively easy [177], [178]. In this field, there are reported works as Biswas et al. [179], in which they obtained a gait stability index sensitive to the change conditions that induce gait instability. Another work with this approach is reported by Xu et al. [180], they used an adaptive neuro-fuzzy inference system (ANFIS) for gait analyzing with problems of cavus foot and flat foot. The process implemented was gait data measurement, extraction, and selection of features and classification with ANFIS. To train the system, they used 300 training data, 500 training periods, and 81 rules.

*Other algorithms* have been tried to provide more accuracy systems for plantar pressure analysis applied in a different area. Some authors have used techniques like KNN-based classifiers. In Liang et al. [181], they analyzed both gait and balance and classified elderly people with a risk of falling. They compared local mean-based k-nearest neighbor (LMKNN), pseudo-nearest neighbor (PNN), and local mean pseudo-nearest neighbor (LMPNN) classification to obtain the best model. Waldecker [182] utilized logistic regression to classify the patients with risk for foot ulcers. Jeon et al. [183] classified the normal step and the step of Parkinson´s disease patients. They used Principal Component Analysis (PCA) to extract 25 features of gait and Support Vector Machine (SVM) with a radial basis function as kernel function for classifying between types. Goulermas et al. [184], applied various data dimensionality reduction techniques for plantar pressure feature extraction in patients with pathological plantar hyperkeratosis, testing different types of Bayesian classifiers. Crea et al. [185], applied the Hidden Markov Model machine-learning method to detect gait phases based on pressure sensors signals.

Table VII presents an updated summary of the reviewed works about automatic plantar pathologies diagnosis since 1983. The systems developed for medical applications must guarantee optimum performance, but very few algorithms have been applied in this field, as shown in Fig. 13 and as discussed above; there is poor use despite its enormous potential to handle large amounts of data. Mainly the reported developments are focused on using algorithms to partition data and classify between healthy and unhealthy people. The most common algorithms are fuzzy C-means and K-means, followed by ANNs from which researchers have obtained important accurate results. Few reported studies are using fuzzy systems for the analysis of plantar pathologies, becoming a vast area of opportunity, given its operation similar to the human brain. Finally, a representative group is integrated by the KNN, PCA, SVM, Hidden Markov Model, and logistic regression algorithms, with which the researchers have obtained promising conclusions.

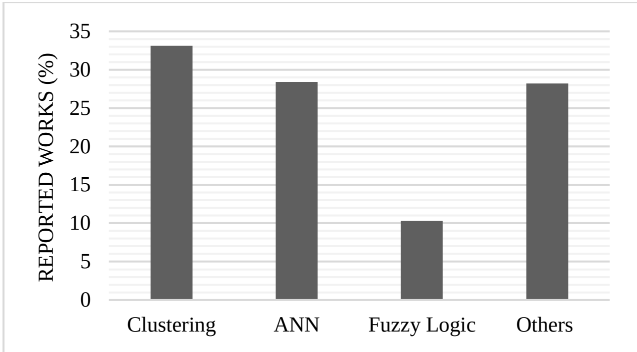


Figure 13. Current use of algorithms for analysis of plantar pressure.

Table VII. Works reported in automatic plantar pathologies diagnosis

| Technique | Author | Application | Acquisition System | Sampled population | Age | Mass | Regions of interest | Sampling Rate | Accuracy |
|---|---|---|---|---|---|---|---|---|---|
| **Fuzzy c-means** | Wang et al. [163] | Anterior cruciate ligament deficiency analysis | Footscan plate | ----- | ----- | ----- | Normal left foot, normal right foot, sick left foot, sick right foot | Walk: 126Hz Run: 500Hz | ----- |
| **K-means** | Bennetts et al. [129] | Typical regional peak plantar pressure distributions | EMED X pressure platform | 819 feet of 438 patients | 59.5+-12.6 | ----- | Hallux, lesser toes (toes2–5), 1st to 5th metatarsal head, midfoot, and heel | 100Hz | ----- |
| | De Cock et al. [165] | Loading patterns during jogging and foot-type classification | Pressure measuring plate RsScan and AMTI force platform | 215 healthy young adults | 18.3+-1.0 | 65.1+-8.6kg | Medial pattern on 2nd metatarsophalangeal, central–lateral pattern central pattern and medial pattern on 1st metatarsophalangeal | 480 Hz | ----- |
| | Giacomozzi et al. [166] | Gait alterations in rheumatoid arthritis | EMED ST-4 pressure platform | 90 rheumatoid arthritis (RA) patients and 30 control patients | RA1: 52.4+-10.3 RA2: 54.2+-10.6 RA3: 58.5+-10.0 Control: 53.2+-12.3 | RA1: 68.5+-11.6kg RA2: 69.7+-12.8 RA3: 75.1+-15.4 Control: 71.5+-14.0 | Peak pressure, peak force, pressure–time integral, force–time integral, duration of stance phase, peak pressure curve, and normalized vertical force curve | 50 Hz | Peak pressure curve: 96.5% Normalized vertical force curve: 96.4% |
| | Niemann et al. [167] | Pressure distributions in diabetic patients | Instrumented insole with 8 sensors | 18 control and 25 diabetics patient | Control: 62.9+-7.6 Diabetic: 64.8+-9.8 | ----- | 1st toe, 1st to 5th metatarsal bone, lateral and calcaneus | ----- | ----- |
| | Deschamps et al. [168], [169] | | Footscan pressure plate | 97 diabetic and 33 control patients | Diabetic: 40-70 Control: 45-70 | Diabetic: 20-40kg/m2 Control:20-40kg/m2 | Hallux, 2nd to 5th toe, 1st to 5th metatarsal heads, midfoot, medial and lateral heel | 200 Hz | ----- |

| | | | | | | | | | |
|---|---|---|---|---|---|---|---|---|---|
| **Artificial Neural Network** | Acharya et al. [176] | Classifier normal, diabetic and neuropathy patients | In-shoe F-Scan system | 63 patients for training and 21 for testing | Control: 14-52<br>Diabetic:32-79<br>Neuropathy:57-84 | Control: 23.52+-4.65kg/m2<br>Diabetic: 26.19+-4.77<br>Neuropathy: 26.12+-4.13kg/m2 | Hallux; 2nd toe; lateral toes; 1st, 2nd and lateral metatarsals; medial and lateral midfoot; medial and lateral heel | ----- | Sensitivity: 100%<br>Specificity: 85% |
| | Keijsers [171] | Classify between patients with and without forefoot pain | Pressure plate Rsscan | 297 patients | Pain: 53+-14<br>No pain: 50+-16 | Pain: 26.0+-4.2kg/m2<br>No pain: 25.7+-4.0kg/m2 | pressure–time integral, mean pressure, and peak pressure | 500 Hz | 70.4% |
| | Sazonov et al. [172] | Identify abnormal gait patterns and reduce risk factors | Instrumented insole with 34 sensors | ----- | ----- | ----- | ----- | 25 Hz | Normal standing: 99.6%<br>Heel dominated standing: 87.6%<br>Normal gait pattern: 92.0%<br>Geriatric gait pattern: 79.5%<br>Forefoot gait pattern: 99.3% |
| | Piecha et al. [173] | Bunion, ischialgia, and paresis | Parotec insole System | ----- | ------ | ------ | 4800 input signals given by the number of steps, feet, sample per step and insole sensors | 300 Hz | 99.9% |
| | Joo et al. [186] | Predict gait speed | Insole Novel Pedar-x system | 20 patients | 24.5+-2.3 | 68.1+-8.9kg | 99 sensors distributed on insole | 100 Hz | Normal walking 96.3%<br>Slow walking 97.8%<br>Fast walking 95% |
| | Joo et al. [175] | | Insole Novel Pedar-x system | 80 patients | 27.9+-7.3 | 65.8+-11.2kg | 3-axis ground reaction force in medial-lateral (GRFML), anterior-posterior (GRFAP) and vertical (GRFV) and 3-axis ground reaction | 100 Hz | Left-foot GRFV, GRMF, GRMT and right-foot GRFAP, GRFML, |

| | | | | | | | | | |
|---|---|---|---|---|---|---|---|---|---|
| | | Predict 6-axis ground reaction forces | | | | | moment in sagittal (GRFS), frontal (GRFF) and transverse (GRFT) | | GRMF, GRMT: 97%<br>left-foot GRFAP, GRFML, GRMS, and right-foot GRFV, GRMS: 98% |
| | Oh et al. [174] | Ground Reaction Force | Insole Novel Pedar-x system<br><br>force plate AMTI | 1 patient | 27 | 68.2kg | Selected 15 and 17 sensors for left and right foot | 100 Hz<br><br>1080 Hz | 80% |
| **Fuzzy Logic** | Biswas et al. [179] | Determine dynamic gait stability index | F-Scan insole | 15 healthy patients | 33.53+-11.85 | 69.21+-11.77kg | Anterior–posterior center of force (CoF) motion, medial–lateral CoF motion, maximum lateral position, cell triggering, stride time, and double support time | 140 Hz | ----- |
| | Xu et al. [180] | Analyze problems of pes cavus and pes planus | Pressure platform | 50 patients, 12 of them with cavus foot and 8 with flat foot | 20-50 | ----- | Staheli Index, Chippaux-Smirak Index, Arch Index and Modified Arch Index | 50 Hz | Normal patients: 96.15%<br>Pes cavus: 92.5%<br>Pes planus: 93.3% |
| **Local mean pseudo-nearest neighbor** | Liang et al. [181] | Analyze the gait and balance to classify elderly people into fallers | Force platform AMTI and MatScan system | 38 patients | 65-84 | 40-90kg | Medial-lateral, anterior-posterior and superior-inferior ground reaction force | ----- | 100% |
| | | | | | | | Time integral forefoot, peak pressure midfoot, pressure time integral heel, and peak pressure heel | | Sensitivity of 73%<br>Specificity of 87% |

| | | | | | | | | | |
|---|---|---|---|---|---|---|---|---|---|
| **Logistic regression** | Waldecker [182] | Classify the patients with risk for foot ulcers | EMED ST 2 Platform systems | Non diabetics: 90 patients; diabetics: 120 patients | ------ | ------ | Peak pressure on metatarsal 4th and 5th, and great toe; pressure time integral on metatarsal 2nd, and 4th; force on metatarsal 4th, force time integral on 2nd toe, and great toe | ----- | Sensitivity of 95% Specificity of 90% |
| **PCA and SVM** | Jeon et al. [183] | Step of Parkinson disease | In-shoe Pedar-X | 21 patients with Parkinson and 17 control | Parkinson: 64.1+-7.34 Control: 62.8+-5.62 | ----- | ----- | ----- | 91.7% |
| **Hidden Markov Model** | Crea et al. [185] | Gait Segmentation Methods | Insole with 64 optoelectronic pressure sensors | 5 patients | 28.8+-3.6 | 72.6+-9.0kg | ----- | 100 Hz | 94.9%-96.8% |

### 2.2.3 Algorithms with potential use

The intelligent algorithms have been tested today with much success in areas such as autonomous vehicles, pattern recognition, speech recognition, and aerospace field, among others [187], [188]. Many researchers have worked with different machine learning algorithms for disease diagnosis, promising to improve the accuracy of perception and diagnosis. In the bio-medical field, the researchers have used different algorithms for many diseases, as is shown in [189], where they obtained promising results. As shown in the previous section, using intelligent algorithms to extract more information from plantar measurement devices and correlate them with pathologies has been low. In the following, we describe the algorithms with potential use in the analysis and diagnosis of plantar pressure, which could help obtain more precise and flexible results.

*Artificial neural networks (ANNs)*

ANNs are widely applied in bio-medicine to solve many non-linear problems by finding a relationship between very complex variables and to converge in a solution. Many works are reported as in [114], [170], [190], [191], where they use different approaches of ANNs to improve the accuracy of predictions. Currently, Deep learning has shown strong potential in the biomedical field. Although it is recent and not thoroughly explored, the main advantage of Deep learning is its ability to learn from the raw data. Conventional methods require sufficient knowledge to extract effective and robust features from data with statistical function and build a prediction or clustering models [191], [192]. The difference with a conventional neural network is its deep architecture, where the number of levels is a free parameter forming multiple levels of data representation.
For developing predictive models using a Deep Learning method, large computing capacity and large databases are needed. Many efforts are made to obtain increasingly efficient computing, perform the many hidden layers' operations, and learn significant abstractions of the data entered in a short time. In the biomedical field, it is possible to obtain large amounts of information from thousands of patients through the different devices of analysis, to detect, diagnose, and monitor patients in different fields of medicine. The authors reported that the deep architectures applied in this field are based on Convolutional Neural Networks, Recurrent Neural Networks, Restricted Boltzmann Machines, and Auto-Encoders [193].

*Fuzzy approach*

Fuzzy logic has an advantage over the previous methods because it does not depend on internal learning parameters as weights and biases or network size, for its performance. Fuzzy logic allows us to reduce the amount of data, facilitating its interpretation and understanding, offering less complexity and faster processing time [194].
The case of Fuzzy-Granular computing is applied in fields like data clustering, machine learning, approximate reasoning, knowledge discovery. In biomedicine have been used by [195], [196]. The principle is to convert the complexity of the problem into computationally simpler algorithms. With this is possible to obtain smaller sub-problems that can be represented by set theory, rough sets and/or fuzzy sets [197], [198].

Fuzzy cognitive maps combine fuzzy logic with cognitive maps theory, obtaining an approach similar to the human decision-making process. They are based on nodes, also known as concepts (states, events, trends, inputs: facts, outputs: decision) that interact with each other. Its interconnections indicate the direction and weight of each relationship. The value for each weight is calculated through inferring from the fuzzy rules that describe the influence between concepts [199], [200]. This method has been used in [201], [202] finding that it is appropriate for support systems in medical diagnosis given its operation similar to human reasoning.
Fuzzy techniques have been well accepted in the medical diagnosis field because the ambiguity and uncertainty are present in real-world knowledge [203]. In many cases, medical diagnoses can be uncertain given the nature of the data, and it is possible to apply methods as fuzzy inference system, fuzzy relation, fuzzy concept lattice [204], intuitionistic fuzzy sets [205], interval type-2 fuzzy [206], among others.

### *Metaheuristic algorithm*

The bio-inspired algorithms have the potential to be applied in the biomedical field. Evolutionary computation is an approach in which researchers have worked to solve complex problems as optimization, automatic programming, circuit design, machine learning, and medicine [207]. The bio-inspired algorithms have the potential to be applied in the biomedical field. Evolutionary computation is an approach in which researchers have worked to solve complex problems as optimization, automatic programming, circuit design, machine learning, and medicine [208]. There are many works reported in medicine that use this algorithm to diagnose Parkinson's disease [209]. In this category, the colony optimization techniques are used to diagnose gastric cancer [210], and pap smear diagnosis [211]. Other techniques that could be applied are particle swarm optimization algorithm, artificial bee colony algorithm, and their hybridizations. These techniques provide ways for solving real-world problems more efficiently and quickly with accuracy [212].

### *Hybrid approach*

Hybrid computational intelligence is an effective combination of intelligent techniques to efficiently solve problems compared with standard intelligent techniques [213]. All computing techniques have different capabilities for different processing phases, from data normalization to decision making. By combining the strengths of the individual components, their performance is enhanced [6]. That is why hybrid approaches are promising, especially in medicine, where many variables have to be taken into account. Hybrid systems must perform better than simple, intelligent approaches, increasing the comprehensibility of the resulting model and improving the speed of the process and the time required to produce a high-performance decision model [213].
There are many works related to this approach in the literature. Table VIII summarizes the reviewed works, where the authors show greater accuracy using hybrid techniques to solve biomedical problems. Hassan et al. [214], used a hybrid genetic algorithm and fuzzy algorithm for the recognition of gait patterns in fall risk patients. They obtained an accuracy of 97.5% with the hybrid genetic algorithm, which is higher than the 89.3% achieved with the fuzzy system.

Table VIII. Some recent works reported using hybridization

| Author | Application | Algorithms | Accuracy |
|---|---|---|---|
| Șahan et al. [215] | Breast cancer diagnosis | Fuzzy-weighting procedure, artificial immune system and k-nearest neighbor | 99.1% |
| Polat et al. [115] | Heart disease diagnosis | Decision tree algorithm, fuzzy weighting pre-processing and artificial immune system | 92.5% |
| Polat et al. [115] | Hepatitis disease diagnosis | Decision tree algorithm, fuzzy weighting pre-processing and artificial immune system | 81.8% |
| Polat et al. [110] | Diabetes disease diagnosis | Principal component analysis and adaptive neuro-fuzzy inference system (ANFIS) | 89.4% |
| Hassan et al. [214] | Falls risk patients | Genetic algorithm and fuzzy set algorithm | 97.5% |
| Parthiban et al. [216] | Heart disease diagnosis | Coactive neuro-fuzzy inference system (CANFIS) | 99.9% |
| Kumar et al. [111] | Diabetes disease diagnosis | Genetic algorithm and perceptron multi-layer Neural Network | 79.1% |
| Martins et al. [217] | Feature selection in walker-assisted gait | Non-dominated sorting genetic algorithm-II and support vector machine | ----- |

Applying different algorithms to solve complex problems with large amounts of data is possible in the current processing speed. Deep learning is a field capable of being applied in the analysis of plantar pressure since it can extract more characteristics from plantar pressure than a human can see. On the other hand, the fuzzy algorithms, given its great capacity to reason similarly to humans, are an advantage to problems where uncertainty and vagueness are handled, as it occasionally happens in medical diagnostic processes. Hybridization is a strategy that brings great advantages to the field of biomedical diagnosis and monitoring, as mentioned. Hybrid systems seek to exploit strong individual components for robust solutions that provide improvements in prediction models reducing the computational cost.

Some of the algorithms that are potential candidates for automating pressure distribution analysis were summarized. We can conclude that the hybrid systems, which include fuzzy concepts, are the most recommended, given their great decision-making capacity similar to humans, by handling uncertain and vague data as it happens in medical diagnosis processes.

# Chapter 3. Plantar Pressure Database Setup

This chapter introduces the steps in obtaining human plantar pressure data using a commercial plantar pressure acquisition platform. The procedure for acquiring and preprocessing these signals is shown, to be used in the classification algorithm and the GUI designed to use the developed system.

## 3.1 Device to Generate the Database

After reviewing the devices for the acquisition of plantar pressure, the main conclusion was that the instrumented insoles are the most flexible and portable system. Still, to build the database, it is easier to use electronic platforms. These devices do not allow portability because of their architecture but are available at many diagnostic centers.

The diagnostic center named PIEDICA located in Mexico City provided us plantar pressure data. PIEDICA Diagnostic Center performs several tests that are applied according to the specific needs of each patient. For this, they use platforms with a density of four sensors per square centimeter (Fig.14), which also has a specialized software (Fig.15) [218].

Figure 14. Baropodometer freeMed [218]

The main features of the acquisition system are resistive pressure sensors with conductive rubber. In configurations up to 40cm per 300cm, durable, compact, ergonomic, and very versatile, it allows a frequency of acquisition of up to 400 Hz in real-time [219]. FreeStep software is a platform for the study of baropodometry, posture, biomechanical analysis, and the patient-space relationship. This software shows both static and dynamic data Fig. 15 and Fig. 16, respectively, and export them to a .scv file for analysis with other methods.

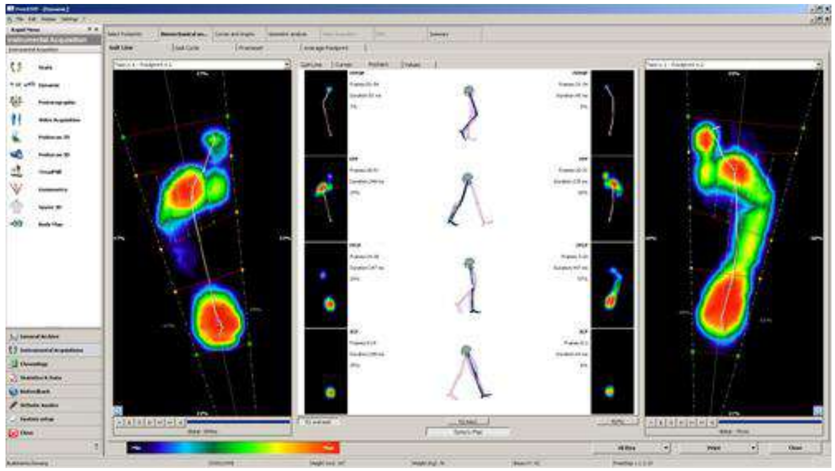

Figure 15. FreeStep software. Static data visualization

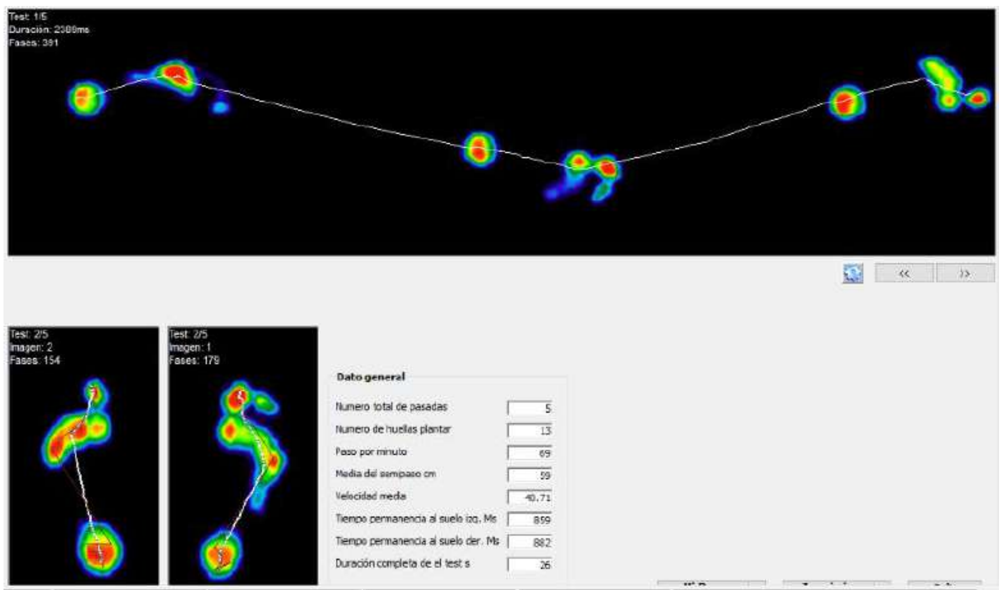


Figure 16. Dyamic data visualization

The diagnostic center provided us the plantar pressure of around 1000 patients with different alterations as cavus foot, flat foot, hallux valgus, fasciitis, spur, among others.

## 3.2 Plantar Pressure Data Extraction

Considering the data distribution in the Excel template generated by the FreeStep software, the process for the extraction of the pressure data is carried out. The exported file by FreeStep software not only has the static and dynamic plantar pressure data, but it also has related data with the height and weight of the patient, and sex. Regardless of the patient, the data is always distributed in the same way within the Excel template. Fig 17. show the data distribution on the template. Data are related to the static plantar pressure of a patient. In this way, it is not comfortable to visualize the static data because each square of the template represents a sensing point of 5x5 mm in the acquisition system.

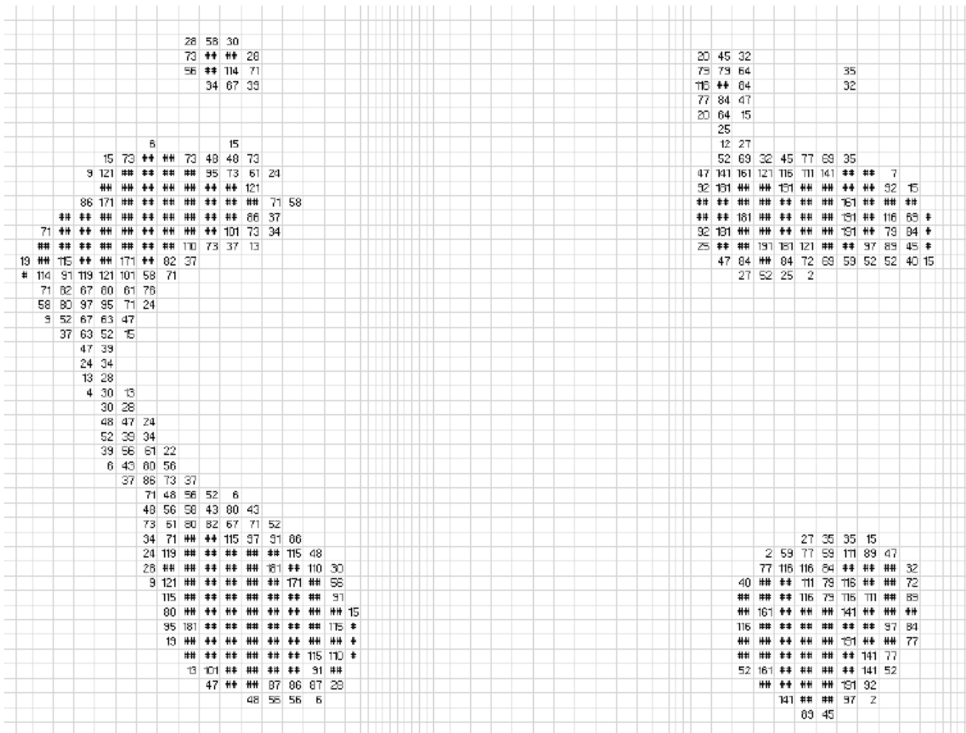

Figure 17. Static plantar pressure data visualized with Excel software

For visualizing in the best way the static and dynamic plantar pressure data, the R software in the Visual Studio framework is used. Visualize the data is very important in this step because it allows confirming that the data were extracted in their entirety. The shapes of the feet were not cut arbitrarily (Fig. 18). The space occupied by static plantar pressure data is always the same; only the amount of these varies according to the size of each patient's foot.

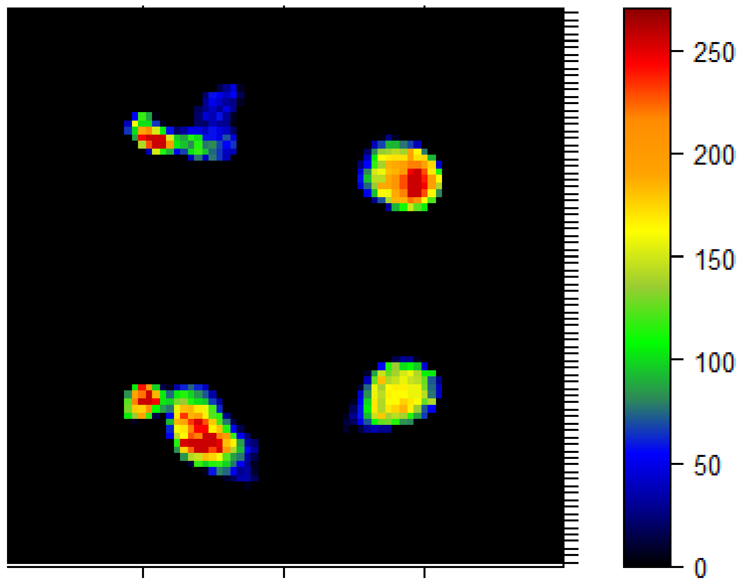


Figure 18. Static plantar pressure data visualized with R software

In this way, now the data are available to use with whatever analysis software and for applying any computational technique for its analysis. Fig 18. shows the static plantar pressure data in levels of colors related to the intensity of each sensing point.

### 3.3 Graphical User Interface (GUI)

A GUI was developed to visualize the plantar pressure of each patient and show the classification result. The development is carried out in the visual study IDE since it presents many advantages of integration with techniques such as databases and the R environment. Fig. 19 shows the GUI's main features, among which are useful for the data extraction and analysis using FCM and features for future use in medical centers for medical decision making.

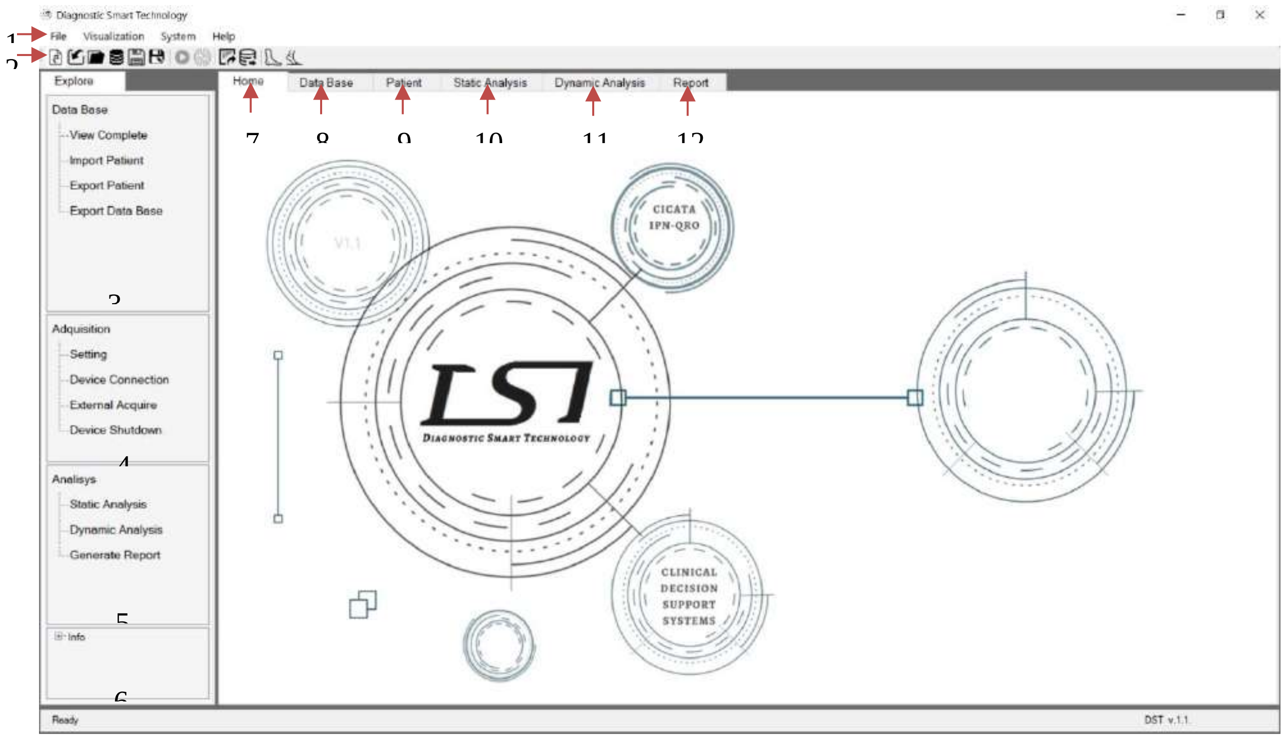


Figure 19. Main window of the GUI

Where:

1. Menu bar
2. Toolbar
3. Database panel
4. Panel of plantar pressure data acquisition
5. Analysis tool panel
6. System information
7.Main window
8. Database management
9. Information of the patient
10. Static analysis of the intelligent algorithm
11. Dynamic analysis of the intelligent algorithm
12. Diagnostic report

The toolbar provides access to all components of the GUI. Button allows creating a new file for a patient, cleaning all the fields of the previous file consulted. Button import a patient file, in this version of the software, the file that can be imported is in the form of the file exported by the FreeStep software from SensorMedica. All open files can be saved for later use, button allows access to the files per patient to re-analyze them or to print a report. With the button it is possible to access all the saved files. Button saves a new file. Button saves changes to a previously saved file. Button extracts all the necessary data from the archive to analyze them and classify the type of foot. Button Analyze the data entered to classify them according to the type of foot. Button export the report for the patient. Button export the entire databases in a .csv file. Button shows static analysis panel. Button shows a dynamic analysis panel.

The panel called *Database* (Fig. 20) contains the tools to import or access patient files with the values of load percentage by area of the foot surface, and additional data such as height, weight, age, shoe size, and sex. As shown in Fig. 20(a), on the right, there is a table with the entire system database and on the left the selected patient information. The buttons allow updating to the database to delete all fields from a previous search, open an existing patient file, export the entire database to a .csv file, save a new patient file, and delete a selected file. Fig. 20(b) shows the panel with the tool to import a new patient file, the button called *File* loads the new file, which is shown in the table below the button.

(a)
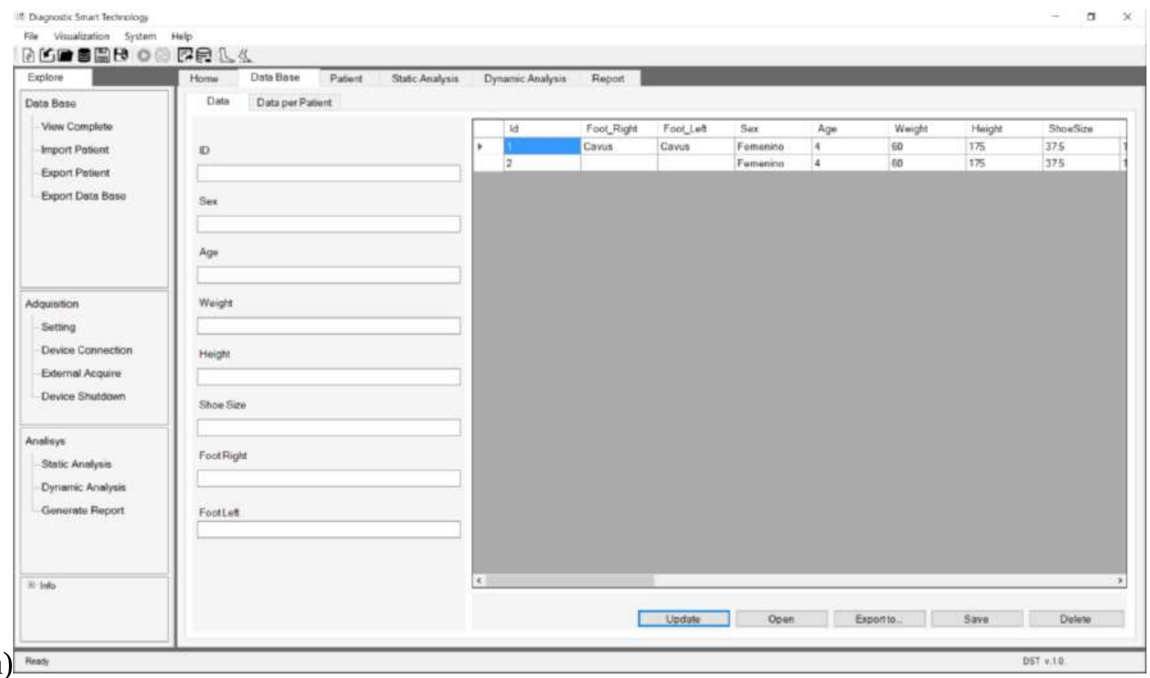

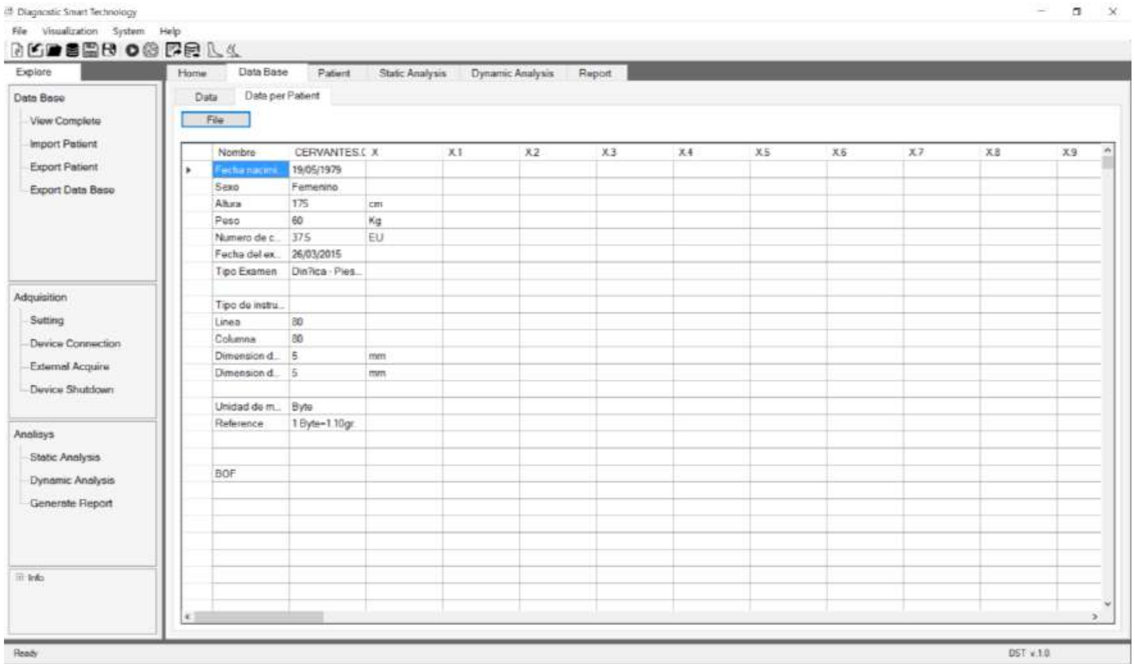

(b)

Figure 20. Data Base panel. (a) Information per selected patient. (b) Visualization of new file imported.

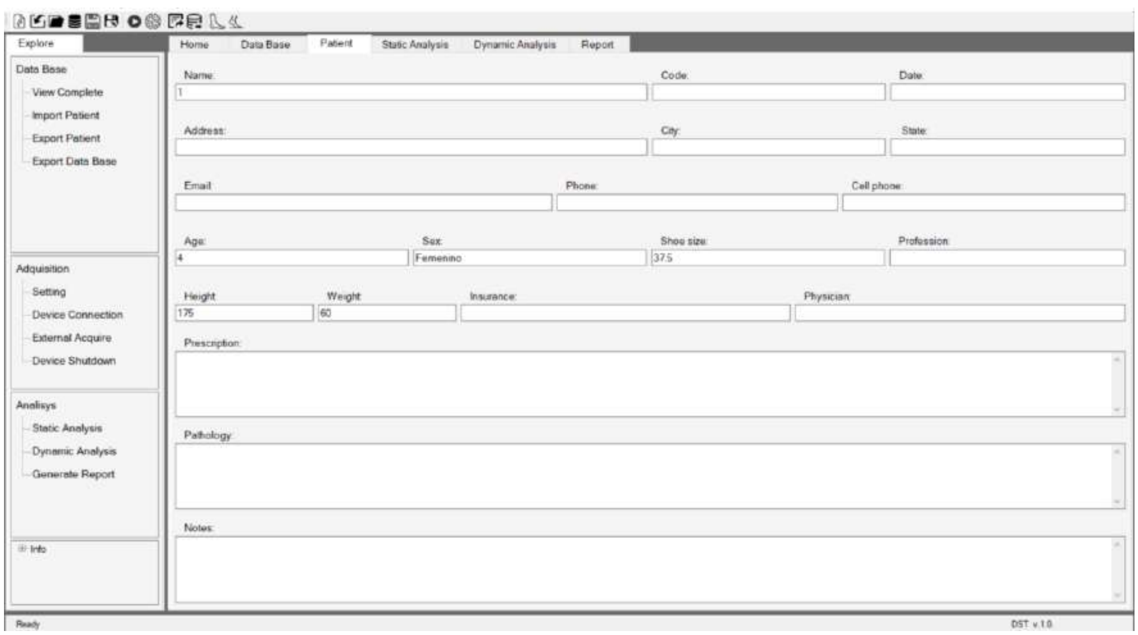


Figure 21. General information of the patient.

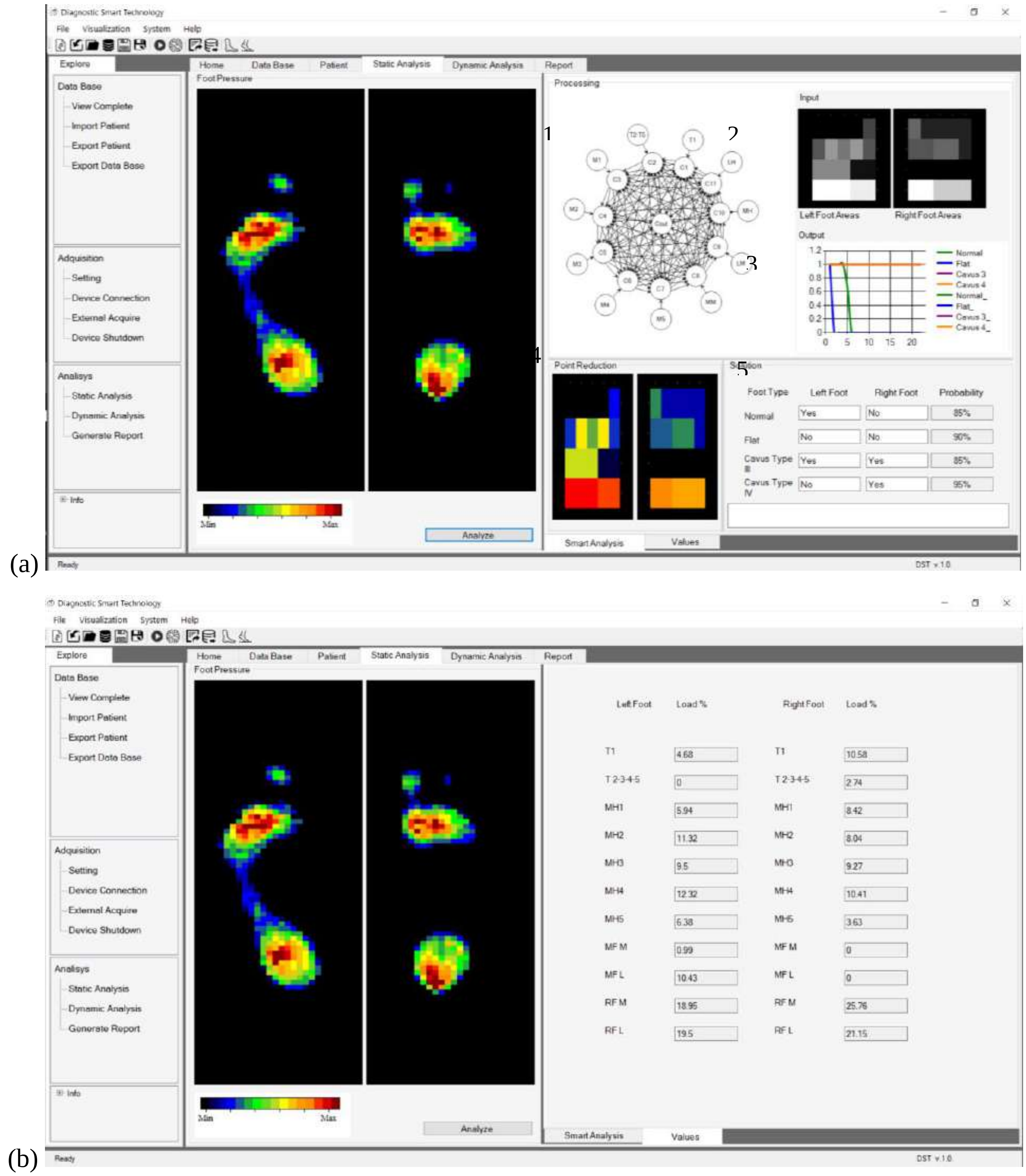


Figure 223. Static analysis panel, all the tools to classify the patient's foot type and visualize the behavior of the system are included. (a) Main analysis panel. (b) Plantar pressure values per area of interest without normalization

The panel shown in Fig. 21 contains the relevant patient information displayed in the previous table, as well as additional patient information and observations that the treating physician deems necessary. This panel was added to the GUI, thinking about in the possible utility in a clinical environment. Only numerical patient information (Plantar pressure data and total patient weight) was necessary for the project. But in a clinical application, contact information, background, insurance data, etc., are needed.

The most important panel of the GUI  presented is shown in Fig. 22. This panel develops the analysis of the data entered. The FCM is activated and generates a classification type alteration report, as well as the simulation performance. Fig. 22(a) the indicators: (1) indicates the configuration of the methodology used for the classification of plantar pressure data. The graph shows the graph of the methodology and how the FCM concepts are related. (2) shows the input data for the classification methodology, since the values must be in the [0-1] range, the figure shows what the system sees to classify, which is the plantar pressure values by areas normalized based on the patient's weight. (3) It shows the FCM simulation's stability graph when it makes the classification decision. If it shows a stable behavior, it means that the system is safe with the decision made. Four lines per foot are showed representing the type of foot that is available to classify (Normal, Flat, Cavo type 3 and Cavo type 4). (4) shows plantar pressure values per area without normalizing. (5) shows the result of the final classification, giving a percentage of probability to each type that can classify. In this way, the system can assist in the diagnosis by the doctor. Fig. 22(b) shows the panel with the numerical data of the load percentages in the areas of interest of the plantar surface.

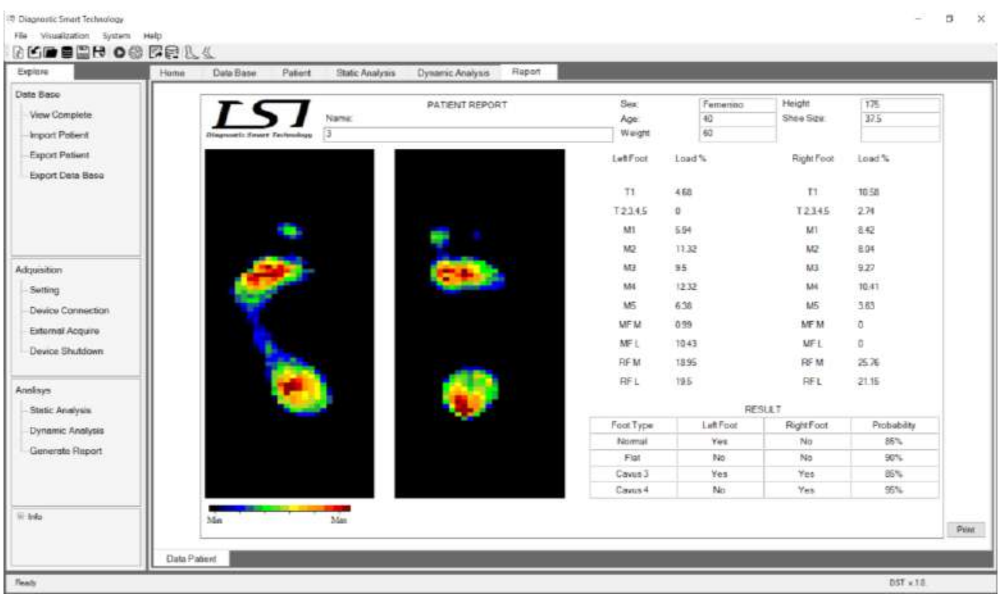


Figure 234.  Report for the patient, contains the input data and the classification result given by the FCM

Fig. 23 shows the final report format for the patient. It includes the graph of the distribution of plantar pressure over the entire plantar surface, the data of the percentage of load by area of interest, relevant personal information, as well as the rates of prediction of plantar alteration found. The file is printed with a .pdf extension and stored in the location that the user wants.

The dynamic analysis panel is not yet available in this version of the software. It can be considered for future work.

### 3.4 System Flow Chart

The system was developed in Visual Studio IDE, integrating SQL to store the database, Window Form for graphic environments, and R for support in extraction, processing, and graphing of plantar pressure data. The flow chart shown in Fig. 24, details the internal operation of the system, the final equations used in the system for plantar pressure data classification are specified in chapter 5 of this document.

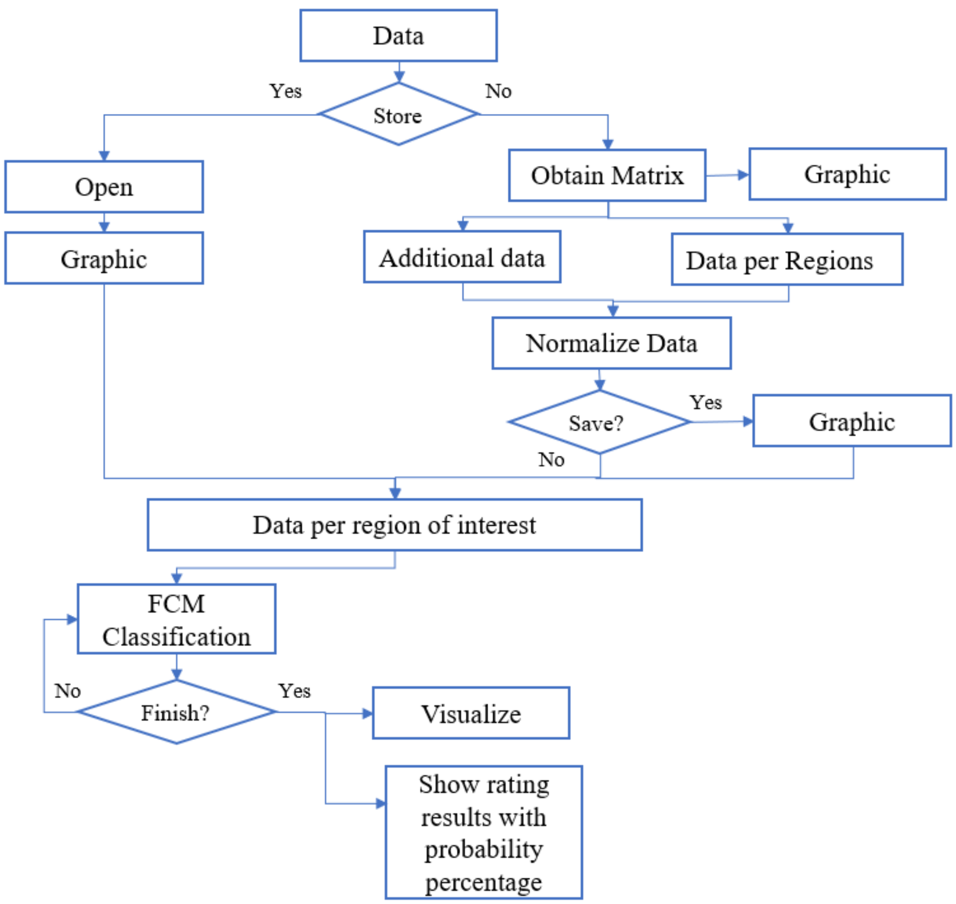


Figure 24. System Flow char

## 3.5 Plantar Pressure Data Sources

The database has two sources. The first set of data was obtained through the database of PIEDICA center, located in Mexico City. The diagnostic center provided us around 1000 plantar pressure data of patients. We observed that only 151 patient data had the appropriate form with the analysis of each of the data. This means that only those patients were diagnosed by qualified medical personnel. The remaining data in this database did not have a label or were empty. To obtain more reliable data through a controlled experiment. We obtain plantar pressure data from the voluntary personnel of the CICATA-IPN Unit Qro. and the Universidad Autónoma de Querétaro, using an electronic platform provided by the PIEDICA center and a medical test protocol (appendix 2.1 y appendix 2.2).

### 3.5.1 Data collection and configuration of plantar pressure values in first experiment

It is used plantar pressure data from the right foot of 151 patients (60% men and 40% women) with flat foot (n=70) and cavus foot (n=81). The initial data classification is carried out by specialized physicians. The age of the patients is between 7 to 77 years-old; their height is between 114 to 196 cm; and their weight was between 17 to 95 Kg. The acquired data was obtained from PIEDICA [218], and was used to test the GA-FCM and MLPNN methodology.

### 3.5.2 Data collection and configuration of plantar pressure values in second experiment

It is used plantar pressure data from the feet of 125 subjects with normal (n=31), cavus type 3 (n=31), cavus type 4 (n=31), and flat foot (n=32) previously diagnosed. The subjects participating in the experiment were 44% women and 56% men with the following features, age between 20 to 68 years-old, height between 150 to 180 cm, and weight between 46.4 to 103 kg. The baropodographic platform was provided by PIEDICA center from Mexico City, which has FreeMed® platforms with an XY resolution of 2.5 dpi and an 8-bit Z resolution [218]..

# Chapter 4. Algorithms and Experiments performed to Classify Plantar Pressure Alterations

This chapter describe the algorithms used for the classification of plantar pressure alterations. Also, it shows the results obtained through two experiments; in the first one, the performance of fuzzy versus non-fuzzy approaches is compared, using small amounts of training data, (appendices 1.3 and 1.4 contain the original documents). The second experiment presents the performance of a modified type II diffuse cognitive map (MFCM-II) trained with the Bacterial Forage Optimization Algorithm (BFOA), (See appendix 1.5).

## 4.1 Fuzzy Cognitive Maps (FCM)

FCM was introduced by Kosko in 1986, and is used for both static and dynamic analysis because of its reasoning approach similar to human reasoning and human decision-making [220]. Specifically, FCM is an artificial neural network represented by a signed fuzzy graph structure with concepts (nodes) and relationships (weighted arcs) [221]. Each concept indicates a key factor of the modeled system, the relationship among themselves is carried out through a weight matrix that indicates the degree of cause and effect. The concepts values ($C_i$) fall within the unit range [0, 1]. The number of connections in the weight matrix ($W_{ij}$) is quadratic in terms of the number of concepts, and the weights assigned to the arcs fall in the range [-1, 1] that indicates the inhibitory or amplification effects [222]. The FCM simulation of the system is carried out by:

$$V_{k(i+1)} = f(W_{(ij)} * V_{k(i)}) \tag{1}$$

Where $V$ represents the current state of concepts, $W$ is the weight matrix that connect the concepts and $f$ is the threshold function that keeps activation values in an allowed range. There are some versions of this function, but the sigmoid function (2) is the most commonly used [220] [223]. The parameter $\lambda$ defines the steepness of the function.

$$\textit{Sigmoid function } f(x) = \frac{1}{1+e^{-\lambda x}} \tag{2}$$

With this structure and some iteration that depends on the study system, the simulation ends up in a fixed-point attractor (which happens when the values of concepts converge to a final stable value), in a limited cycle (which happens when a series of $n$ state concepts appears with a certain pattern but do not converge in a stable state), or the simulation may have a chaotic behavior [222]. When the knowledge to build the weight matrix is not available due to the complexity of the system, the main approach is to compute a weight matrix that fits best with the decision-making and prediction problems. With learning algorithms, the strength connections (weights) between the concepts of FCM can be obtained, as in the case of synapses of neural networks. In most of the studies reported to train FCM, the expert provides the set of concept labels $C$ (input/output), and the matrix $W$ is obtained through a series of historical data [224]–[226]. The most important approaches to get the weight matrix are Hebbian-based, population-based, and hybrid learning [226], [224]. Hebbian-based methods are unsupervised learning algorithms based on the modified Hebbian law and historical data, in which the FCM weights are adjusted in each iteration until they reach the desired structure [225]–[228]. Population-based algorithms like genetic and evolutionary algorithms, particle swarm optimization, bacterial foraging optimization are optimization techniques. These techniques can replace the expert knowledge through historical input data to train FCMs but they have high computation demand [227], [225]. Hybrid approaches combine the two types of learning mentioned above. The main goal of this technique is to improve the resulting outcome based on initial experience and historical data [227], [225].

In the case presented to learn the weight matrix, a genetic algorithm (GA) is used, which has been successfully applied in different learning processes of FCMs [225], [229]. GA is a general-purpose algorithm based on genetic evolution to solve problems, originally presented by Holland in 1975 [230]. In this algorithm, as in real life, the fittest individuals survive and are selected for reproduction to produce improved individuals and the weak individuals disappear [231]. The initial weight matrix generated by GA is random, then GA calculates the next weight matrix using (3) as the objective function.

$$Error = \sum_{i=1}^{n} abs(A_i(t) - A_j^P(t)) + abs(SE(t)) \tag{3}$$

where $n$ is number of output concepts, $A_i(t)$ is output concept values expected, $A_j^P(t)$ is concept values proposed by GA-FCM and $SE(t)$ is the stabilization error of the model to reach a fixed-point attractor.

### 4.2 Fuzzy Cognitive Maps Type-II (FCM-II)

In the FCM Type-II model, the previous value of each concept is considered. In this way, the new value of the concept is calculated through the multiplication of a portion to the state vector and the weight matrix and the adding of a portion of the previous concept value [232]. This formulation is represented by (4) [232].

$$x_i(\mathrm{t}) = f\left[k_1 \sum_{\substack{j=1 \\ j\neq i}}^{n} x_j(t-1)\, W_{ji} + k_2 x_i(t-1)\right] \tag{4}$$

Where $k_1$ expresses the influence [0-1] of the new value in the interconnected concepts, $k_2$ is the portion [0-1] of the previous concept considered and $x_i(t-1)$ is the values of the concept $C_i$ at time $t$-$1$. Initially, $k_1$ is fixed with a higher value, and $k_2$ is fixed with a lower value, but during the training process of the FCM both parameters vary according to the simulated system [232]. Inference rules are applied in the amount of iteration required until the detention criteria are satisfied [222].

## 4.3 Multi-Layer Perceptron Neural Network (MLPNN)

MLPNN is a system of interconnected neurons (except between the nodes in the same layer neurons), through weights and output signals, which are the sum of the input values to each node modified by an activation function nonlinear. This modification is part of the learning process, the widely used algorithm is back-propagation (BP) [233]–[235]. This type of NN is characterized by an input layer, an output layer and may have one or more hidden layers.

The method to establish the number of hidden layer nodes is described in the following equation [234]:

$$N_h = INT\sqrt{N_i * N_o} \tag{5}$$

Where**,** $N_i$ refer to the number of input layer nodes, $N_o$ is the number of output layer nodes, and *INT* function approximate to a next integer.

The main objective of training the neural network is to reduce an error function. This procedure is done by adapting the input and output weights of each neuron. Backpropagation uses the resulting error to modify the weights using a method such as the descending gradient to locate the absolute error in the workspace [233]. The error function used is the sum of squared error (6) or cross entropy (7).

$$E_{sse} = \frac{1}{2}\sum_{l=1}^{L}\sum_{h=1}^{H}(o_{lh} - y_{lh})^2 \tag{6}$$

$$E_{ce} = \frac{1}{2}\sum_{l=1}^{L}\sum_{h=1}^{H}[y_{lh}\log(o_{lh}) + (1 - y_{lh})\log(1 - o_{lh})] \tag{7}$$

Where, $l$ is the index of $L$ observations, $h$ is the index of $H$ output nodes, $o$ is the predicted output and $y$ is the real output.

To find a minimum error the absolute partial derivatives of the error function (6) or (7) are used with respect to weight ($\partial E/\partial w$), when each new weight given by (8) is based on the actual weight $w_k$ [235].

$$w_k^{(t+1)} = w_k^{(1)} - \eta\frac{\partial E^{(t)}}{w_k^{(t)}} \tag{8}$$

where $\eta$ is the learning rate.

## 4.4 Bacterial Foraging Optimization Algorithm (BFOA)

BFOA was proposed by Kevin Passino (2002) to solve numerical optimization problems. This technique is based on mimicking the foraging behavior of *E. coli bacteria*, and it has shown a competitive performance against well-known nature-inspired optimization algorithms [236] [237]. The key idea of BFOA is the application of group foraging strategy of a swarm of *Escherichia coli bacteria* in multi-optimal function optimization. Bacteria search for nutrients in a manner to maximize energy obtained per unit time. There are four main phases in BFOA [238] [239]:

*Chemotaxis*: This process simulates the movements of an *Escherichia coli* cell through swimming and tumbling via flagella. A bacterium may swim for a period in the same direction, or it may tumble and alternate between these two modes of operation for all their life. In computational chemotaxis, the movement of the bacterium may be represented by (9).

$$\theta^{i}(\mathrm{j}+1, \mathrm{k}, \mathrm{l}) = \theta^{i}(\mathrm{j}, \mathrm{k}, \mathrm{l}) + \mathrm{c}(\mathrm{i}) = \frac{\Delta(\mathrm{i})}{\sqrt{\Delta^{T}(\mathrm{i}) * \Delta(\mathrm{i})}} \tag{9}$$

Where Δ is a vector in the random direction whose elements lie in [-1,1], *j-th* is the chemotactic step, *k-th* is the reproduction step, *l-th* is the elimination-dispersal step, *θi(j,k,l)* is the *i-th* bacterium at *j-th* chemotactic and *C(i)* is the size of the step.

*Swarming:* The cell with better environment sends signal to attract others, forming swarm. The cell-to-cell signaling in *Escherichia coli* swarm may be represented by (10).

$$J_{cc}\big(\theta, P(j,k,l)\big) = \sum_{i=1}^{S} J_{cc}\left(\theta, \theta^{i}(j,k,l)\right) =$$

$$= \sum_{i=1}^{S} [-d_{attract} exp^{(-w_{attract} \sum_{m=1}^{P} (\theta_m - \theta_m^i)^2)}] + \sum_{i=1}^{S} [h_{repell} exp^{(-w_{repell} \sum_{m=1}^{P} (\theta_m - \theta_m^i)^2)}] \tag{10}$$

Where *S* is the total number of bacteria, *Jcc (θ, P(j,k))* is the objective function to reduce; *P* is the number of variables to optimize; *T* is the point in the *p-dimensional* search domain; *dattrac*, *wattrac*, *hrepell*, and *wrepell* are coefficients [1,9].

*Reproduction:* Less healthy bacteria die, while each of the fittest bacteria asexually split into two bacteria, which are then placed in the same location, keeping the swarm size constant.

*Elimination and dispersal:* some bacteria are randomly liquidated with a very small probability, while new replacements are randomly initialized in the search space.

## 4.5 First Experiment: GA-FCM against MLPNN

In the first experiment the operation of GA-FCM and MLPNN is tested. To simplify the model, foot surface was divided into 14 areas (toe 1st to 5th (T1–T5), metatarsal joint 1st to 5th (M1–M5), lateral midfoot (LM), medial midfoot (MM), lateral heel (LH), medial heel (MH)), as Fig. 25. reported by [240]. The percentage of weight supported by each area was calculated and then normalized according to the total weight of the patient. In a later step, these areas will represent each input concept in the FCM model and MLPNN.

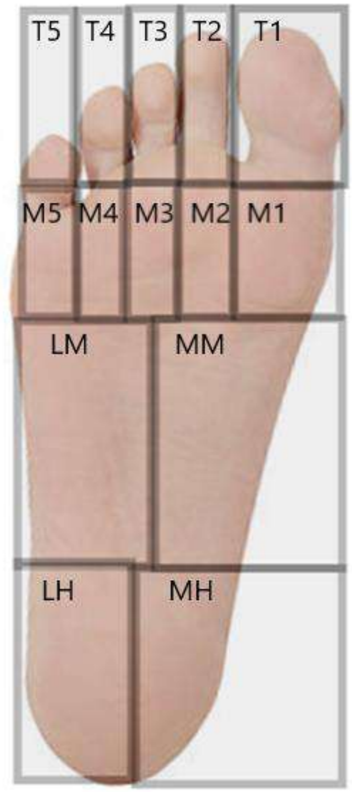


Figure 255. Main regions on the foot surface that reduce the number of sensing points of the acquisition system.

### 4.5.1 GA-FCM method

The concept vector is built with three parts, the first part contains 14 plantar pressure values per area, the second part are 4 intermediate concepts and the last part are 3 output concepts, such as it is shown in Fig. 26. The quantity of intermediate concepts (*IC*) in the second part of the state concept vector is fixed on 4 concepts. This value was obtained after testing 3 to 14 concepts, with 4 being the best value. A three-bit binary combination is proposed for the output concepts in the last part of the state vector concept. With this combination of 3 output concept values, it is possible to classify 8 different foot alterations.

FCM simulation calculates the future states of the system through a series of iterations using (1) and (2). In each iteration, the FCM generates a new state vector that becomes the current state, generating the behavior of the system, which is reflected as one of the three possible states mentioned above. The concept vector is formed as shown in Fig. 27, where values of the input concepts are given by the values of plantar pressure in each normalized region. Data normalization was performed based on the unit, considering the weight of each patient as a reference value. Since the value of intermediate concepts is not known, 0.5 is assumed because it is in the middle of the range of values specified by the FCM methodology (0 to 1). The values of the output concepts are given by the established binary combination, and its initial value is 0.5. In this way, it is expected that for a Flat foot the system will respond as 001 and for a Cavus foot 011 when a fixed-point attractor is reached (Fig. 28).

When FCM simulation converges in a fixed attractor point, the first 14 concepts are the attractor points of each input concept, the next 4 concepts represent the attractor point of each intermediate concept, and the last 3 values represent the value for a specific alteration. Under these conditions, the proposed FCM model is shown in Figure 29.

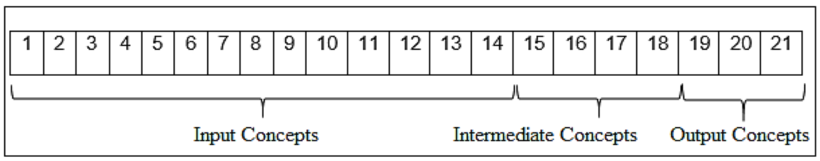


Figure 26. Division of the complete concept vector for the Fuzzy approach methodology

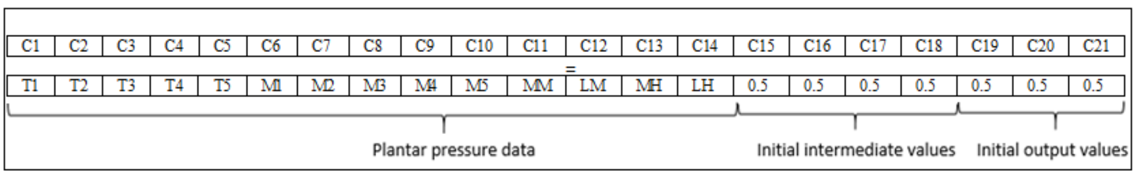


Figure 27. Encoding schema of the initial concepts for FCM-GA methodology

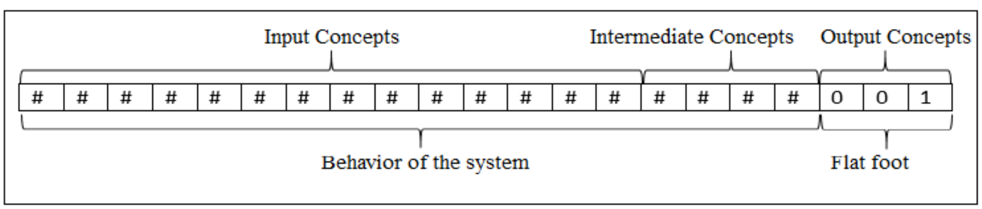


Figure 28. Example of the behavior of the concepts when a fixed attractor point is reached.

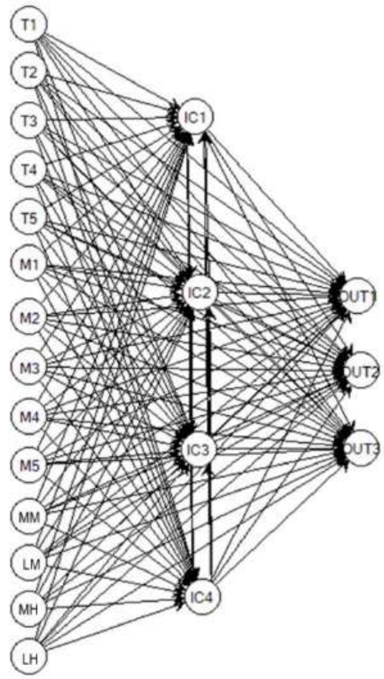


Figure 29. Graph of the proposed FCM, where the circles show concepts and the arrows represent weighted connections. The first layer indicates input concepts, the second layer indicates intermediate concepts and the last layer indicates output concepts.

The Relationships not considered are: between input concepts, from intermediate concepts to input concepts, from output concepts to input concepts, from output concepts to intermediate concepts and between output concepts.

After the above process to arrange the concepts of the state vector, the next step is to solve the FCM weight matrix. The genetic algorithm used in our experiments to obtain the weight matrix has a chromosomal representation, since each value of the weight matrix is a chromosome in the algorithm. It means that in each iteration, GA proposes a new weight matrix that is assessed in the FCM simulation. When an FCM simulator reaches a fixed-point attractor or after a certain number of iterations, the output concepts and the stabilization of the systems is assessed. If the output values in the simulation are the target and the system is stable, the objective function will be zero and the system will stop, but if one of these conditions are not fulfilled, the GA will need to calculate a new weight matrix.

The values of the GA configuration parameters are shown in Table IX, values for the probability of mutation and population size were obtained through tests in a range of 0.009 to 0.050 and 50 to 150, respectively. The encoding gene is composed of 127 values of the matrix of weights and 1 value for the number of iterations. In this way, the genetic algorithm defines when the system is stable for all elements of the training set. The complete algorithm shown in Fig. 30, was implemented in C++ using Visual Studio IDE.

Table IX. Configuration parameters of GA

| **Parameter** | **Factor** |
|---|---|
| Recombination operator | single point |
| Mutation | Random |
| Probability of mutation | 0.009 |
| Population size | 120 |
| Number of genes | 127 |
| Max. number of generations | 5000 |
| Fitness function | (7) |
| Termination method | Maximum iteration |

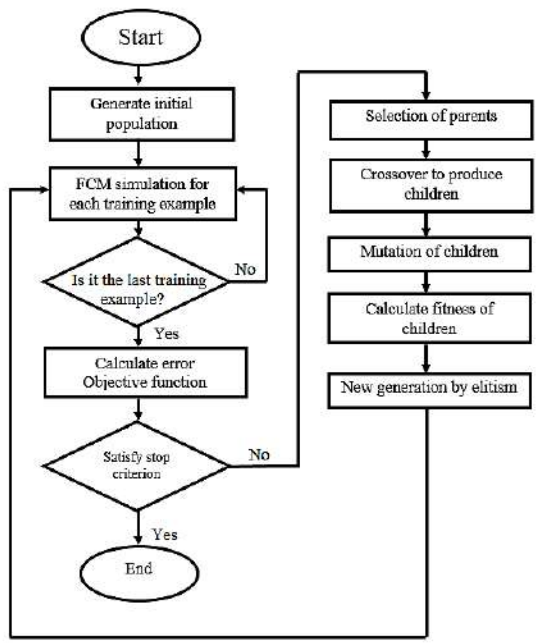


Figure 30. Flowchart describing the GA-FCM methodology.

### 4.5.2 MLPNN method

The input layer nodes of the neural network, as for the GA-FCM method, were given by the regions of interest of the plantar surface. To calculate the number of nodes in the hidden layer is used (5) and the resulting value was 4 nodes. The output layer has only one node, in this way the Flat foot label was coded with 0 and the Cavus foot with 1.

Table X shows the configuration parameters for MLPNN. Considering to keep the same conditions for both methodologies, the parameters were set in the best configuration. Fig. 31 shows the graph of the implemented MLPNN. For the experiment, R software environment was used in the Visual Studio IDE, and the library called NeuralNet.

Table X. Configuration parameters of MLPNN

| Parameter | Value |
|---|---|
| Maximum steps | 100000 |
| Repetitions | 50 |
| Learning rate | 0.5 |
| Training algorithm | Backpropagation |
| Error function | Sum of square errors |
| Activation Function | Logistic |
| Threshold value | 0.01 |

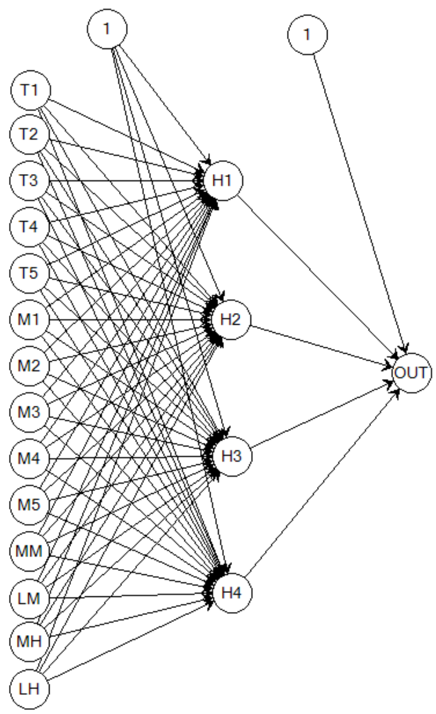


Figure 31. MLPNN chart describing the input layer, a hidden layer, the output layer and biases, the circles show nodes and arrows representing weight connections.

## 4.6 Second Experiment: MFCM-II Method

A modification is carried out to the FCM Type-II in the calculation rule used. Considering a part of the value of the past concept, according to the following equation:

$$x_i(\mathrm{t}) = f[\sum_{\substack{j=1 \\ j\neq i}}^{n} x_j(t-1)\, W_{ji} + k\ (x_i(t-1))] \tag{11}$$

Where k is the portion between 0 to 1of the previous concept that is considered to calculate the new concept value, $x_i(t-1)$ is the value of the concept *Ci* at time *t-1*, $W_{ji}$ is the weight matrix, $x_j(t-1)$ is the value of the concept *Cj* at time *t-1* and *f* is the threshold function (2). To calculate the weight matrix that interconnects the concepts and the steepness parameter in the threshold function, a BFOA and the historical data from 250 feet from 125 subjects with normal, flat, cavus type 3, and cavus type 4 foot, is used.

The use of each resolution point as a concept in the FCM makes the graph complex. For avoiding this condition, the division of the foot surface was used as reported with a small modification [240]. In this experiment, the data from the T2 to T5 were combined, because, the device used does not provide relevant information in these regions, the value merged is denoted by TM. This change generates a less division of the foot surface in just 11 regions (Fig. 32). The data of the regions of interest were obtained through the software of the baropodographic device.


Figure 326. Main regions on the foot surface.

The value of each defined region in the input stage is taken as the percentage load value for each region of the foot, which was normalized according to the unit using the weight of each patient, to establish each value in the range of 0 to 1. The state vector consists of 11 input concepts, and 1 output concept, the initial values of the input concepts are the plantar value of each patient.The initial value of the output concept is 0.5, (Fig. 33) this value is fixed considering the middle of the range than handle the FCM theory.

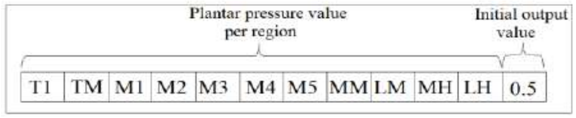


Figure 33. Encoding scheme of concepts

The algorithm used has a bacterium representation in which each one is formed by 132 values that compone the weight matrix, and one value for the steepness parameter (2), the number of iteration and the constant *k* (11). The optimization algorithm in each iteration tries to find the fittest values to reduce the error function (3). This means that the algorithm generates new vales for the next weight matrix and the parameters for performing the FCM simulation, as shown in Fig. 34.

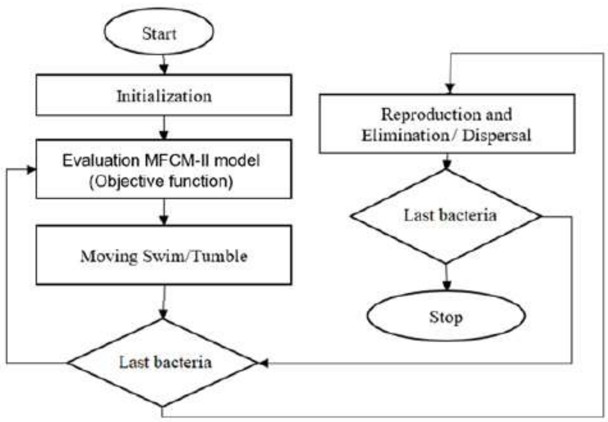


Figure 34. Flowchart describing the BFOA-MFCM-II method

In the processing stage, the input concepts are assumed to have an external input with their weight as [232]. Allowing the input variables to remain unchanged, but each auxiliary concept (representing a region of interest of the plantar surface) may relate to each other to know the behavior of the system (Fig. 35).

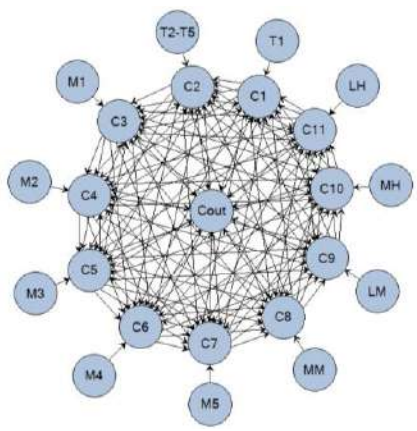


Figure 35. Graph of the MFCM-II proposed. Circles mean concepts, and arrows represent weighted connections.

If the error function (3) is satisfied, taking into account the stability of the system and that the desired output value is very close to the proposed value (±0.01), the values are considered an acceptable solution; otherwise, the algorithm calculates new parameters to be assessed. The set-up values for the BFOA are shown in Table XI.

The output stage was established considering 1 if a specific alteration is true or 0 if it is false, thus classifying the type of foot.

Table XI. Set-up values for the bfoa

| Parameter | Value |
|---|---|
| Population size | 30.0 |
| Number of splits | 15.0 |
| Step size | 0.3 |
| Number of elimination-dispersal events | 20.0 |
| Number of reproduction steps | 10.0 |
| Number of chemotactic steps | 20.0 |
| Swim length | 10.0 |
| Eliminate probability | 0.01 |
| Depth of the attractant | 5.0 |
| Width of the attractant signal | 5.0 |
| Height of the repellant effect | 5.0 |
| Width of the repellant | 10.0 |

### 4.6.1 GA-FCM against MLPNN

A 4-fold cross validation was performed to obtain a reliable result. The folds were obtained using the Caret library of R. In each fold, 90% of the data were chosen for training and 10% for testing. The symmetry between the number of flat foot and cavus foot in each fold was not considered.

In the case of GA-FCM methodology, in each run of the algorithm with the corresponding data, the classification error was adjusted on average to 16.25% of the training data of the 4 folds. The FCM simulation shows a stable response for the classification of alterations that were established. The system response is stable after the tenth iteration for a flat foot (001) and a Cavus foot (011).

As the genetic algorithm calculates the parameter of the number of iterations, the output reached a fixed-point attractor, avoiding the limit cycle and chaotic behavior. The parameter $\lambda$ (2) was chosen using a range of 1 to 10 in 0.1 steps, in which 5 was found as the best value.

The algorithm found the best solution in a different number of iterations for each execution because the data are differents. Table XII shows partial data of the conceptual matrix of the GA-FCM methodology for the training and test fold, where concepts C1 to C14 represent the main regions of the foot considering and concepts C15 to C21 are the intermediate concepts initialized by 0.5. In the table XII, identifiers 1 and 2 are plantar pressure data of patients with a Flat foot and identifiers 3 and 4 represent data of patients with a Cavus foot. To train the system, the algorithm required two files, one corresponding to the plantar pressure data of the patient and another file with the labels corresponding to each alteration. This means that the input data had a corresponding output value, which the genetic algorithm had to adjust. Considering the allowed connection conditions between concepts, the resulting density of the weight matrix is 22.8%.

Table XII. Initial state concept matrix in fold 1. C1 to C14 are normalized plantar pressure values and C15 to C21 are the established initial value

| **Data** | | **Initial Concepts** | | | | | | | | | | | | | | |
|---|---|---|---|---|---|---|---|---|---|---|---|---|---|---|---|---|
| | **ID** | **C1** | **C2** | **C3** | **C4** | **C5** | **C6** | **C7** | **C8** | **C9** | **C10** | **C11** | **C12** | **C13** | **C14** | **C15-C21** |
| **Training** | 1 | 0.040 | 0.006 | 0 | 0 | 0 | 0.046 | 0.127 | 0.167 | 0.150 | 0.046 | 0 | 0.171 | 0.114 | 0.127 | 0.5 |
| | 2 | 0.046 | 0.029 | 0 | 0 | 0 | 0.144 | 0.112 | 0.044 | 0.052 | 0 | 0.255 | 0.064 | 0.155 | 0.094 | 0.5 |
| | 3 | 0.085 | 0 | 0 | 0 | 0 | 0.071 | 0.080 | 0.095 | 0 | 0 | 0 | 0 | 0.316 | 0.350 | 0.5 |
| | 4 | 0.040 | 0 | 0 | 0 | 0 | 0.074 | 0.172 | 0.137 | 0.135 | 0.078 | 0 | 0.008 | 0.195 | 0.155 | 0.5 |
| **Testing** | 1 | 0.035 | 0 | 0 | 0 | 0 | 0.037 | 0.046 | 0.045 | 0.05 | 0.021 | 0.058 | 0.134 | 0.338 | 0.225 | 0.5 |
| | 2 | 0.071 | 0.015 | 0 | 0 | 0 | 0.084 | 0.088 | 0.129 | 0.069 | 0.028 | 0.034 | 0.177 | 0.163 | 0.137 | 0.5 |
| | 3 | 0.113 | 0.008 | 0 | 0 | 0 | 0.206 | 0.132 | 0.123 | 0.139 | 0.042 | 0.023 | 0.055 | 0.110 | 0.044 | 0.5 |
| | 4 | 0.043 | 0 | 0 | 0 | 0 | 0.103 | 0.066 | 0.068 | 0.066 | 0.021 | 0 | 0.034 | 0.250 | 0.345 | 0.5 |

The data sets with which the system was trained produced a matrix of different weights for each case. As an example, Table XIII shows the matrix of weights obtained for the first fold. To carry out the validation, the data were entered without labels. In this way, the score observed in Table XIII was obtained as a result. The identifiers in Table XIII mean the number of each fold used for validation.

Table XII. Weight matrix given by GA in fold 1

| | **C1-14** | **C15** | **C16** | **C17** | **C18** | **C19** | **C20** | **C21** |
|---|---|---|---|---|---|---|---|---|
| **C1** | 0 | -0.64611 | -0.50456 | -0.05734 | -0.81616 | -0.88318 | -0.86792 | 0.291177 |
| **C2** | 0 | 0.256935 | -0.14188 | -0.46574 | 0.793634 | 0.18894 | -0.62676 | 0.712455 |
| **C3** | 0 | 0.757866 | -0.79968 | 0.695303 | 0.210181 | 0.133213 | 0.561449 | 0.277566 |
| **C4** | 0 | 0.348308 | 0.813593 | -0.61968 | 0.80694 | -0.89721 | -0.99408 | -0.54198 |
| **C5** | 0 | -0.03879 | 0.840754 | 0.714103 | -0.47801 | 0.922544 | 0.923093 | 0.291116 |
| **C6** | 0 | -0.84899 | -0.54088 | 0.493332 | -0.67858 | -0.29557 | 0.388897 | 0.522202 |
| **C7** | 0 | -0.61834 | 0.251259 | 0.092746 | 0.147679 | -0.54625 | 0.024323 | 0.898801 |
| **C8** | 0 | -0.58824 | 0.260659 | -0.9234 | 0.102573 | 0.917173 | 0.506394 | -0.48973 |
| **C9** | 0 | 0.573412 | -0.00955 | 0.427168 | 0.052095 | 0.531236 | 0.906186 | -0.66417 |
| **C10** | 0 | -0.71294 | 0.034761 | -0.31382 | 0.72808 | -0.44029 | 0.355937 | 0.627918 |
| **C11** | 0 | 0.077975 | -0.01083 | 0.599231 | -0.17783 | 0.531053 | 0.093478 | 0.871822 |
| **C12** | 0 | 0.892758 | 0.503769 | -0.47264 | 0.067171 | -0.03147 | 0.329691 | -0.54094 |
| **C13** | 0 | -0.90582 | -0.0903 | -0.9118 | 0.492477 | -0.77532 | -0.20469 | -0.85656 |
| **C14** | 0 | 0 | 0.961608 | -0.20823 | -0.32554 | 0.517319 | 0.355754 | -0.64867 |
| **C15** | 0 | 0 | 0.199316 | 0.07242 | -0.68059 | -0.01419 | -0.4782 | -0.369 |

| | | | | | | | | |
|---|---|---|---|---|---|---|---|---|
| **C16** | 0 | 0.977844 | 0 | 0.130284 | -0.98779 | -0.92883 | -0.69939 | 0.676565 |
| **C17** | 0 | 0.472518 | -0.12442 | 0 | -0.10617 | -0.87329 | -0.55449 | -0.71667 |
| **C18** | 0 | -0.52458 | -0.67046 | -0.22935 | 0 | -0.72155 | 0.405927 | 0.394208 |
| **C19-C21** | 0 | 0 | 0 | 0 | 0 | 0 | 0 | 0 |

Density of the model is calculated with (12).

$$Density = \frac{W_{non-zero}}{N^2 - N} \tag{12}$$

Where $W_{non-zero}$ is the weight numbers without including the zero-diagonal and $N$ indicate the number of concepts.

In the case of MLPNN, the training classification error was adjusted on average to 18.25%, as shown in Table XIII. If the neural network is adjusted too close to the training data, the probability of classifying the test data decreases. The classification has a stable response to the established alterations. For the validation process, only the file with the plantar pressure data was required. Table XIV shows the values obtained from the weights of the neural network, including the two biases, with the first set of training data. This matrix was chosen because these values gave the best classification result, as the GA-FCM methodology showed.

Comparing the classification results in Table XIII, close indexes were obtained, where the GA-FCM methodology classify 91.17% and MLPNN 87.29% of the test data on average. To obtain a more detailed analysis of the classification performance for both methodologies, a confusion matrix was made with the results obtained. Table XV shows the average of true positives (TP), false positives (FP), false negatives (FN), and true negatives (TN) of both techniques for the classification of Cavus and Flatfoot. Equations 13 to 15 show the rates computed from the confusion matrices, where:

$$Sensitivity = TP/(TP + FN) \tag{13}$$

$$Specificity = TN/(FP + TN) \tag{14}$$

$$Accuracy = (TP + TN)/(TP + FP + FN + TN) \tag{15}$$

These rates were chosen to obtain the classification results with greater precision and compare the performance of both techniques.

The results are shown in Table XVI, for the average of the test fold. In this table, sensitivity allows the GA-FCM methodology to have a greater capacity to detect plantar alteration in patients who have it.

Through specificity, GA-FCM has more capacity to detect the absence of the specific plantar alteration. And finally, observing the accuracy, GA-FCM has the best proximity of the measurements, with a value of 0.91 against 0.87 of the MLPNN.

Table XIII. Score of each fold for GA-FCM and MLPNN methodologies

| Technique | Fold | Score training data | Score testing data | Average score traning | Average score testing |
|---|---|---|---|---|---|
| **GA-FCM** | 1 | 85% | 100.0% | 83.75% | 91.17% |
| | 2 | 85% | 91.66% | | |
| | 3 | 83% | 83.33% | | |
| | 4 | 82% | 85.71% | | |
| **MLPNN** | 1 | 78% | 100.0% | 81.75% | 87.29% |
| | 2 | 65% | 100.0% | | |
| | 3 | 92% | 77.77% | | |
| | 4 | 92% | 71.42% | | |

Table XIV. Weight matrix of MLPNN in fold 1

| Input Layer | Hidden node 1 | Hidden node 2 | Hidden node 3 | Hidden node 4 | Bias |
|---|---|---|---|---|---|
| **Bias** | 1.01072 | 2.31514 | -1.71659 | -0.65134 | |
| **C1** | 2.76455 | -20.12813 | 68.42477 | -14.40239 | |
| **C2** | 538.88379 | -53.43668 | 7.97747 | -0.96111 | |
| **C3** | -1.70239 | -0.99529 | -1.88439 | -1.14712 | |
| **C4** | -1.09829 | 0.57721 | -0.77540 | -0.30279 | |
| **C5** | 0.06019 | -0.63408 | 0.57891 | 0.41863 | |
| **C6** | 2.96899 | -3.22786 | -103.6708 | 84.97005 | |
| **C7** | 30.22780 | -35.09383 | -93.56199 | 149.93200 | |
| **C8** | 5.47972 | 82.44947 | -26.96725 | 183.36702 | |
| **C9** | 2.83560 | 61.32675 | -37.96629 | -67.05491 | |
| **C10** | -67.92741 | -81.39720 | 43.74652 | -98.45673 | |
| **C11** | -48.15851 | 563.2206 | -20.86826 | -119.2881 | |

| | | | | | |
|---|---|---|---|---|---|
| **C12** | -23.79057 | -19.26990 | -5.57095 | -319.2177 | |
| **C13** | 53.10472 | 44.73620 | 2.65627 | -54.69429 | |
| **C14** | -45.91110 | -43.92571 | -8.04353 | 81.97045 | |
| **Output** | -1.72081 | -1.72081 | 2.19841 | 2.23394 | 0.4994 |

Table XV. Confusion matrix comparison for GA-FCM and MLPNN methods

| | **Predicted Flat foot** | **Predicted Cavus foot** |
|---|---|---|
| | **GA-FCM** | |
| **Real Flat foot** | **6.7** | 0.9 |
| **Real Cavus foot** | 0.4 | **6.3** |
| | **MLPNN** | |
| **Real Flat foot** | **6.1** | 1.5 |
| **Real Cavus foot** | 0.4 | **6.2** |

Table XVI. Validation results in term of sensivity, specifity and accurancy

| **Technique** | **Sensitivity** | **Specificity** | **Accuracy** |
|---|---|---|---|
| **GA-FCM** | 0.94 | 0.87 | 0.91 |
| **MLPNN** | 0.93 | 0.80 | 0.87 |

### 4.6.2 MFCM-II models

Five MFCM-II models were implemented, to obtain one that represents each alteration that was being considered. The independent model can differentiate between what is a specific alteration and what is not. Graphically, the alteration analysis in this study has the structure shown in Fig. 36(a-d). The grayscale images in Fig. 36(e-h) is the view considering the main regions on the surface of the foot. It is clear to note the differences between types, but these conditions may have small variations in all people.

The numerical modifications have the form shown in Table XVII (T1-LH), in which the data were normalized according to the weight of the subject to obtain each of the data in a range of 1 to 0. In the experiment, 5-fold cross-validation was performed to get more consistent results. Each fold has 90% of the data for training and the remaining 10% for testing. The type of alteration was coded to handle it in a computer program. The normal foot is treated as 1, flat foot as 2, cavus foot type 3 as 3, and cavus foot type 4 as 4 (Table XVII).

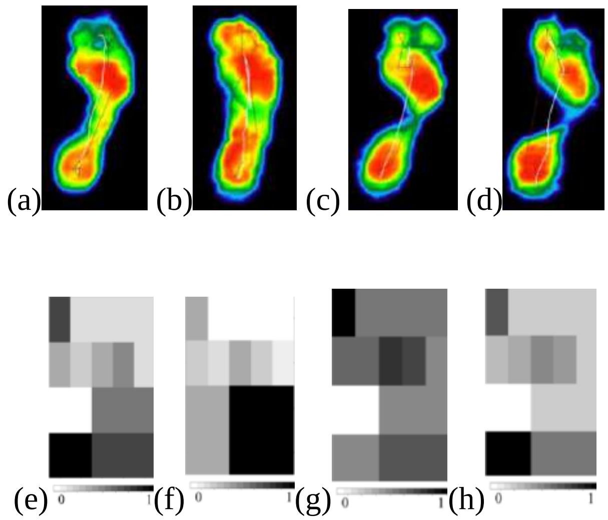

Figure 36. Shape of the foot surface. (a) Normal foot. (b) Flat foot. (c) Cavus foot type 3. (d) Cavus foot type 4. (e) Main regions for normal foot. (f) Main regions for flat foot. (g) Main regions for cavus foot type 3. (h) Main regions for cavus foot type 4.

Table XVII. Initial state concept vector

| Alteration | Normalized Values | | | | | | | | | | | | |
|---|---|---|---|---|---|---|---|---|---|---|---|---|---|
| ID | T1 | TM | M1 | M2 | M3 | M4 | M5 | MM | LM | MH | LH | AC | Cout |
| | C0.1 | C0.2 | C0.3 | C0.4 | C0.5 | C0.6 | C0.7 | C0.8 | C0.9 | C0.10 | C0.11 | C1-11 | C12 |
| 1 | 0.142 | 0.049 | 0.065 | 0.079 | 0.109 | 0.100 | 0.049 | 0.023 | 0.050 | 0.204 | 0.120 | 0.5 | 0.5 |
| 2 | 0.153 | 0.081 | 0.095 | 0.097 | 0.126 | 0.114 | 0.072 | 0.006 | 0.071 | 0.079 | 0.101 | 0.5 | 0.5 |
| 3 | 0.085 | 0.045 | 0.054 | 0.110 | 0.128 | 0.095 | 0.049 | 0.024 | 0.100 | 0.168 | 0.130 | 0.5 | 0.5 |
| 4 | 0.1422 | 0.049 | 0.065 | 0.079 | 0.109 | 0.100 | 0.049 | 0.023 | 0.050 | 0.204 | 0.120 | 0.5 | 0.5 |

The weight matrices required by the proposed model and produced by BFOA have a density of 24.95%, which means that on all possible connections, 75.05% was not used, to obtain a simpler graph. The model representing each alteration has a different weight matrix, so four weight matrices were obtained that show the behavior of each system.

During the MFCM-II simulation, the relationship between concepts produces a behavior between interest areas, which change until the MFCM-II simulation reaches a fixed-point attractor. This different behavior for each model allows knowing which were the areas of interest that at the time of the simulation considered to converge on the expected result, as it is shown in Fig. 37. This figure shows the behavior of the system when the alteration is present and when it is not present.

In the classification results, the MFCM-II simulation reached a fixed-point attractor. Fig 38. shows the stabilization behavior of the output concepts for all the alterations considered in this study, after 12th iterations, the system achieves the stability that allows obtaining the expected result and observing the behavior between the concepts.

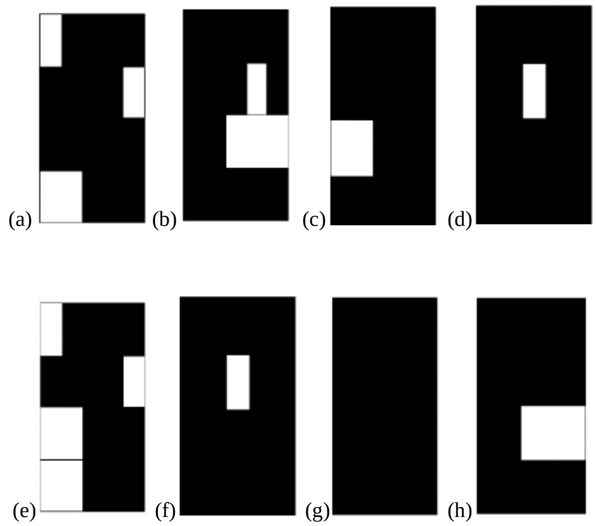


Figure 37. Behavior of the concepts when a fixed-point attractor is reached. (a) Flat foot detected. (b) Cavus foot type 4 detected. (c) Cavus foot type 3 detected. (d) Normal foot detected. (e) Non-Flat foot detected. (f) Non-Cavus foot type 4 detected. (g) Non-Cavus foot type 3 detected. (h) Non-normal foot detected.

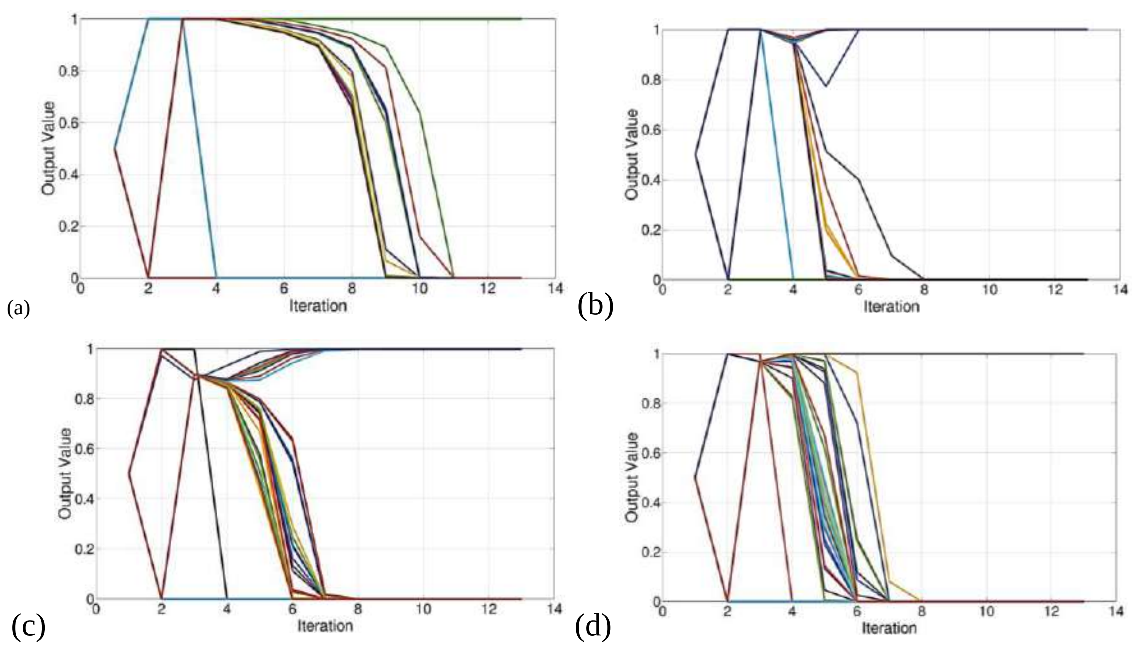


Figure 38. Subsequent values of output concepts till convergence for all the models in fold 1. (a) Normal foot. (b) Flat foot. (c) Cavus foot type 3. (d) Cavus foot type 4.

Parameter $\lambda$ (2), and the number of state vectors were chosen by the optimization algorithm that allows the output to reach a fixed-point attractor efficiently before the *12th* iteration for alteration (1) and non-alteration (0) avoiding limit cycle and chaotic behavior. The simulation of the FCM for normal foot requires more iterations to reach a fixed-point, while the simulations for the remaining alterations, reach stability before the *9th* iteration. The result is because the relationship between the regions is closer and difficult to find. For each model, the algorithm found the best solution with different parameters in terms of the weight matrix, parameter $\lambda$ (2), and constant $k$ (11).

Table XVIII shows the results of the classification of the system in each fold. The identifiers mean the number of each fold used for validation. The classification error rate with the training data was adjusted around 10% for all the alterations and folds used, as shown in Table XVIII. The probability that the system could correctly classify the test data for each model was adjusted by 89% on average.

The confusion matrices were made to obtain a more detailed result of the performance in the classification task with the proposed method. Table XIX shows the average of TP, FP, FN, and TN for the classification of Normal foot, Flat foot, Cavus foot type 3 and Cavus foot type 4. Through each confusion matrix, equations 13 to 15 showing the sensitivity, specificity, and precision of the models were calculated. Table XX shows the calculated results for the average of the test fold for each alteration.

The BFOA-MFCM-II methodology has a high capacity to detect alterations with a sensitivity value around 0.93, but the capacity to detect the absence of a specific plantar alteration is lower with a specificity value around of 0.80, as shown in Table XX. The accuracy of the methodology applied has a value of 0.84 on average, considering that the methodology is not a black box; it has good proximity to the measurements.

Table XVIII. Score of each fold for classify between alterations

| Type of foot | Fold | Score testing data | Average score testing | Average score training |
|---|---|---|---|---|
| Normal vs non-normal foot | 1 | 86.6% | 83.7% | 85% |
| | 2 | 80.6% | | |
| | 3 | 84.3% | | |
| | 4 | 80.4% | | |
| | 5 | 86.6% | | |
| Flat vs non-flat foot | 1 | 91.1% | | |
| | 2 | 93.5% | | |

| | | | | |
|---|---|---|---|---|
| | 3 | 96.8% | 90.7% | 90% |
| | 4 | 90.2% | | |
| | 5 | 82.5% | | |
| Cavus foot type 3 vs non-cavus foot type 3 | 1 | 88.8% | 84.1% | 85% |
| | 2 | 80.6% | | |
| | 3 | 81.2% | | |
| | 4 | 80.4% | | |
| | 5 | 89.4% | | |
| Cavus foot type 4 vs non-cavus foot type 4 | 1 | 91.1% | 96.5% | 95% |
| | 2 | 100% | | |
| | 3 | 93.7% | | |
| | 4 | 100% | | |
| | 5 | 97.7% | | |

Table XIX. Confusion matrices for each model obtained with the bfoa-mfcm-ii methodology

| | Normal foot | |
|---|---|---|
| | Predicted normal foot | Predicted non-normal foot |
| Real normal foot | 10.6 | 1.6 |
| Real non-normal foot | 6 | 22.4 |
| | Flat foot | |
| | Predicted flat foot | Predicted non-flat foot |
| Real flat foot | 8.6 | 0.4 |
| Real non-flat foot | 5 | 26.6 |
| | Cavus type foot 3 | |
| | Predicted cavus foot type 3 | Predicted non-cavus foot type 3 |
| Real cavus foot type 3 | 8.6 | 0.8 |

| | | |
|---|---|---|
| Real non-cavus foot type 3 | 7.6 | 24 |
| | Cavus foot type 4 | |
| | Predicted cavus foot type 4 | Predicted non-cavus foot type 4 |
| Real cavus foot type 4 | 9.6 | 0 |
| Real non-cavus foot type 4 | 3 | 27.2 |

Table XX. Validation results in term of sensivity, specifity and accurancy

| Type of Foot | Sensitivity | Specificity | Accuracy |
|---|---|---|---|
| Normal foot | 0.86 | 0.78 | 0.81 |
| Flat foot | 0.95 | 0.84 | 0.86 |
| Cavus foot type 3 | 0.91 | 0.76 | 0.74 |
| Cavus foot type 4 | 1 | 0.78 | 0.92 |

### 4.7 Discussion of results obtained with different methods

Diagnosing or detecting disorders are essential challenges. Using effective, efficient computerized knowledge systems, it is possible to include recommendations for treatment, prescribe preventive health tasks, and improve people's quality of life [240][119]. Studies to treat or detect different diseases with promising results have been reported [241][242]. On the biomedical field, plantar pressure through static and dynamic measurements allows for understanding the human foot's mechanical behavior for detecting, monitoring, and treating many other diseases reflected in the abnormal distribution of loads. Abnormal foot posture (flat foot or cavus foot) has been associated with lower limb injuries, such as patellofemoral joint pain, medial tibial stress syndrome, Achilles tendinopathy, patellar tendinopathy, plantar fasciitis, medial midfoot arthritis, and posterior tibial tendon dysfunction [243]–[246]. A deeper researcher is needed, for a deeper analysis of plantar information correlated with alterations to improve therapeutic or surgical strategies for patients and obtain more efficient support systems [247][245][248], in [240] the different techniques used to detect diabetic foot, orthopedic alterations, plantar hyperkeratosis, among others, are reported.

Despite, pressure platforms are restricted to be used in laboratories by its structure made of a flat and a rigid array of pressure sensing elements embedded in the ground. Platforms can be used for dynamic and static studies easily. The appropriate cost-resolution relationship allows carrying out different studies as presented. The resolution of the pressure platforms produces large amounts of data by the sensing points. In the specific device used provided by Piedica, the tool produces an average of 450 detection points per foot, producing a complex graph. For simplifying the model, the first experiment foot surface was divided into 14 areas (toe 1st to 5th, metatarsal joint 1st to 5th, lateral midfoot, medial midfoot, lateral heel, medial heel). In the second experiment, the foot surface was divided into 11 areas (toe 1st, toe 2nd to 5th, metatarsal joint 1st to 5th, lateral midfoot, medial midfoot, lateral heel, medial heel) as reported. This division of the foot surface provides efficient and precise plantar pressure measurements without losing information because these areas support body weight and adjust the balance. This information may be analyzed to identify patterns and correlate them with medical diseases. Nevertheless, analyze this data requires efficient techniques to deal with the inaccuracy, vagueness, and uncertainty present in medical and biological data [249][250]. In addition, these systems should be easy to interpret, where the same prediction model may clearly explain the results.

Traditional classifiers, such as neural networks, have higher prediction rates but are considered black-boxes, in which each node has no meaning related to the problem, making it difficult to interpret the results [251][249]. Fuzzy Cognitive Maps (FCM) have proven to overcome those difficulties because they are a useful tool to design knowledge-based systems that behave like human reasoning, giving interpretability to their network. In an FCM, each node represents a specific variable that models the problem, resulting in versatile models that help to explain the solution [252][253][254]. Different proposals to calculate the rule of Fuzzy Cognitive Maps have been reported [232][255], in addition to being used for modeling complex systems, including medical decision support systems [252][256][257][258].

### 4.7.1 Specific discussion from first experiment

In the classification task, the performance of the Fuzzy approach was compared against a non-Fuzzy approach, specifically an MLPNN for finding the best methodology for classification using small amounts of data. The results obtained show a better performance of the Fuzzy approach, improving the classification score by 4%. The GA-FCM methodology can detect 94% of patients who have the alteration, and can detect 87% of patients who do not actually have it (considering the confusion matrix).

Reported indexes have between 80% and 94% of accuracy in the classification of alterations and have been obtained handling both different complexities in the systems and the different number of interest areas [180] [176] [180]. The work that shows the highest classification score was developed applying Adaptive Neuro-Fuzzy Inference System (ANFIS), but it has a complex architecture (software or hardware), with at least 162 nodes. Otherwise, the GA-FCM methodology shows an apparent advantage being one of the highest classification indexes with a simple and understandable architecture of 21 nodes and direct data from the most representative areas that provide reliable information about the load distribution on the human foot surface.

FCM achieves better performance compared to MLPNN since fuzzy models handle uncertainty better because human behavior is considered and can work with limited amounts of data. On the other hand, MLPNN needs training samples that are large and representative enough to avoid possible over-fitting. In addition, the results are difficult to interpret because each node does not have a meaning related to the problem.

Although the GA-FCM methodology achieved 91% accuracy, the knowledge produced by the database used is not enough for decision support in actual clinical practice. Future work should focus on building a complete database of plantar pressure and integrating more sources of knowledge. In addition, the adaptation of the weight matrix of the FCM can be improved by applying other methods such as unsupervised learning based on the Hebbian method, supervised with the use of Bacterial Evolutionary Algorithms (BEA) and/or gradient-based methods.

### 4.7.2 Specific discussion from second experiment

In the presented model, each node has a specific meaning that represents the interest areas of the foot surface. To evaluate the methodology, two physicians classified a sample of 50 patient data from the same database, and their classification result was compared. In this way, physicians agree 60% in the classification of the normal foot, 75% in flat foot, 50% in cavus foot type 3, and 25% in cavus foot type 4. Each physician classified the different types of the foot according to their criteria by viewing images with pressure levels as in Fig. 46(a-d). This is not an easy classification task since confusion may occur when the plantar pressure levels of a subject resemble the two-foot types, it should be taken into account that basic alterations were used, such as a flat foot and not combinations, for example flat-valgus foot.

Authors as [180], [176] have applied different techniques to use plantar pressure information to detect alterations and provide physicians with useful analysis tools. Table XXI shows a comparison of previous studies using fuzzy and non-fuzzy approaches for the classification of plantar foot alterations.

The proposed methodology shows a high classification score when the classification is evident, as is the case of differentiating between what is a flat foot and what is not, and between what is a cavus foot type 4 and what is not is. In these cases, it was possible to achieve up to 100% success in the classification. By including more classes, the ranking score decreases because it becomes more difficult to find the pattern because the differences that identify them are more subtle.

Table XXI. Classification of plantar foot alterations by different approaches

| Technique | Reference | Classification task | Number of patients | Parameters of interest | Simplicity of the model | Classification rate |
|---|---|---|---|---|---|---|
| ANFIS | [180] | Classifies between normal, flat and cavus foot | 50 | Staheli Index (SI), Chippaux-Smirak Index (CSI), Arch Index (AI) and Modified Arch Index (MAI). | 81 Fuzzy rules | 93.9% |
| BP Neural Network | | | | | ------- | 84.0% |

| | | | | | | |
|---|---|---|---|---|---|---|
| BP Neural Network | [176] | Classifies between normal, diabetic Type 2 with and without neuropathy patients | 84 | Toe 1st (T1), toe 2nd (T2), toe 3rd to 5th (T3–T5), metatarsal joint 1s (M1), metatarsal joint 2nd (M2), metatarsal joint 3rd to 5th (M3–M5), lateral midfoot (LM), medial midfoot (MM), lateral heel (LH), medial heel (MH). | 20 nodes | 90.4% |
| GMM | | | | | ------- | 80.9% |
| GA-FCM | Applied model | Classifies between flat and cavus foot | Right foot of 151 patients | Toe 1st, to toe 5th (T1–T5), metatarsal joint 1st to 5th (M1–M5), lateral midfoot (LM), medial midfoot (MM), lateral heel (LH), medial heel (MH). | 21 nodes | 91.17% |
| MLPNN | Applied model | Classifies between flat and cavus foot | Right foot of 151 patients | Toe 1st, to toe 5th (T1–T5), metatarsal joint 1st to 5th (M1–M5), lateral midfoot (LM), medial midfoot (MM), lateral heel (LH), medial heel (MH). | 21 nodes | 87.29% |
| BFOA-MFCM-II | Applied model | Classifies between normal, flat, cavus type 3 and cavus type 4 foot | 250 feet of 125 patients | Toe 1st, toe 2nd to 5th (T2–T5), metatarsal joint 1st to 5th (M1–M5), lateral midfoot (LM), medial midfoot (MM), lateral heel (LH), medial heel (MH). | 23 nodes | 89% |
| Classification by physicians | Applied method | Classifies between normal, flat, cavus type 3 and cavus type 4 foot | 100 feet of 50 patients | Toe 1st, toe 2nd to 5th (T2–T5), metatarsal joint 1st to 5th (M1–M5), lateral midfoot (LM), medial midfoot (MM), lateral heel (LH), medial heel (MH). | ------ | 52.5% |

The BFOA-MFCM-II methodology, which considers the past of the concept, proved to be more efficient in the classification task of plantar pressures. Besides, it was possible to eliminate the black boxes of the model, since each concept has a definite meaning. It is possible to see each one's behavior to converge to a solution. In this sense, to improve the classification results of plantar alterations with very sensitive patterns, more concepts should be considered. One option is to divide the surface of the foot into more areas, and another option is to consider postural Inputs such as in ankles: dorsal/plantar flexion, inversion/eversion, internal/external rotation; in knees: flexion/extension, valgus/varus, internal/external rotation; in hips: flexion/extension, adduction/abduction and in foot internal/external rotation. These variables also make the classification of plantar alterations more precise and efficient, since not only the plantar pressure variables but also the postural variables of the patients would be considered.

# Chapter 5. Conclusion and final remarks

## 5.1 Conclusion

In the review of the literature carried out in this research, it was evident the work that different authors in different universities around the world are doing to obtain models and systems that can be applied to the detection of plantar foot alterations using data from electronic devices of acquisition. In addition to algorithms to analyze plantar pressure data, the development of electronic devices has been a relevant issue, as shown in the review. The most used tools to acquire pressure information on the surface of the foot are electronic insoles and baropodometers, the first being the most flexible for use, but the second most used in research by the adequate resolution-costs relationship.

Dividing the surface of the foot by regions and considering the load percentages in each one, makes the analysis of the information more efficient, as reported. This strategy provides efficient and accurate plantar pressure measurements without losing information because these areas support body weight and adjust balance. On the other hand, the graph obtained is simple to interpret and use with the methodologies.

Methodology FCM with GA proved to be better than MLPNN in the classification with small amounts of patient plantar pressure data. Although the system is not over-fitted, the learning method must be improved to reduce convergence time. The final model is easy to understand, with 21 total nodes divided as follows: 14 nodes representing each region of interest of the plantar surface; 4 intermediate nodes proposed as a hidden layer and 3 output nodes for the binary combination established by the classification between flat and cavus foot.

MFCM-II with BFOA proves to be a useful methodology, because through a simple structure, easy to understand and by using an effective decision-making mechanism similar to that of humans. It is possible to classify the plantar pressure data and know the interaction between regions, which the system considered to achieve the result. On the other hand, the response of the system is stable and achieved with few iterations, where this number of iterations varies when it is more difficult to find the pattern that represents. It has a low computational cost with 11 input nodes representing each interest region of the plantar surface, depending on the percentage of the load. Plus 11 auxiliary nodes proposed to improve the performance of the graph and observe the relationship between the concepts of input, and an output node, removing black boxes.

The support system for the detection of alterations in the human footprint using plantar The support system for the detection of alterations in the human footprint using plantar pressures, proved to be a useful tool, as shown in Chapter 7, due to the complexity and decision-making based on the criteria of each specialist, low ranking rates may be obtained. With the system, it was possible to get high rates in the classification task. It can be improved using the knowledge of many physicians in the training process to achieve results with the least possible bias. During the development of the investigation, it was evidenced that for obtaining a more generalized model, more population with similar morphological characteristics of other countries must be included to get results that may be applicable and scalable in other places. The GUI has the necessary functionalities to work stably in real environments. Through different methods, the GUI can receive plantar pressure data from new patients, analyze them with the MFCM-II methodology, and print a classification result with graphic information related to plantar pressures entered.

## 5.2 Final remarks

Currently, the development of plantar pressure acquisition systems is an activity that works in both academic and commercial settings. The academic developments have the disadvantage that they are built specifically for a particular application; on the other hand, commercial developments have a high economic cost. I recommend designing and building the own plantar pressure acquisition system (electronic platform or template system). The thesis presented has all the necessary information regarding the requirement to build it and would bring many benefits for future research in this area.

The methodology showed good results to classify planting alternations pressure, but to improve outcomes in future work should consider two fundamental aspects. First, increasing the sample size of the study subjects, including populations from other countries with similar morphological characteristics. And second, to use a larger group of specialists. With these considerations, it will be possible to get a more general model of plantar foot alterations with the least bias.

I recommend to analyze the relationship between body posture and foot changes. The classification of plantar alterations is more precise and efficient, when considering postural variables such as: inversion/eversion and internal/external rotation, in the ankles; flexion/extension, valgus/varus, internal/external rotation, in knees; flexion/extension and adduction/abduction, in hips; and internal/external rotation of the foot. Since plantar foot alterations are reflected in the surface of the foot (through pressure leves) and in the posture of the human body.

## Appendices

Appendix 1 shows the products derived from the thesis, all of them have been published except for appendix 1.5, which is under review. Appendix 2 shows the documents used to carry out the experiments considering medical protocols.

Appendix 1. Products

1.1. J. A. Ramirez-Bautista, J. A. Huerta-Ruelas, S. L. Chaparro-Cardenas, and A. Hernandez-Zavala, "A Review in Detection and Monitoring Gait Disorders Using In-Shoe Plantar Measurement Systems," IEEE Rev. Biomed. Eng., vol. 10, no. c, pp. 299–309, 2017.

1.2. J. A. R. Bautista, S. L. C. Cárdenas, A. H. Zavala, and J. A. Huerta-Ruelas, "Review on plantar data analysis for disease diagnosis," Biocybern. Biomed. Eng., vol. 8, 2018.

1.3. J. A. Ramirez-Bautista, A. Hernández-Zavala, J. A. Huerta-Ruelas, M. F. Hatwágner, S. L. haparro-Cárdenas and L. T. Kóczy, "Detection of Human Footprint Alterations by Fuzzy Cognitive Maps Trained with Genetic Algorithm," IEEE procc. MICAI 2018.

1.4. J. A. Ramirez-Bautista, A. Hernández-Zavala, J. A. Huerta-Ruelas, M. F. Hatwágner, S. L. Chaparro-Cárdenas and L. T. Kóczy, "Classification of Plantar Foot Alterations by Fuzzy Cognitive Maps against Multi-Layer Perceptron Neural Network" Biocybern. Biomed. Eng., vol. 40, 2020.

1.5. Julian Andres Ramirez-Bautista, Student Member, IEEE, Antonio Hernández-Zavala, Ruth Magdalena Gallegos-Torres, Silvia L. Chaparro-Cárdenas, Student Member, IEEE, Martha Lucía Zequera, Yosabad Tovar-Barrera, Juan Manuel Pradilla-Gómez and Jorge A. Huerta-Ruelas, "Modified Fuzzy Cognitive Map Type-II and Bacterial Foraging Optimization Algorithm for Classify Plantar Foot Alterations,". under review.

Appendix 2. Protocols and Informed Consent

2.1. Protocol used for plantar pressure acquisition, "Protocolo para Obtención de Datos de Presión Plantar".

2.2. Information document and Informed Consent.

## References


[1] M. Woźniak, D. Połap, R. K. Nowicki, C. Napoli, G. Pappalardo, and E. Tramontana, "Novel approach toward medical signals classifier," *Proc. Int. Jt. Conf. Neural Networks*, vol. 2015-Septe, 2015, doi: 10.1109/IJCNN.2015.7280556.

[2] A. H. Abdul Razak, A. Zayegh, R. K. Begg, and Y. Wahab, "Foot plantar pressure measurement system: A review," *Sensors (Switzerland)*, vol. 12, no. 7, pp. 9884–9912, 2012, doi: 10.3390/s120709884.

[3] J. H. Bauman and P. W. Brand, "Measurement of pressure between foot and shoe," *Lancet*, vol. 281, no. 7282, pp. 629–632, 1963, doi: 10.1016/S0140-6736(63)91271-6.

[4] T. L. Lawrence and R. N. Schmidt, "Wireless In-shoe Force System," *Proc. 19th Annu. Int. Conf. Ieee Eng. Med. Biol. Soc. Vol 19, Pts 1-6*, vol. 19, no. C, pp. 2238–2241, 1997, doi: 10.1109/IEMBS.1997.758805.

[5] N. Hegde, M. Bries, and E. Sazonov, "A Comparative Review of Footwear-Based Wearable Systems," *Electronics*, vol. 5, no. 3, p. 48, 2016, doi: 10.3390/electronics5030048.

[6] M. Woźniak, M. Graña, and E. Corchado, "A survey of multiple classifier systems as hybrid systems," *Inf. Fusion*, vol. 16, no. 1, pp. 3–17, 2014, doi: 10.1016/j.inffus.2013.04.006.

[7] D. T. H. H. Lai, R. K. Begg, and M. Palaniswami, "Computational Intelligence in Gait Research : A Perspective on Current Applications and Future Challenges," *Technology*, vol. 13, no. 5, pp. 687–702, 2009, doi: 10.1109/TITB.2009.2022913.

[8] Y. Guo and W. Lanmei, "Recent Advance in Plantar Pressure Measurement System," *Sens. Transducers*, vol. 145, no. 10, pp. 96–105, 2012, doi: 1726-5479.

[9] V. Racic, A. Pavic, and J. M. W. Brownjohn, "Modern facilities for experimental measurement of dynamic loads induced by humans: A literature review," *Shock Vib.*, vol. 20, no. 1, pp. 53–67, 2013, doi: 10.3233/SAV-2012-0727.

[10] L. Wafai, A. Zayegh, J. Woulfe, S. M. Aziz, and R. Begg, "Identification of Foot Pathologies Based on Plantar Pressure Asymmetry.," *Sensors (Basel).*, vol. 15, no. 8, pp. 20392–20408, 2015, doi: 10.3390/s150820392.

[11] P. S. Dyer and S. J. M. Bamberg, "Instrumented insole vs. force plate: A comparison of center of plantar pressure," *Proc. Annu. Int. Conf. IEEE Eng. Med. Biol. Soc. EMBS*, pp. 6805–6809, 2011, doi: 10.1109/IEMBS.2011.6091678.

[12] L. Shu, T. Hua, Y. Wang, Q. Qiao Li, D. D. Feng, and X. Tao, "In-shoe plantar pressure measurement and analysis system based on fabric pressure sensing array.," *IEEE Trans. Inf. Technol. Biomed.*, vol. 14, no. 3, pp. 767–775, 2010, doi: 10.1109/TITB.2009.2038904.

[13] A. M. Tan, F. K. Fuss, Y. Weizman, Y. Woudstra, and O. Troynikov, "Design of Low Cost Smart Insole for Real Time Measurement of Plantar Pressure," *Procedia Technol.*, vol. 20, no. May 2016, pp. 117–122, 2015, doi: 10.1016/j.protcy.2015.07.020.

[14] W. Xu, Z. Li, M. C. Huang, N. Amini, and M. Sarrafzadeh, "eCushion: An eTextile device

for sitting posture monitoring," *Proc. - 2011 Int. Conf. Body Sens. Networks, BSN 2011*, vol. 1, no. c, pp. 194–199, 2011, doi: 10.1109/BSN.2011.24.

[15] C. A. Macleod, B. A. Conway, D. B. Allan, and S. S. Galen, "Development and validation of a low-cost, portable and wireless gait assessment tool," *Med. Eng. Phys.*, vol. 36, no. 4, pp. 541–546, 2014, doi: 10.1016/j.medengphy.2013.11.011.

[16] B. Horsak *et al.*, "SONIGait: a wireless instrumented insole device for real-time sonification of gait," *J. Multimodal User Interfaces*, vol. 10, no. 3, pp. 195–206, 2016, doi: 10.1007/s12193-016-0216-9.

[17] J. Park, Y. Na, G. Gu, and J. Kim, "Flexible insole ground reaction force measurement shoes for jumping and running," *Proc. IEEE RAS EMBS Int. Conf. Biomed. Robot. Biomechatronics*, vol. 2016-July, pp. 1062–1067, 2016, doi: 10.1109/BIOROB.2016.7523772.

[18] F. Pineda López, A. Guerra, E. Montes, and D. S. Benítez, "A Low Cost Baropodometric System for Children's Postural and Gait Analysis," in *Communications and Computing (COLCOM), 2016 IEEE Colombian Conference on*, 2016, pp. 1–4, doi: 10.1109/ColComCon.2016.7516381.

[19] J. Pauk, K. Daunoraviciene, M. Ihnatouski, J. Griskevicius, and J. V. Raso, "Analysis of the plantar pressure distribution in children with foot deformities," *Acta Bioeng. Biomech.*, vol. 12, no. 1, pp. 29–34, 2010.

[20] J. Torres, A. García, C. Villarraga, A. Egel, and R. Polanía, "DESARROLLO DE UN SISTEMA ELECTRÓNICO PARA MEDIR AMBULATORIAMENTE PRESIONES EN LA PLANTA DEL PIE INSENSIBLE," in *IBEROAMERICAN WORKSHOP IBERCHIP*, 2007, pp. 1–4.

[21] I. González, J. Fontecha, R. Hervás, and J. Bravo, "An Ambulatory System for Gait Monitoring Based on Wireless Sensorized Insoles," *Sensors (Basel).*, vol. 15, no. 7, pp. 16589–16613, 2015, doi: 10.3390/s150716589.

[22] L. Shu *et al.*, "Monitoring diabetic patients by novel intelligent footwear system," *ICCH 2012 Proc. - Int. Conf. Comput. Healthc.*, pp. 91–94, 2012, doi: 10.1109/ICCH.2012.6724478.

[23] K. Kong, J. Bae, and M. Tomizuka, "Detection of abnormalities in a human gait using smart shoes," *Proc. SPIE*, vol. 6932, pp. 69322G-69322G–10, 2008, doi: 10.1117/12.776003.

[24] C. S. Morère, A. Sura, A. R. Pérez-tabernero, E. Vihriälä, and T. Myllylä, "MEMS Technology Sensors as a More Advantageous Technique for Measuring Foot Plantar Pressure and Balance in Humans," vol. 2016, 2016, doi: 10.1155/2016/6590252.

[25] E. S. Sazonov, G. Fulk, J. Hill, Y. Schutz, and R. Browning, "Monitoring of posture allocations and activities by a shoe-based wearable sensor," *IEEE Trans. Biomed. Eng.*, vol. 58, no. 4, pp. 983–990, 2011, doi: 10.1109/TBME.2010.2046738.

[26] S. Urry, "Plantar pressure-measurement sensors," *Meas. Sci. Technol.*, vol. 16, no. 1, pp.

16–32, Jan. 1999, doi: 10.1088/0957-0233/10/1/017.

[27] Y. Wahab, “Design and Implementation of MEMS Biomechanical Sensors for Real-Life Measurements of Gait Parameters,” Victoria University, Australia, 2009.

[28] Moticon GmbH, “Plantillas electrónicas para investigación y deporte,” Munich, 2015.

[29] Moticon GmbH, “Moticon Science,” *Product Home*, 2015. [Online]. Available: http://www.moticon.de/products/product-home. [Accessed: 03-Nov-2016].

[30] Sennotech Co. Ltd., “Sennotech sensing innovative,” *Insole Smart & Natural*. [Online]. Available: http://www.sennotech.com/EN/product/insole.php. [Accessed: 03-Nov-2016].

[31] Tekscan, “F-Scan In-Shoe Analysis System.” [Online]. Available: https://www.tekscan.com/products-solutions/systems/t-scan. [Accessed: 08-Jun-2016].

[32] Novel, “Pedar -X ® system - The quality in-shoe dynamic pressure measuring system,” *The pedar®*, 2008. [Online]. Available: http://novel.de/novelcontent/pedar. [Accessed: 03-Nov-2016].

[33] amcube, “In-Shoe Pressure Measurement | Mobile Foot Pressure Measurement,” *IN-SHOE PRESSURE MEASUREMENT Mobile & Practical*. [Online]. Available: http://www.amcube.co.uk/products/in-shoe-pressure-measurement/. [Accessed: 15-Sep-2016].

[34] Instituto de Biomecánica de Valencia, “Sistema Biofoot / IBV,” Valencia, 4, 2012.

[35] Paromed, “paroTec: The high-precision foot pressure measurement system,” *Products*. [Online]. Available: http://www.paromed.biz/paroTec-3-2.html. [Accessed: 12-Oct-2016].

[36] Techno concepts, “DYNAFOOT 2,” France, 2015.

[37] WIISEL, “Wireless Insole for Independent and Safe Elderly Living,” 2013. [Online]. Available: http://www.wiisel.eu/?q=content/documents. [Accessed: 25-Nov-2016].

[38] medilogic, “Medilogic Insole Science,” *2016*. [Online]. Available: http://www.medilogic.com/en/products-human/footpressure-measurement/medilogic-insole/. [Accessed: 24-Nov-2016].

[39] ORPYX Medical Technologies, “LogR - Orpyx Medical Technologies,” *Real-time measurement of plantar pressure for analysis by researchers*, 2016. [Online]. Available: https://orpyx.com/pages/logr. [Accessed: 18-Oct-2016].

[40] Sensor Medica, “sensor medica cataloge,” *Design & Development by Sensor Medica*, 2017. [Online]. Available: http://www.sensormedica.com/site/SM_catalogue_2017.pdf. [Accessed: 23-Jun-2017].

[41] S. Corbellini, C. Ramella, C. Fallauto, M. Pirola, S. Stassi, and G. Canavese, “Low-cost wearable measurement system for continuous real-time pedobarography,” *2015 IEEE Int. Symp. Med. Meas. Appl. Proc.*, pp. 639–644, 2015, doi: 10.1109/MeMeA.2015.7145281.

[42] M. Donati *et al.*, “A flexible sensor technology for the distributed measurement of

interaction pressure," *Sensors (Switzerland),* vol. 13, no. 1, pp. 1021–1045, 2013, doi: 10.3390/s130101021.

[43] K. Leemets, T. Terasmaa, P. Jaakson, A. Kume, and T. Tamm, "Development of A Smart Insole System for Gait and Performance Monitoring," no. Icmsa, pp. 713–718, 2015.

[44] Z. Ahmad, M. R. Azizan, I. Mat Sahat, and Z. Ghazalli, "A Low-Cost of Foot Plantar Shoes for Gait Monitoring System," *Annu. Conf. Eng. Informations Technol.*, no. April 2016, 2015.

[45] F. Neaga, D. Moga, D. Petreus, M. Munteanu, and N. Stroia, "A Wireless System for Monitoring the Progressive Loading of Lower Limb in Post-Traumatic Rehabilitation," *Int. Conf. Adv. Med. Heal. Care through Technol.*, vol. 36, pp. 54–59, 2011, doi: 10.1007/978-3-642-22586-4.

[46] S. Bamberg, A. Y. Benbasat, D. M. Scarborough, D. E. Krebs, and J. A. Paradiso, "Gait analysis using a shoe-integrated wireless sensor system," *Inf. Technol. Biomed. IEEE Trans.*, vol. 12, no. 4, pp. 413–423, 2008.

[47] J. M. Hausdorff, Z. Ladin, and J. Y. Wei, "Footswitch system for measurement of the temporal parameters of gait," *J. Biomech.*, vol. 28, no. 3, pp. 347–351, 1995.

[48] E. Campo, Y. Charlon, and D. Brulin, "Instrumented Insole for Weight Measurement of Frail People," *Proc. 8th ACM Int. Conf. PErvasive Technol. Relat. to Assist. Environ.*, pp. 60:1--60:6, 2015, doi: 10.1145/2769493.2769525.

[49] A. M. Cristiani, G. M. Bertolotti, E. Marenzi, S. Member, and S. Ramat, "An Instrumented Insole for Long Term Monitoring," vol. 14, no. 5, pp. 1564–1572, 2014.

[50] V. David, H. Jagos, S. Litzenberger, and M. Reichel, "Instrumented insole for mobile and long distance motion pattern measurement," *Procedia Eng.*, vol. 34, pp. 760–765, 2012, doi: 10.1016/j.proeng.2012.04.130.

[51] I. P. I. Pappas, T. Keller, S. Mangold, M. R. Popovic, V. Dietz, and M. Morari, "A Reliable Gyroscope-Based Gait-Phase Detection Sensor Embedded in a Shoe Insole," *IEEE Sens. J.*, vol. 4, no. 2, pp. 268–274, 2004, doi: 10.1109/JSEN.2004.823671.

[52] M. Chen, B. Huang, and Y. Xu, "Intelligent shoes for abnormal gait detection," *Proc. - IEEE Int. Conf. Robot. Autom.*, pp. 2019–2024, 2008, doi: 10.1109/ROBOT.2008.4543503.

[53] H. Tanwar, L. Nguyen, and N. Stergiou, "Force Sensitive Resistor (FSR)-based wireless gait analysis device," in *Proceedings of the 3rd IASTED International Conference on Telehealth*, 2007.

[54] W. Srivises, I. Nilkhamhang, and K. Tungpimolrut, "Design of a Smart Shoe for Reliable Gait Analysis Using State Transition Theory," in *9th International Conference on*, 2012, pp. 1–4, doi: 10.1109/ECTICon.2012.6254200.

[55] J. C. Ayena, L. D. C. T., M. J. D. Otis, and B. A. J. Menelas, "An efficient home-based risk of falling assessment test based on Smartphone and instrumented insole," *Med. Meas. Appl.*

*(MeMeA), 2015 IEEE Int. Symp.*, pp. 416–421, 2015, doi: 10.1109/MeMeA.2015.7145239.

[56] H. Ma and W.-H. Liao, “Human Gait Modeling and Analysis Using a Semi-Markov Process with Ground Reaction Forces,” *IEEE Trans. Neural Syst. Rehabil. Eng.*, vol. 25, no. 6, pp. 1–1, Jun. 2016, doi: 10.1109/TNSRE.2016.2584923.

[57] L. Y. Qin, H. Ma, and W. H. Liao, “Insole plantar pressure systems in the gait analysis of post-stroke rehabilitation,” *2015 IEEE Int. Conf. Inf. Autom. ICIA 2015 - conjunction with 2015 IEEE Int. Conf. Autom. Logist.*, no. August, pp. 1784–1789, 2015, doi: 10.1109/ICInfA.2015.7279576.

[58] J. Torres, A. García, C. Villarraga, A. Egel, and R. Polanía, “DESARROLLO DE UN SISTEMA ELECTRÓNICO PARA MEDIR AMBULATORIAMENTE PRESIONES EN LA PLANTA DEL PIE INSENSIBLE,” in *IBERCHIP*, 2007.

[59] S. L. Patil, A. Madhuri, and U. M. Chaskar, “Development of Planter Foot Pressure Distribution System Using Flexi Force Sensors,” *Sensors & Transducers*, vol. 108, no. 9, pp. 73–79, 2009, doi: 1726-5479.

[60] H. Zhu, N. Maalej, J. G. Webster, W. J. Tompkins, P. Bach-Y-Rita, and J. J. Wertsch, “An umbilical data-acquisition system for measuring pressures between the foot and shoe,” *IEEE Trans. Biomed. Eng.*, vol. 37, no. 9, pp. 908–911, 1990, doi: 10.1109/10.58601.

[61] A. S. Benbakhti, S. Boukhenous, C. Zizoua, and M. Attari, “An instrumented shoe for ambulatory prevention of diabetic foot ulceration,” *Proc. 2014 4th Int. Conf. Wirel. Mob. Commun. Healthc. - "Transforming Healthc. Through Innov. Mob. Wirel. Technol. MOBIHEALTH 2014*, pp. 43–46, 2015, doi: 10.1109/MOBIHEALTH.2014.7015905.

[62] L. Yang, P. S. Dyer, R. J. Carson, J. B. Webster, K. Bo Foreman, and S. J. M. Bamberg, “Utilization of a lower extremity ambulatory feedback system to reduce gait asymmetry in transtibial amputation gait,” *Gait Posture*, vol. 36, no. 3, pp. 631–634, 2012, doi: 10.1016/j.gaitpost.2012.04.004.

[63] L. Claverie, A. Ille, and P. Moretto, “Discrete sensors distribution for accurate plantar pressure analyses,” *Med. Eng. Phys.*, vol. 38, no. 12, pp. 1489–1494, 2016, doi: 10.1016/j.medengphy.2016.09.021.

[64] A. C. Guerra and E. G. Montes, “Diseño e implementación de un sistema de baropodometría electrónica para niños,” vol. 5, no. 1, p. 153, 2014.

[65] H. P. Noce, “An In-shoe Instrument for Acquisition and Storage of Plantar Pressure,” Oregon State University, 2005.

[66] R. Eguchi, A. Yorozu, T. Fukumoto, and M. Takahashi, “Ground Reaction Force Estimation Using Insole Plantar Pressure Measurement System from Single-Leg Standing,” no. Mfi, pp. 19–21, 2016.

[67] O. Mazumder, A. S. Kundu, and S. Bhaumik, “Development of wireless insole foot pressure data acquisition device,” *Commun. Devices Intell. Syst. (CODIS), 2012 Int. Conf.*, pp. 302–305, 2012, doi: 10.1109/codis.2012.6422198.

[68] T. Salpavaara, J. Verho, J. Lekkala, and J. Halttunen, “Wireless Insole Sensor System for Plantar Force Measurements during Sport Events,” *XIX IMEKO World Congr. Fundam. Appl. Metrol.*, pp. 2118–2123, 2009.

[69] F. Martínez-Martí, M. S. Martínez-García, S. G. García-Díaz, J. García-Jiménez, A. J. Palma, and M. A. Carvajal, “Embedded sensor insole for wireless measurement of gait parameters,” *Australas. Phys. Eng. Sci. Med.*, vol. 37, no. 1, pp. 25–35, 2014, doi: 10.1007/s13246-013-0236-7.

[70] P. Paulick, H. Djalilian, and M. Bachman, “StabilitySole: Embedded sensor insole for balance and gait monitoring,” *Lect. Notes Comput. Sci. (including Subser. Lect. Notes Artif. Intell. Lect. Notes Bioinformatics)*, vol. 6777 LNCS, pp. 171–177, 2011, doi: 10.1007/978-3-642-21799-9_19.

[71] E. Klimiec, J. Piekarski, W. Zaraska, and B. Jasiewicz, “Electronic measurement system of foot plantar pressure,” *Microelectron. Int.*, vol. 31, no. 3, pp. 229–234, 2014, doi: 10.1108/MI-11-2013-0074.

[72] C. N. Lescano, R. H. Rodrigo, and S. E. Rodrigo, “PRESIONES PLANTARES,” *Rev. Iberoam. Ing. Mecánica*, vol. 19, no. 1, pp. 49–58, 2015.

[73] F. Chedevergne, A. Faivre, and M. Dahan, “Development of a mechatronical device to measure plantar pressure for medical prevention of gait issues,” *2006 IEEE Int. Conf. Mechatronics Autom. ICMA 2006*, vol. 2006, pp. 928–932, 2006, doi: 10.1109/ICMA.2006.257749.

[74] Y. S. A. Mustufa, J. Barton, B. O’Flynn, R. Davies, P. McCullagh, and H. Zheng, “Design of a smart insole for ambulatory assessment of gait,” in *2015 IEEE 12th International Conference on Wearable and Implantable Body Sensor Networks (BSN)*, 2015, pp. 1–5, doi: 10.1109/BSN.2015.7299383.

[75] J. Munk-stander, “Evaluation of Piezoelectric Film Sensors for In-Shoe Pressure Measurement Jacob Munk-Stander ( Joint technical report with University of Cambridge ) Evaluation of Piezoelectric Film Sensors for In-Shoe Pressure Measurement,” no. 06.

[76] J. J. Wertsch, J. G. Webster, and W. J. Tompkins, “A portable insole plantar pressure measurement system,” *J. Rehabil. Res. Dev.*, vol. 29, no. 1, p. 13, 1992, doi: 10.1682/JRRD.1992.01.0013.

[77] M. Hannula, A. Säkkinen, and A. Kylmänen, “Development of EMFI-sensor based pressure sensitive insole for gait analysis,” *MeMeA 2007 2nd - IEEE Int. Work. Med. Meas. Appl.*, pp. 18–20, 2007, doi: 10.1109/MEMEA.2007.4285153.

[78] M. Saito *et al.*, “An in-shoe device to measure plantar pressure during daily human activity,” *Med. Eng. Phys.*, vol. 33, no. 5, pp. 638–645, 2011, doi: 10.1016/j.medengphy.2011.01.001.

[79] Kyoungchul Kong and M. Tomizuka, “A Gait Monitoring System Based on Air Pressure Sensors Embedded in a Shoe,” *IEEE/ASME Trans. Mechatronics*, vol. 14, no. 3, pp. 358–370, Jun. 2009, doi: 10.1109/TMECH.2008.2008803.

[80] Y. Cong and M. Zhang, "Measurement of in-shoe plantar triaxial stresses in high-heeled shoes," *Proc. - 2010 3rd Int. Conf. Biomed. Eng. Informatics, BMEI 2010*, vol. 4, no. Bmei, pp. 1760–1763, 2010, doi: 10.1109/BMEI.2010.5639873.

[81] T. Liu, Y. Inoue, and K. Shibata, "A wearable ground reaction force sensor system and its application to the measurement of extrinsic gait variability," *Sensors (Switzerland)*, vol. 10, no. 11, pp. 10240–10255, 2010, doi: 10.3390/s101110240.

[82] G. Li, T. Liu, J. Yi, H. Wang, J. Li, and Y. Inoue, "The lower limbs kinematics analysis by wearable sensor shoes," *IEEE Sens. J.*, vol. 16, no. 8, pp. 2627–2638, 2016, doi: 10.1109/JSEN.2016.2515101.

[83] M. F. Domingues *et al.*, "Insole optical fiber Bragg grating sensors network for dynamic vertical force monitoring," *J. Biomed. Opt.*, vol. 22, no. 9, p. 091507, 2017, doi: 10.1117/1.JBO.22.9.091507.

[84] T. Holleczek, A. Ru, H. Harms, and G. Tro, "Textile pressure sensors for sports applications," in *2010 IEEE Sensors*, 2010, pp. 732–737, doi: 10.1109/ICSENS.2010.5690041.

[85] W. Xu, J. J. Liu, M.-C. Huang, L. He, N. Amini, and M. Sarrafzadeh, "Smart Insole : A Wearable System for Gait Analysis," *Proc. 5th Int. Conf. Pervasive Technol. Relat. to Assist. Environ.*, pp. 1–4, 2012, doi: 10.1145/2413097.2413120.

[86] Y. Wu, W. Xu, J. J. Liu, M. C. Huang, S. Luan, and Y. Lee, "An Energy-Efficient Adaptive Sensing Framework for Gait Monitoring Using Smart Insole," *IEEE Sens. J.*, vol. 15, no. 4, pp. 2335–2343, 2015, doi: 10.1109/JSEN.2014.2372694.

[87] Z. Ahmad, M. R. Azizan, I. Mat Sahat, and Z. Ghazalli, "A Low-Cost of Foot Plantar Shoes for Gait Monitoring System," in *The 3rd Annual Conference on Engineering and Informations Technology*, 2015, no. March 2015, pp. 1–10.

[88] E. S. Sazonov, S. Member, N. Hegde, and W. Tang, "Development of SmartStep : an insole - based physical activity monitor," pp. 7209–7212, 2013.

[89] I. Tekscan, "F-Scan System | Tekscan," *F-Scan System*. [Online]. Available: https://www.tekscan.com/products-solutions/systems/f-scan-system?tab=add-ons. [Accessed: 16-Oct-2016].

[90] C. Kirtley, "an Instrumented Insole for Kinematic and Kinetic Gait Measurements," *Proc. 5th Symp. Footwear Biomech.*, no. Vcm, pp. 52–53, 2001.

[91] F. Martínez-Martí *et al.*, "Embedded sensor insole for wireless measurement of gait parameters," *Australas. Phys. Eng. Sci. Med.*, vol. 37, no. 1, pp. 25–35, 2014, doi: 10.1007/s13246-013-0236-7.

[92] J. Munk-stander, "Evaluation of Piezoelectric Film Sensors for In-Shoe Pressure Measurement," Denmark, 2006.

[93] B. Saggin, D. Scaccabarozzi, and M. Tarabini, "Metrological performances of a plantar

pressure measurement system," *IEEE Trans. Instrum. Meas.*, vol. 62, no. 4, pp. 766–776, 2013, doi: 10.1109/TIM.2013.2245185.

[94] H. Kato, T. Takada, T. Kawamura, N. Hotta, and S. Torii, "The reduction and redistribution of plantar pressures using foot orthoses in diabetic patients," *Diabetes Res. Clin. Pract.*, vol. 31, no. 1–3, pp. 115–118, 1996, doi: 10.1016/0168-8227(96)01214-4.

[95] D. De León Rodriguez *et al.*, "Biofeedback can reduce foot pressure to a safe level and without causing new at-risk zones in patients with diabetes and peripheral neuropathy," *Diabetes Metab Res*, vol. 29, no. 2, pp. 139–144, Feb. 2013, doi: 10.1002/dmrr.2366.

[96] G. Talavera *et al.*, *Ambient Intelligence for Health*, vol. 9456. Cham: Springer International Publishing, 2015.

[97] R. G. Frykberg, L. A. Lavery, H. Pham, C. Harvey, L. Harkless, and A. Veves, "Role of Neuropathy and High Foot Pressures in Diabetic Foot Ulceration," *Diabetes Care*, vol. 21, no. 10, pp. 1714–1719, 1998.

[98] L. S. Lincoln and S. J. M. Bamberg, "Insole sensor system for real-time detection of biped slip," *2010 Annu. Int. Conf. IEEE Eng. Med. Biol. Soc. EMBC'10*, pp. 1449–1452, 2010, doi: 10.1109/IEMBS.2010.5626859.

[99] H. Abou Ghaida, S. Mottet, and J. M. Goujon, "A real time study of the human equilibrium using an instrumented insole with 3 pressure sensors," *Conf. Proc. ... Annu. Int. Conf. IEEE Eng. Med. Biol. Soc. IEEE Eng. Med. Biol. Soc. Annu. Conf.*, vol. 2014, pp. 4968–4971, 2014, doi: 10.1109/EMBC.2014.6944739.

[100] F. Kawsar, M. K. Hasan, R. Love, and S. I. Ahamed, "A Novel Activity Detection System Using Plantar Pressure Sensors and Smartphone," *IEEE 39th Annu. Comput. Softw. Appl. Conf.*, pp. 44–49, 2015, doi: 10.1109/COMPSAC.2015.201.

[101] C. Wada *et al.*, "Development of a rehabilitation support system with a shoe-type measurement device for walking," *SICE Annu. Conf. 2010, Proc.*, pp. 2534–2537, 2010.

[102] S. Guillén, M. Arredondo, and E. Catellano, "A Survey of Commercial Wearable Systems for Sport Application," in *Wearable Monitoring Systems*, Springer Science+Business Media, 2011, pp. 1–296.

[103] R. M. Queen, B. B. Haynes, W. M. Hardaker, and W. E. Garrett, "Forefoot loading during 3 athletic tasks.," *Am. J. Sports Med.*, vol. 35, no. 4, pp. 630–6, Apr. 2007.

[104] A. ;Mallio. Gioftsidou P.;Pafis, G.;Beneka, A.;Godolias, G.;Maganaris, C. N., "The effects of soccer training and timing of balance training on balance ability," *Eur.J Appl Physiol*, vol. 96, no. 6, pp. 659–664, 2006, doi: 10.1007/s00421-005-0123-3.

[105] L. Mertz, "Technology Comes to the Playing Field," *IEEE Pulse*, vol. 4, no. 5, pp. 12–17, 2013.

[106] B. Braunstein, N. Schulze, M. Sanno, and G.-P. Brüggemann, "COMFORT AND PLANTAR PRESSURE PATTERN DURING RUNNING WITH PREFABRICATED

INSOLES German Sport University Cologne , Institute of Biomechanics and Orthopaedics , Germany German Research Centre of Elite Sport , Cologne , Germany Center for Health and Integrati," pp. 3–6, 2014.

[107] M. Abdullah, "Disease Diagnosis using Soft Computing Model : A Digest," vol. 102, no. 10, pp. 43–47, 2014.

[108] K. C. Tan, Q. Yu, C. M. Heng, and T. H. Lee, "Evolutionary computing for knowledge discovery in medical diagnosis," *Artif. Intell. Med.*, vol. 27, no. 2, pp. 129–154, 2003, doi: 10.1016/S0933-3657(03)00002-2.

[109] I. Kononenko, "Machine learning for medical diagnosis: history, state of the art and perspective," *Artif Intell Med*, vol. 23, no. 1, pp. 89–109, 2001, doi: 10.1016/S0933-3657(01)00077-X.

[110] K. Polat and S. Güneş, "An expert system approach based on principal component analysis and adaptive neuro-fuzzy inference system to diagnosis of diabetes disease," *Digit. Signal Process.*, vol. 17, no. 4, pp. 702–710, 2007, doi: 10.1016/j.dsp.2006.09.005.

[111] D. K. Choubey and S. Paul, "GA_MLP NN: A Hybrid Intelligent System for Diabetes Disease Diagnosis," *Int. J. Intell. Syst. Appl.*, vol. 8, no. 1, pp. 49–59, 2016, doi: 10.5815/ijisa.2016.01.06.

[112] D. Giveki, H. Salimi, G. Bahmanyar, and Y. Khademian, "Automatic Detection of Diabetes Diagnosis using Feature Weighted Support Vector Machines based on Mutual Information and Modified Cuckoo Search," 2012.

[113] O. Y. Atkov *et al.*, "Coronary heart disease diagnosis by artificial neural networks including genetic polymorphisms and clinical parameters," *J. Cardiol.*, vol. 59, no. 2, pp. 190–194, 2012, doi: 10.1016/j.jjcc.2011.11.005.

[114] M. S. Bascil and H. Oztekin, "A study on hepatitis disease diagnosis using probabilistic neural network," *J. Med. Syst.*, vol. 36, no. 3, pp. 1603–1606, 2012, doi: 10.1007/s10916-010-9621-x.

[115] K. Polat and S. Güneş, "A hybrid approach to medical decision support systems: Combining feature selection, fuzzy weighted pre-processing and AIRS," *Comput. Methods Programs Biomed.*, vol. 88, no. 2, pp. 164–174, 2007, doi: 10.1016/j.cmpb.2007.07.013.

[116] E. Dogantekin, A. Dogantekin, and D. Avci, "Automatic hepatitis diagnosis system based on Linear Discriminant Analysis and Adaptive Network based on Fuzzy Inference System," *Expert Syst. Appl.*, vol. 36, no. 8, pp. 11282–11286, 2009, doi: 10.1016/j.eswa.2009.03.021.

[117] N. K. Ghanad and S. Ahmadi, "Combination of PSO Algorithm and Naive Bayesian Classification for Parkinson Disease Diagnosis," *Adv. Comput. Sci. an Int. J.*, vol. 4, no. 4, pp. 119–125, 2015.

[118] Z. Li, W. Chen, J. Wang, and J. Liu, "An automatic recognition system for patients with movement disorders based on wearable sensors," *Proc. 2014 9th IEEE Conf. Ind. Electron. Appl. ICIEA 2014*, pp. 1948–1953, 2014, doi: 10.1109/ICIEA.2014.6931487.

[119] J. A. Ramirez-Bautista, J. A. Huerta-Ruelas, S. L. Chaparro-Cardenas, and A. Hernandez-Zavala, "A Review in Detection and Monitoring Gait Disorders Using In-Shoe Plantar Measurement Systems," *IEEE Rev. Biomed. Eng.*, vol. 10, no. c, pp. 299–309, 2017, doi: 10.1109/RBME.2017.2747402.

[120] D. Rosenbaum and H.-P. Becker, "Plantar pressure distribution measurements. Technical background and clinical applications," *Foot Ankle Surg.*, vol. 3, no. 1, pp. 1–14, 1997, doi: 10.1046/j.1460-9584.1997.00043.x.

[121] Z. Pataky *et al.*, "The impact of callosities on the magnitude and duration of plantar pressure in patients with diabetes mellitus.," *Diabetes Metab*, vol. 28, no. 5, pp. 356–361, 2002, doi: MDOI-DM-11-2002-28-5-1262-3636-101019-ART2 [pii].

[122] T. A. Bacarin, I. C. N. Sacco, and E. M. Hennig, "Plantar pressure distribution patterns during gait in diabetic neuropathy patients with a history of foot ulcers.," *Clinics (Sao Paulo).*, vol. 64, no. 2, pp. 113–120, 2009, doi: 10.1590/S1807-59322009000200008.

[123] C.-W. Lung, E. T. Hsiao-Wecksler, S. Burns, F. Lin, and Y.-K. Jan, "Quantifying Dynamic Changes in Plantar Pressure Gradient in Diabetics with Peripheral Neuropathy," *Front. Bioeng. Biotechnol.*, vol. 4, no. 4, pp. 543389–54, Jul. 2016, doi: 10.3389/fbioe.2016.00054.

[124] K. R. Ford *et al.*, "Comparison of in-shoe foot loading patterns on natural grass and synthetic turf," *J. Sci. Med. Sport*, vol. 9, no. 6, pp. 433–440, 2006, doi: 10.1016/j.jsams.2006.03.019.

[125] S. Kimmeskamp and E. M. Hennig, "Heel to toe motion characteristics in Parkinson patients during free walking," *Clin. Biomech.*, vol. 16, no. 9, pp. 806–812, 2001, doi: 10.1016/S0268-0033(01)00069-9.

[126] T. Duckworth, A. J. Boulton, R. P. Betts, C. I. Franks, and J. D. Ward, "Plantar pressure measurements and the prevention of ulceration in the diabetic foot," *J Bone Jt. Surg Br*, vol. 67, no. 1, pp. 79–85, 1985.

[127] J. Wen, Q. Ding, Z. Yu, W. Sun, Q. Wang, and K. Wei, "Adaptive changes of foot pressure in hallux valgus patients," *Gait Posture*, vol. 36, no. 3, pp. 344–349, 2012, doi: 10.1016/j.gaitpost.2012.03.030.

[128] M. V Madavi and S. D. Giripunje, "Design and Implementation of Wearable Device for Neuropathic Diabetic Foot Patients," in *7th International Conference on Emerging Trends in Engineering & Technology Design*, 2015, pp. 23–27, doi: 10.1109/ICETET.2015.14.

[129] C. J. Bennetts, T. M. Owings, A. Erdemir, G. Botek, and P. R. Cavanagh, "Clustering and classification of regional peak plantar pressures of diabetic feet," *J. Biomech.*, vol. 46, no. 1, pp. 19–25, 2013, doi: 10.1016/j.jbiomech.2012.09.007.

[130] Z. Pataky, J. P. Assal, P. Conne, H. Vuagnat, and a Golay, "Plantar pressure distribution in Type 2 diabetic patients without peripheral neuropathy and peripheral vascular disease," *Diabet. Med.*, vol. 22, no. 6, pp. 762–767, 2005, doi: 10.1111/j.1464-5491.2005.01520.x.

[131] L. Wafai, A. Zayegh, R. Begg, and J. Woulfe, "Asymmetry detection during pathological

gait using a plantar pressure sensing system," *2013 7th IEEE GCC Conf. Exhib. GCC 2013*, pp. 182–187, 2013, doi: 10.1109/IEEEGCC.2013.6705772.

[132] A. Veves, H. J. Murray, M. J. Young, and A. J. M. Boulton, "Diabetologia," vol. 30, pp. 660–663, 1992.

[133] M. L. Zequera, S. E. Solomonidis, F. Vega, and L. M. Rondon, "STUDY OF THE PLANTAR PRESSURE DISTRIBUTION ON THE SOLE OF THE FOOT OF NORMAL AND DIABETIC SUBJECTS IN THE EARLY STAGES BY USING A WYDROCELL PRESSURE SENSOR," in *25' Annual lntemationai Conference ofthe IEEE EMBS*, 2003, pp. 1874–1877.

[134] D. V Rai and L. M. Aggarwal, "The Study of Plantar Pressure Distribution in Normal and Pathological Foot," *Polish J. Med. Phys. Eng.*, vol. 12, no. 1, pp. 25–34, 2006.

[135] Piédica, "Plantillas ortopédicas," *Pie plano adultos*, 2016. [Online]. Available: http://www.piedica.com/blog-dolor-de-pies/pie-plano-en-adulto. [Accessed: 03-Jul-2017].

[136] L. Vorlickova and P. Korvas, "Evaluation of rehabilitation influence on flat foot in children by plantar pressure analysis," *J. Hum. Sport Exerc.*, vol. 9, no. 1 (special issue), pp. 5–7, 2014, doi: 10.14198/jhse.2014.9.Proc1.42.

[137] Piédica and Centro de Diagnostico Piédica, "Plantillas ortopédicas," 2016. [Online]. Available: http://www.piedica.com/blog-dolor-de-pies/pie-cavo. [Accessed: 03-Jul-2017].

[138] U. Koller, M. Willegger, R. Windhager, A. Wanivenhaus, H. J. Trnka, and R. Schuh, "Plantar pressure characteristics in hallux valgus feet," *J. Orthop. Res.*, vol. 32, no. 12, pp. 1688–1693, 2014, doi: 10.1002/jor.22707.

[139] W. R. Ledoux and H. J. Hillstrom, "The distributed plantar vertical force of neutrally aligned and pes planus feet," *Gait Posture*, vol. 15, no. 1, pp. 1–9, 2002, doi: 10.1016/S0966-6362(01)00165-5.

[140] R. M. Queen, N. A. Mall, J. A. Nunley, and B. Chuckpaiwong, "Differences in plantar loading between flat and normal feet during different athletic tasks," *Gait Posture*, vol. 29, no. 4, pp. 582–586, 2009, doi: 10.1016/j.gaitpost.2008.12.010.

[141] L. M. Fern??ndez-Segu??n, J. A. Diaz Mancha, R. S??nchez Rodr??guez, E. Escamilla Mart??nez, B. G??mez Mart??n, and J. Ramos Ortega, "Comparison of plantar pressures and contact area between normal and cavus foot," *Gait Posture*, vol. 39, no. 2, pp. 789–792, 2014, doi: 10.1016/j.gaitpost.2013.10.018.

[142] J. Burns, J. Crosbie, A. Hunt, and R. Ouvrier, "The effect of pes cavus on foot pain and plantar pressure," *Clin. Biomech.*, vol. 20, no. 9, pp. 877–882, 2005, doi: 10.1016/j.clinbiomech.2005.03.006.

[143] C. Giacomozzi and J. A. Stebbins, "Anatomical masking of pressure footprints based on the Oxford Foot Model: validation and clinical relevance," *Gait Posture*, vol. 53, pp. 131–138, 2017, doi: 10.1016/j.gaitpost.2016.12.022.

[144] M. Costea, B. Sarghie, A. Mihai, and E. Rezus, “Classification of the Elderly Foot Types Based on Plantar Footprints,” *Procedia Eng.*, vol. 181, pp. 36–43, 2017, doi: 10.1016/j.proeng.2017.02.360.

[145] H. Rouhani, X. Crevoisier, J. Favre, and K. Aminian, “Outcome evaluation of ankle osteoarthritis treatments: Plantar pressure analysis during relatively long-distance walking,” *Clin. Biomech.*, vol. 26, no. 4, pp. 397–404, 2011, doi: 10.1016/j.clinbiomech.2010.11.011.

[146] G. V. Zammit, H. B. Menz, S. E. Munteanu, and K. B. Landorf, “Plantar pressure distribution in older people with osteoarthritis of the first metatarsophalangeal joint (Hallux limitus/rigidus),” *J. Orthop. Res.*, vol. 26, no. 12, pp. 1665–1669, 2008, doi: 10.1002/jor.20700.

[147] A. Schmiegel, D. Rosenbaum, A. Schorat, A. Hilker, and M. Gaubitz, “Assessment of foot impairment in rheumatoid arthritis patients by dynamic pedobarography,” *Gait Posture*, vol. 27, no. 1, pp. 110–114, 2008, doi: 10.1016/j.gaitpost.2007.02.008.

[148] D. Rosenbaum and H. Becker, “Review article Plantar pressure distribution measurements . Technical background and clinical applications,” *Foot Ankle Surg.*, no. 3, pp. 1–14, 1997.

[149] N. Hayafune, Y. Hayafune, and H. a. C. Jacob, “Pressure and force distribution characteristics under the normal foot during the push-off phase in gait,” *Foot*, vol. 9, no. 2, pp. 88–92, 1999, doi: 10.1054/foot.1999.0518.

[150] Z. O. Abu-faraj and M. Abdul-Al, “Leg Length Discrepancy : A Study on In-Shoe Plantar Pressure Distribution,” in *8th International Conference on BioMedical Engineering and Informatics (BMEI 2015)*, 2015, pp. 381–385.

[151] S. Choi, H. Cho, B. Kang, D. H. Lee, M. J. Kim, and S. H. Jang, “Slip-related changes in plantar pressure distribution, and parameters for early detection of slip events,” *Ann. Rehabil. Med.*, vol. 39, no. 6, pp. 897–904, 2015, doi: 10.5535/arm.2015.39.6.897.

[152] E. Eils, S. Nolte, M. Tewes, L. Thorwesten, K. Völker, and D. Rosenbaum, “Modified pressure distribution patterns in walking following reduction of plantar sensation,” *J. Biomech.*, vol. 35, no. 10, pp. 1307–1313, 2002, doi: 10.1016/S0021-9290(02)00168-9.

[153] R. Okuno, S. Fujimoto, J. Akazawa, M. Yokoe, S. Sakoda, and K. Akazawa, “Analysis of spatial temporal plantar pressure pattern during gait in Parkinson’s disease,” in *2008 30th Annual International Conference of the IEEE Engineering in Medicine and Biology Society*, 2008, pp. 1765–1768, doi: 10.1109/IEMBS.2008.4649519.

[154] S. Meyring, R. Diehl, T. Milani, E. Hennig, and P. Berlit, “Dynamic plantar pressure distribution measurements in hemiparetic patients,” *Clin. Biomech.*, vol. 12, no. 1, pp. 60–65, 1997, doi: 10.1016/S0268-0033(96)00050-2.

[155] Á. S. Machado, G. D. Bombach, J. Duysens, and F. P. Carpes, “Differences in foot sensitivity and plantar pressure between young adults and elderly,” *Arch. Gerontol. Geriatr.*, vol. 63, pp. 67–71, 2016, doi: 10.1016/j.archger.2015.11.005.

[156] E. M. Hennig, a Staats, and D. Rosenbaum, “Plantar pressure distribution patterns of young

school children in comparison to adults," *Foot Ankle Int*, vol. 15, no. 1, pp. 35-40., 1994.

[157] M. Birtane and H. Tuna, "The evaluation of plantar pressure distribution in obese and non-obese adults," *Clin. Biomech.*, vol. 19, no. 10, pp. 1055–1059, 2004, doi: 10.1016/j.clinbiomech.2004.07.008.

[158] A. P. Hills, E. M. Hennig, M. McDonald, and O. Bar-Or, "Plantar pressure differences between obese and non-obese adults: a biomechanical analysis.," *Int. J. Obes. Relat. Metab. Disord.*, vol. 25, no. 11, pp. 1674–9, 2001, doi: 10.1038/sj.ijo.0801785.

[159] Z. O. Abu-Faraj, Y. T. Faraj, K. H. Mohtar, and M. M. Rammal, "Characterization of plantar pressures in visually impaired individuals: A pilot study," *Int. IEEE/EMBS Conf. Neural Eng. NER*, pp. 1549–1553, 2013, doi: 10.1109/NER.2013.6696242.

[160] H. B. Menz and M. E. Morris, "Clinical determinants of plantar forces and pressures during walking in older people," *Gait Posture*, vol. 24, no. 2, pp. 229–236, 2006, doi: 10.1016/j.gaitpost.2005.09.002.

[161] A. K. Jain, M. N. Murty, and P. J. Flynn, "Data Clustering : A Review," *ACM Comp. Surv.*, vol. 31, no. 3, pp. 264–323, 1999.

[162] B. Zhang, S. Qin, W. Wang, D. Wang, and L. Xue, "Data stream clustering based on Fuzzy C-Mean algorithm and entropy theory," *Signal Processing*, vol. 126, pp. 111–116, 2016, doi: 10.1016/j.sigpro.2015.10.014.

[163] J. Wang, H. Huang, X. Li, and Y. Ao, "Application of the fuzzy C-means clustering algorithm in plantar pressure analysis," in *28th Chinese Control and Decision Conference (CCDC)*, 2016, pp. 2089–2094.

[164] K. Wagstaff, C. Cardie, S. Rogers, and S. Schroedl, "Constrained K-means Clustering with Background Knowledge," *Int. Conf. Mach. Learn.*, pp. 577–584, 2001, doi: 10.1109/TPAMI.2002.1017616.

[165] A. De Cock, T. Willems, E. Witvrouw, J. Vanrenterghem, and D. De Clercq, "A functional foot type classification with cluster analysis based on plantar pressure distribution during jogging," *Gait Posture*, vol. 23, no. 3, pp. 339–347, 2006, doi: 10.1016/j.gaitpost.2005.04.011.

[166] C. Giacomozzi, F. Martelli, A. Nagel, A. Schmiegel, and D. Rosenbaum, "Cluster analysis to classify gait alterations in rheumatoid arthritis using peak pressure curves," *Gait Posture*, vol. 29, no. 2, pp. 220–224, 2009, doi: 10.1016/j.gaitpost.2008.08.004.

[167] U. Niemann *et al.*, "Comparative clustering of plantar pressure distributions in diabetics with polyneuropathy may be applied to reveal inappropriate biomechanical stress," *PLoS One*, vol. 11, no. 8, pp. 1–12, 2016, doi: 10.1371/journal.pone.0161326.

[168] K. Deschamps *et al.*, "Classification of forefoot plantar pressure distribution in persons with diabetes: A novel perspective for the mechanical management of diabetic foot?," *PLoS One*, vol. 8, no. 11, 2013, doi: 10.1371/journal.pone.0079924.

[169] K. Deschamps *et al.*, “Classification of forefoot plantar pressure distribution in patients with diabetes: a biomechanical approach based on relative regional impulses and non-hierachical clustering,” in *24th Congress of the International Society of Biomechanics (ISB 2013) ; 15th Brazilian Congress of Biomechanics*, 2013, pp. 8–9, doi: 5947772.

[170] F. Amato, A. López, E. M. Peña-Méndez, P. Vaňhara, A. Hampl, and J. Havel, “Artificial neural networks in medical diagnosis,” *J. Appl. Biomed.*, vol. 11, no. 2, pp. 47–58, 2013, doi: 10.2478/v10136-012-0031-x.

[171] N. L. W. Keijsers, N. M. Stolwijk, J. W. K. Louwerens, and J. Duysens, “Classification of forefoot pain based on plantar pressure measurements,” *Clin. Biomech.*, vol. 28, no. 3, pp. 350–356, 2013, doi: 10.1016/j.clinbiomech.2013.01.012.

[172] E. S. Sazonov, T. Bumpus, S. Zeigler, and S. Marocco, “Classification of plantar pressure and heel acceleration patterns using neural networks,” in *Proceedings. 2005 IEEE International Joint Conference on Neural Networks, 2005.*, 2005, vol. 5, pp. 3007–3010, doi: 10.1109/IJCNN.2005.1556404.

[173] J. Piecha, “The Neural Network Selection for a Medical Diagnostic System using an Artificial Data Set,” *J. Comput. Inf. Technol.*, pp. 123–132, 2001.

[174] S. E. Oh, S. Joo, H. W. Jung, H. M. Heo, J. H. Mun, and N. Gmbh, “Development of Algorithm for Ground Reaction Force Prediction using Plantar Pressure during a Harvesting Posture,” korea, 2015.

[175] S. Bin Joo, S. E. Oh, and J. H. Mun, “Improving the ground reaction force prediction accuracy using one-axis plantar pressure: Expansion of input variable for neural network,” *J. Biomech.*, vol. 49, no. 14, pp. 3153–3161, 2016, doi: 10.1016/j.jbiomech.2016.07.029.

[176] R. Acharya U *et al.*, “Automated identification of diabetic type 2 subjects with and without neuropathy using wavelet transform on pedobarograph,” *J. Med. Syst.*, vol. 32, no. 1, pp. 21–29, 2008, doi: 10.1007/s10916-007-9103-y.

[177] J. H. T. Bates and M. P. Young, “Applying Fuzzy Logic to Medical Decision Making in the Intensive Care Unit,” *Am. J. Respir. Crit. Care Med.*, vol. 167, no. 7, pp. 948–952, 2003, doi: 10.1164/rccm.200207-777CP.

[178] N. H. Phuong and V. Kreinovich, “Fuzzy logic and its applications in medicine,” *Int. J. Med. Inform.*, vol. 62, no. 2–3, pp. 165–173, 2001, doi: 10.1016/S1386-5056(01)00160-5.

[179] A. Biswas, E. D. Lemaire, and J. Kofman, “Dynamic gait stability index based on plantar pressures and fuzzy logic,” *J. Biomech.*, vol. 41, no. 7, pp. 1574–1581, 2008, doi: 10.1016/j.jbiomech.2008.02.009.

[180] S. Xu, X. Zhou, and Y.-N. Sun, “A novel gait analysis system based on adaptive neuro-fuzzy inference system,” *Expert Syst. Appl.*, vol. 37, no. 2, pp. 1265–1269, 2010, doi: 10.1016/j.eswa.2009.06.026.

[181] S. Liang *et al.*, “Feature Selection and Predictors of Falls with Foot Force Sensors Using KNN-Based Algorithms,” *Sensor*, vol. 15, pp. 29393–29407, 2015, doi:

10.3390/s151129393.

[182] U. Waldecker, “Foot and Ankle Surgery Pedographic classification and ulcer detection in the diabetic foot,” *Foot Ankle Surg.*, vol. 18, no. 1, pp. 42–49, 2012, doi: 10.1016/j.fas.2011.03.004.

[183] H.-S. Jeon, J. Han, W.-J. Yi, B. Jeon, and K. S. Park, “Classification of Parkinson gait and normal gait using Spatial-Temporal Image of Plantar pressure.,” *Conf. Proc. ... Annu. Int. Conf. IEEE Eng. Med. Biol. Soc. IEEE Eng. Med. Biol. Soc. Annu. Conf.*, vol. 2008, pp. 4672–5, 2008, doi: 10.1109/IEMBS.2008.4650255.

[184] J. Y. Goulermas, A. H. Findlow, C. J. Nester, D. Howard, and P. Bowker, “Automated design of robust discriminant analysis classifier for foot pressure lesions using kinematic data,” *Biomed. Eng. IEEE Trans.*, vol. 52, no. 9, pp. 1549–1562, 2005, doi: 10.1109/TBME.2005.851519.

[185] S. Crea *et al.*, “Development of gait segmentation methods for wearable foot pressure sensors,” *Proc. Annu. Int. Conf. IEEE Eng. Med. Biol. Soc. EMBS*, pp. 5018–5021, 2012, doi: 10.1109/EMBC.2012.6347120.

[186] S.-B. Joo *et al.*, “Prediction of gait speed from plantar pressure using artificial neural networks,” *Expert Syst. Appl.*, vol. 41, no. 16, pp. 7398–7405, 2014, doi: 10.1016/j.eswa.2014.06.002.

[187] M. Forsting, “Hot Topics: Will Machine Learning Change Medicine?,” *J. Nucl. Med.*, p. jnumed.117.190397, 2017, doi: 10.2967/jnumed.117.190397.

[188] Z. Obermeyer and E. J. Emanuel, “Predicting the Future — Big Data, Machine Learning, and Clinical Medicine,” vol. 13, no. 13, pp. 1216–1219, 2016, doi: 10.1056/NEJMp1609300.

[189] M. Fatima and M. Pasha, “Survey of Machine Learning Algorithms for Disease Diagnostic,” *J. Intell. Learn. Syst. Appl.*, vol. 09, no. 01, pp. 1–16, 2017, doi: 10.4236/jilsa.2017.91001.

[190] O. Er, N. Yumusak, and F. Temurtas, “Chest diseases diagnosis using artificial neural networks,” *Expert Syst. Appl.*, vol. 37, no. 12, pp. 7648–7655, 2010, doi: 10.1016/j.eswa.2010.04.078.

[191] R. Miotto, F. Wang, S. Wang, X. Jiang, and J. T. Dudley, “Deep learning for healthcare: review, opportunities and challenges,” *Brief. Bioinform.*, vol. 201, no. February, pp. 1135–44, 2017, doi: 10.1093/bib/bbx044.

[192] D. Shen, G. Wu, and H.-I. Suk, “Deep Learning in Medical Image Analysis,” *Annu. Rev. Biomed. Eng.*, vol. 19, no. 1, p. annurev-bioeng-071516-044442, 2017, doi: 10.1146/annurev-bioeng-071516-044442.

[193] Y. LeCun, Y. Bengio, and G. Hinton, “Deep learning,” *Nature*, vol. 521, no. 7553, pp. 436–444, May 2015, doi: 10.1038/nature14539.

[194] M. Alaqtash, H. Yu, R. Brower, A. Abdelgawad, and T. Sarkodie-Gyan, "Application of wearable sensors for human gait analysis using fuzzy computational algorithm," *Eng. Appl. Artif. Intell.*, vol. 24, no. 6, pp. 1018–1025, 2011, doi: 10.1016/j.engappai.2011.04.010.

[195] M. a. Bogale, H. Yu, T. Sarkodie-Gyan, M. Alaqtash, J. Moody, and R. Brower, "Case Study on Assessment of Mild Traumatic Brain Injury Using Granular Computing," *Engineering*, vol. 04, no. 10, pp. 11–15, 2012, doi: 10.4236/eng.2012.410B004.

[196] M. A. Bogale, H. Yu, T. Sarkodie-gyan, and A. Abdelgawad, "Characterization and quantification of gait deficits within gait phases using fuzzy-granular computing *," vol. 2012, no. December, pp. 720–728, 2012.

[197] Y. Qian, Y. Li, J. Liang, G. Lin, and C. Dang, "Fuzzy Granular Structure Distance," *IEEE Trans. Fuzzy Syst.*, vol. 23, no. 6, pp. 2245–2259, 2015, doi: 10.1109/TFUZZ.2015.2417893.

[198] T. Y. Lin, "Modeling the Real World for Data Mining: Granular Computing Approach," *Conf. Proc. Jt. 9th IFSA World Congr. 20th NAFIPS Int. Conf.*, pp. 3044–3049, 2001.

[199] M. F. Hatwagner, A. Buruzs, A. Torma, and L. T. Koczy, "Introduction of Modeling Complex Management Systems using Fuzzy Cognitive Map," *7th Int. Conf. Inf. Technol.*, vol. 2015, pp. 508–514, 2015, doi: 10.15849/icit.2015.0092.

[200] C. D. Stylios and V. C. Georgopoulos, "Fuzzy cognitive maps structure for medical decision support systems," *Stud. Fuzziness Soft Comput.*, vol. 218, pp. 151–174, 2008, doi: 10.1007/978-3-540-73185-6_7.

[201] V. C. Georgopoulos, G. A. Malandraki, and C. D. Stylios, "A fuzzy cognitive map approach to differential diagnosis of specific language impairment," *Artif. Intell. Med.*, vol. 29, no. 3, pp. 261–278, 2003, doi: 10.1016/S0933-3657(02)00076-3.

[202] N. Douali, "Clinical Decision Support System based on Fuzzy Cognitive Maps," *J. Comput. Sci. Syst. Biol.*, vol. 8, no. 2, pp. 112–120, 2015, doi: 10.4172/jcsb.1000177.

[203] A. Manimaran, V. M. Chandrasekaran, and B. Praba, "A review of fuzzy environmental study in medical diagnosis system," *Res. J. Pharm. Technol.*, vol. 9, no. 2, pp. 707–709, 2016, doi: 10.5958/0974-360X.2016.00032.9.

[204] C. Zou and H. Deng, "Using Fuzzy Concept Lattice for Intelligent Disease Diagnosis," *IEEE Access*, vol. 5, pp. 236–242, 2017, doi: 10.1109/ACCESS.2016.2638848.

[205] S. K. De, R. Biswas, and A. R. Roy, "An application of intuitionistic fuzzy sets in medical diagnosis," *Fuzzy Sets Syst.*, vol. 117, no. 2, pp. 209–213, Jan. 2001, doi: 10.1016/S0165-0114(98)00235-8.

[206] M. Pota, M. Esposito, and G. De Pietro, "Interval type-2 fuzzy DSS for unbiased medical diagnosis," *2016 IEEE Int. Conf. Syst. Man, Cybern. SMC 2016 - Conf. Proc.*, pp. 3340–3345, 2017, doi: 10.1109/SMC.2016.7844750.

[207] C. A. Peña-Reyes and M. Sipper, "Evolutionary Computation in Medicine: an Overview,"

*Artif. Intell. Med.*, vol. 19, pp. 1–23, 2000, doi: S0933-3657(99)00047-0.

[208] U. Maulik, "Medical image segmentation using genetic algorithms.," *IEEE Trans. Inf. Technol. Biomed.*, vol. 13, no. 2, pp. 166–173, 2009, doi: 10.1109/TITB.2008.2007301.

[209] S. L. Smith, P. Gaughan, D. M. Halliday, Q. Ju, N. M. Aly, and J. R. Playfer, "Diagnosis of Parkinson's disease using evolutionary algorithms," *Genet. Program. Evolvable Mach.*, vol. 8, no. 4, pp. 433–447, 2007, doi: 10.1007/s10710-007-9043-9.

[210] M. S. Bergholt *et al.*, "In vivo diagnosis of gastric cancer using Raman endoscopy and ant colony optimization techniques," *Int. J. Cancer*, vol. 128, no. 11, pp. 2673–2680, 2011, doi: 10.1002/ijc.25618.

[211] Y. MARINAKIS and G. DOUNIAS, "NATURE INSPIRED INTELLIGENCE IN MEDICINE: ANT COLONY OPTIMIZATION FOR PAP-SMEAR DIAGNOSIS," *Int. J. Artif. Intell. Tools*, vol. 17, no. 02, pp. 279–301, Apr. 2008, doi: 10.1142/S0218213008003893.

[212] C. Selvaraj, S. Kumar, and M. Karnan, "A Survey on Application of Bio-Inspired Algorithms," *Int. J. Comput. Sci. Inf. Technol.*, vol. 5, no. 6, pp. 366–370, 2014, doi: 0975-9646.

[213] G. Dounias, "Hybrid computational intelligence in medicine," *Univ. Aegean. Dept. Bus. …*, 2003.

[214] M. R. Hassan, S. M. Arafat, and R. K. Begg, "Fuzzy-Genetic Model for the Identification of Falls Risk Gait," *Procedia Comput. Sci.*, vol. 82, no. March, pp. 4–11, 2016, doi: 10.1016/j.procs.2016.04.002.

[215] S. Şahan, K. Polat, H. Kodaz, and S. Güneş, "A new hybrid method based on fuzzy-artificial immune system and k-nn algorithm for breast cancer diagnosis," *Comput. Biol. Med.*, vol. 37, no. 3, pp. 415–423, 2007, doi: 10.1016/j.compbiomed.2006.05.003.

[216] L. Parthiban and R. Subramanian, "Intelligent Heart Disease Prediction System using CANFIS and Genetic Algorithm," *Int. J. Biol. Med. Sci.*, vol. 3, no. 3, pp. 157–160, 2008.

[217] M. Martins, L. Costa, A. Frizera, R. Ceres, and C. Santos, "Hybridization between multi-objective genetic algorithm and support vector machine for feature selection in walker-assisted gait," *Comput. Methods Programs Biomed.*, vol. 113, no. 3, pp. 736–748, 2014, doi: 10.1016/j.cmpb.2013.12.005.

[218] Piedica, "Baropodometría — Plantillas ortopédicas." [Online]. Available: https://www.piedica.com/baropodometria/. [Accessed: 10-May-2018].

[219] "FreeMed Sensor Medica." [Online]. Available: http://www.sensormedica.mx/baropodometro. [Accessed: 10-May-2018].

[220] M. F. Hatwagner and L. T. Koczy, "Parameterization and concept optimization of FCM models," *IEEE Int. Conf. Fuzzy Syst.*, vol. 2015-Novem, 2015, doi: 10.1109/FUZZ-IEEE.2015.7337888.

[221] M. F. Hatwágner, V. A. Niskanen, and L. T. Kóczy, “Behavioral analysis of fuzzy cognitive map models by simulation,” *IFSA-SCIS 2017 - Jt. 17th World Congr. Int. Fuzzy Syst. Assoc. 9th Int. Conf. Soft Comput. Intell. Syst.*, 2017, doi: 10.1109/IFSA-SCIS.2017.8023345.

[222] M. F. Hatwágner, G. Vastag, V. A. Niskanen, and L. T. Kóczy, “Banking applications of FCM models,” *Springer-Verlag*, pp. 1–9, 2011.

[223] W. Stach, L. Kurgan, W. Pedrycz, and M. Reformat, “Genetic learning of fuzzy cognitive maps,” *Fuzzy Sets Syst.*, vol. 153, no. 3, pp. 371–401, 2005, doi: 10.1016/j.fss.2005.01.009.

[224] A. V. Huerga, “A balanced differential learning algorithm in fuzzy cognitive maps,” *Proc. 16th Int. Work. Qual. Reason.*, pp. 1–7, 2002.

[225] E. I. Papageorgiou, “Learning algorithms for fuzzy cognitive maps - A review study,” *IEEE Trans. Syst. Man Cybern. Part C Appl. Rev.*, vol. 42, no. 2, pp. 150–163, 2012, doi: 10.1109/TSMCC.2011.2138694.

[226] G. Felix, G. Nápoles, R. Falcon, W. Froelich, K. Vanhoof, and R. Bello, “A review on methods and software for fuzzy cognitive maps,” *Artif. Intell. Rev.*, pp. 1–31, 2017, doi: 10.1007/s10462-017-9575-1.

[227] E. I. Papageorgiou and J. L. Salmeron, *Fuzzy Cognitive Maps for Applied Sciences and Engineering*, vol. 54. Berlin, Heidelberg: Springer Berlin Heidelberg, 2014.

[228] E. I. Papageorgiou, C. D. Stylios, and P. P. Groumpos, “Active Hebbian learning algorithm to train fuzzy cognitive maps,” *Int. J. Approx. Reason.*, vol. 37, no. 3, pp. 219–249, 2004, doi: 10.1016/j.ijar.2004.01.001.

[229] C. D. Stylios and V. C. Georgopoulos, “Genetic algorithm enhanced Fuzzy Cognitive Maps for medical diagnosis,” in *2008 IEEE International Conference on Fuzzy Systems (IEEE World Congress on Computational Intelligence)*, 2008, pp. 2123–2128, doi: 10.1109/FUZZY.2008.4630663.

[230] J. H. Holland, *Adaptation in Natural and Artificial Systems*. University of Michigan Press, 1975.

[231] O. Cordón, F. Herrera, F. Hoffmann, and L. Magdalena, *Genetic Fuzzy Systems*, vol. 19. WORLD SCIENTIFIC, 2001.

[232] C. D. Stylios and P. P. Groumpos, “Mathematical formulation of fuzzy cognitive maps,” *Proc. 7th Mediterr. Conf. Control Autom.*, pp. 2251–2261, 1999.

[233] M. W. Gardner and S. R. Dorling, “Artificial Neural Networks ( the Multilayer Perceptron )— a Review of Applications in the Atmospheric Sciences,” vol. 32, no. 14, pp. 2627–2636, 1998.

[234] X. Hu and Q. Weng, “Estimating impervious surfaces from medium spatial resolution imagery using the self-organizing map and multi-layer perceptron neural networks,” *Remote Sens. Environ.*, vol. 113, no. 10, pp. 2089–2102, 2009, doi: 10.1016/j.rse.2009.05.014.

[235] Z. Zhang, "Neural networks: further insights into error function, generalized weights and others," *Ann. Transl. Med.*, vol. 4, no. 16, pp. 300–300, 2016, doi: 10.21037/atm.2016.05.37.

[236] B. Hernandez-Ocana, E. Mezura-Montes, and P. Pozos-Parra, "A review of the bacterial foraging algorithm in constrained numerical optimization," *2013 IEEE Congr. Evol. Comput. CEC 2013*, pp. 2695–2702, 2013, doi: 10.1109/CEC.2013.6557895.

[237] K. M. Passino, "Bacterial Foraging Optimization," *Int. J. Swarm Intell. Res.*, vol. 1, no. 1, pp. 1–16, 2010, doi: 10.4018/jsir.2010010101.

[238] N. K. Jhankal and D. Adhyaru, "Comparative Analysis of Bacterial Foraging Optimization Algorithm with Simulated Annealing," vol. 3, no. 3, pp. 10–13, 2014.

[239] S. Das, A. Biswas, S. Dasgupta, and A. Abraham, "Bacterial Foraging Optimization Algorithm: Theoretical Foundations, Analysis, and Applications," pp. 23–55, 2009, doi: 10.1007/978-3-642-01085-9_2.

[240] J. A. R. Bautista, S. L. C. Cárdenas, A. H. Zavala, and J. A. Huerta-Ruelas, "Review on plantar data analysis for disease diagnosis," *Biocybern. Biomed. Eng.*, vol. 8, 2018, doi: 10.1016/j.bbe.2018.02.004.

[241] E. Papageorgiou, N. Papandrianos, D. Apostolopoulos, and P. Vassilakos, "Fuzzy Cognitive Map Based Decision Support System for Thyroid Diagnosis Management," *Ieee Int. Conf. Fuzzy Syst.*, vol. 1, pp. 1204–1211, 2008.

[242] G. Nápoles, I. Grau, R. Bello, and R. Grau, "Two-steps learning of Fuzzy Cognitive Maps for prediction and knowledge discovery on the HIV-1 drug resistance," *Expert Syst. Appl.*, vol. 41, no. 3, pp. 821–830, 2014, doi: 10.1016/j.eswa.2013.08.012.

[243] D. R. Bonanno, K. Ledchumanasarma, K. B. Landorf, S. E. Munteanu, G. S. Murley, and H. B. Menz, "Effects of a contoured foot orthosis and flat insole on plantar pressure and tibial acceleration while walking in defence boots," *Sci. Rep.*, vol. 9, no. 1, pp. 1–10, 2019, doi: 10.1038/s41598-018-35830-5.

[244] A. K. Buldt, S. Forghany, K. B. Landorf, P. Levinger, G. S. Murley, and H. B. Menz, "Foot posture is associated with plantar pressure during gait: A comparison of normal, planus and cavus feet," *Gait Posture*, vol. 62, no. October 2017, pp. 235–240, 2018, doi: 10.1016/j.gaitpost.2018.03.005.

[245] U. K. Hofmann, M. Götze, K. Wiesenreiter, O. Müller, M. Wünschel, and F. Mittag, "Transfer of plantar pressure from the medial to the central forefoot in patients with hallux valgus," *BMC Musculoskelet. Disord.*, vol. 20, no. 1, pp. 1–8, 2019, doi: 10.1186/s12891-019-2531-2.

[246] A. K. Buldt, J. J. Allan, K. B. Landorf, and H. B. Menz, "The relationship between foot posture and plantar pressure during walking in adults: A systematic review," *Gait Posture*, vol. 62, no. January, pp. 56–67, 2018, doi: 10.1016/j.gaitpost.2018.02.026.

[247] A. M. Said, M. Justine, and H. Manaf, "Plantar pressure distribution among older persons

with different types of foot and its correlation with functional reach distance," *J. Nanomater.*, vol. 2016, 2016, doi: 10.1155/2016/8564020.

[248] W. M. Williams, "The Accuracy and Reliability of Plantar Pressure Measurements for the Early Diagnosis of Foot Deformities in Patients Suffering from Rheumatoid Arthritis," *Divers. Equal. Heal. Care*, vol. 14, no. 4, pp. 193–202, 2017, doi: 10.21767/2049-5471.1000111.

[249] D. A. Pelta, C. Cruz, A. D. Masegosa, E. Onieva, P. Lopez-garcia, and E. Osaba, *Soft Computing Based Optimization and Decision Models*, Springer I., vol. 360. Cham, Switzerland: Springer, 2018.

[250] S. Sujamol, S. Ashok, and U. K. Kumar, "Study of Fuzzy Cognitive Maps for Modeling Clinical Support Systems," vol. 119, no. 12, pp. 15433–15445, 2018.

[251] G. Nápoles, E. Papageorgiou, R. Bello, and K. Vanhoof, "Learning and Convergence of Fuzzy Cognitive Maps Used in Pattern Recognition," *Neural Process. Lett.*, vol. 45, no. 2, pp. 431–444, 2017, doi: 10.1007/s11063-016-9534-x.

[252] C. D. Stylios, V. C. Georgopoulos, G. A. Malandraki, and S. Chouliara, "Fuzzy cognitive map architectures for medical decision support systems," *Appl. Soft Comput. J.*, vol. 8, no. 3, pp. 1243–1251, 2008, doi: 10.1016/j.asoc.2007.02.022.

[253] G. A. PAPAKOSTAS, Y. S. BOUTALIS, D. E. KOULOURIOTIS, and B. G. MERTZIOS, "Fuzzy Cognitive Maps for Pattern Recognition Applications," *Int. J. Pattern Recognit. Artif. Intell.*, vol. 22, no. 08, pp. 1461–1486, 2009, doi: 10.1142/s0218001408006910.

[254] J. S. Papageorgiou, EI, "A review of fuzzy cognitive map research at the last decade," *Ieeexplore.Ieee.Org*, vol. 21, no. 1, pp. 66–79, 2013.

[255] G. Papakostas and D. E. Koulouriotis, "Classifying Patterns Using Fuzzy Cognitive Maps," in *Fuzzy cognitive maps*, 2010, vol. 247, pp. 291–306, doi: 10.1016/S0020-7373(86)80040-2.

[256] P. P. Groumpos and A. P. Anninou, "A theoretical mathematical modeling of Parkinson's disease using Fuzzy Cognitive Maps," *IEEE 12th Int. Conf. Bioinforma. Bioeng. BIBE 2012*, no. November, pp. 677–682, 2012, doi: 10.1109/BIBE.2012.6399748.

[257] E. I. Papageorgiou, C. D. Stylios, and P. P. Groumpos, "An Integrated Two-Level Hierarchical System for Decision Making in Radiation Therapy Based on Fuzzy Cognitive Maps," *IEEE Trans. Biomed. Eng.*, vol. 50, no. 12, pp. 1326–1339, 2003, doi: 10.1109/TBME.2003.819845.

[258] P. Oikonomou and E. I. Papageorgiou, "Particle Swarm Optimization approach for fuzzy cognitive maps applied to autism classification," in *IFIP Advances in Information and Communication Technology*, 2013, vol. 412, pp. 516–526, doi: 10.1007/978-3-642-41142-7_52.